ERDC/GSL TR-14-14

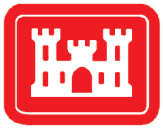

US Army Corps
of Engineers®
Engineer Research and
Development Center

ERDC
INNOVATIVE SOLUTIONS
for a safer, better world

Geotechnical Centrifuge Experiments to Evaluate Piping in Foundation Soils

Daniel A. Leavell, Johannes L. Wibowo, Donald E. Yule,
and Ryan C. Strange

May 2014

Geotechnical and Structures Laboratory

The US Army Engineer Research and Development Center (ERDC) solves the nation's toughest engineering and environmental challenges. ERDC develops innovative solutions in civil and military engineering, geospatial sciences, water resources, and environmental sciences for the Army, the Department of Defense, civilian agencies, and our nation's public good. Find out more at www.erdc.usace.army.mil.

To search for other technical reports published by ERDC, visit the ERDC online library at http://acwc.sdp.sirsi.net/client/default.

ERDC/GSL TR-14-14
May 2014

Geotechnical Centrifuge Experiments to Evaluate Piping in Foundation Soils

Johannes L. Wibowo, Donald E. Yule, and Ryan A. Strange

Geotechnical and Structures Laboratory
US Army Engineer Research and Development Center
3909 Halls Ferry Road
Vicksburg, MS 39180-6199

Daniel A. Leavell

Bowhead Science and Technology
3401 Halls Ferry Road, Suite 6
Vicksburg, MS 39180

Final report

Prepared for US Army Corps of Engineers
Washington, DC 20314-1000

Abstract

The general objectives of the centrifuge tests for this research were to model a realistic geologic prototype of a levee with a foundation containing a sand layer that is susceptible to an internal erosion/piping failure mechanism with objectives to initiate and monitor piping. Parameters that could influence piping/erosion in levee foundation soils were evaluated (i.e., depth of erodible material, density of erodible material, and confining stress). Centrifuge testing and numerical modeling were performed on three geotechnical models constructed with soils similar to those found in the US Army Corps of Engineers levee portfolio. Models 1 and 2 had a clay levee that was founded on a Nevada Sand layer sandwiched between two Longhorn Red Clay layers. Model 3 had a foundation consisting of a Longhorn Red Clay top layer, then a clayey sand layer, followed by Nevada Sand and, finally, a bottom layer of Longhorn Red Clay. Varying gravity loadings were selected based on a prototype structure 5 to 12 ft. in height. All models developed piping that moved from a downstream relief hole back under the levee toward the upstream reservoir. The results from the three centrifuge tests showed that subsurface erosion could be modeled in a centrifuge.

Contents

Figures and Tables

Figures

Tables

Preface

This study was conducted for the Headquarters, US Army Corps of Engineers (USACE) Civil Works research program, Flood Risk Management and Water Control Infrastructure Resiliency and Reliability Program under the Flood and Coastal Storm Damage Reduction (FCDR) Research and Development Program. William R. Curtis was the Technical Director of the Coastal and Hydraulics Laboratory (CHL), US Army Engineer and Development Center, for the FCDR program. The Program Manager for FCDR was Dr. Cary A. Talbot, CHL. Dr. Michael K. Sharp was the Technical Director for the Water Resources Infrastructure Research, Geotechnical and Structures Laboratory (GSL). The Technical Monitor was Dr. Maureen K. Corcoran, GSL.

The work was performed by the Geotechnical Engineering and Geosciences Branch (GEGB) of the GSL Geosciences and Structures Division (GSD). At the time of publication, Chad A. Gartrell was Chief, GEGB, and Bartley P. Durst was Chief, GSD. The Deputy Director of ERDC-GSL was Dr. William P. Grogan, and the Director was Dr. David W. Pittman.

Centrifuge testing was conducted at the US Army Geotechnical Centrifuge Research Center (CRC) in Vicksburg, Mississippi. The director of the CRC was Wipawi Vanadit-Ellis. David Daley of the ERDC Information Technology Laboratory provided instrumentation support.

COL Jeffrey R. Eckstein was Commander of ERDC, and Dr. Jeffery P. Holland was Director.

Unit Conversion Factors

Multiply	By	To Obtain
cubic feet	0.02831685	cubic meters
cubic inches	1.6387064 E-05	cubic meters
degrees (angle)	0.01745329	radians
feet	0.3048	meters
inches	0.0254	meters
pounds (force)	4.448222	newtons
pounds (force) per foot	14.59390	newtons per meter
pounds (force) per inch	175.1268	newtons per meter
pounds (force) per square foot	47.88026	pascals
pounds (force) per square inch	6.894757	kilopascals
pounds (mass)	0.45359237	kilograms
pounds (mass) per cubic foot	16.01846	kilograms per cubic meter
pounds (mass) per cubic inch	2.757990 E+04	kilograms per cubic meter
pounds (mass) per square foot	4.882428	kilograms per square meter
square feet	0.09290304	square meters
square inches	6.4516 E-04	square meters

1 Introduction

Internal erosion of embankments and their foundations is the most frequent failure mode observed in dams and levees. As part of an overall assessment of the current state-of-knowledge to increase the understanding of this failure mode, physical modeling (geotechnical centrifuge model tests, in this case) was conducted. This report documents the investigation of physical modeling tests conducted in a geotechnical centrifuge at the US Army Engineer Research and Development Center (ERDC) Centrifuge Research Center in Vicksburg, Mississippi.

The tests described and discussed in this report were performed on a 1256 *g*-ton centrifuge (Figure 1) located at the Centrifuge Research Center, Geotechnical and Structures Laboratory, ERDC, Vicksburg. The centrifuge has a platform radius of 21.3 ft, a maximum payload of 8800 lb at 143 *g*, platform area of 20 sq ft, and a maximum gravity range of 350 *g*.

Additional technical information for the centrifuge can be obtained from the Director, Centrifuge Research Center, 3909 Halls Ferry Road, Vicksburg, MS 39180-6199.

Figure 1. US Army Corps of Engineers' centrifuge.

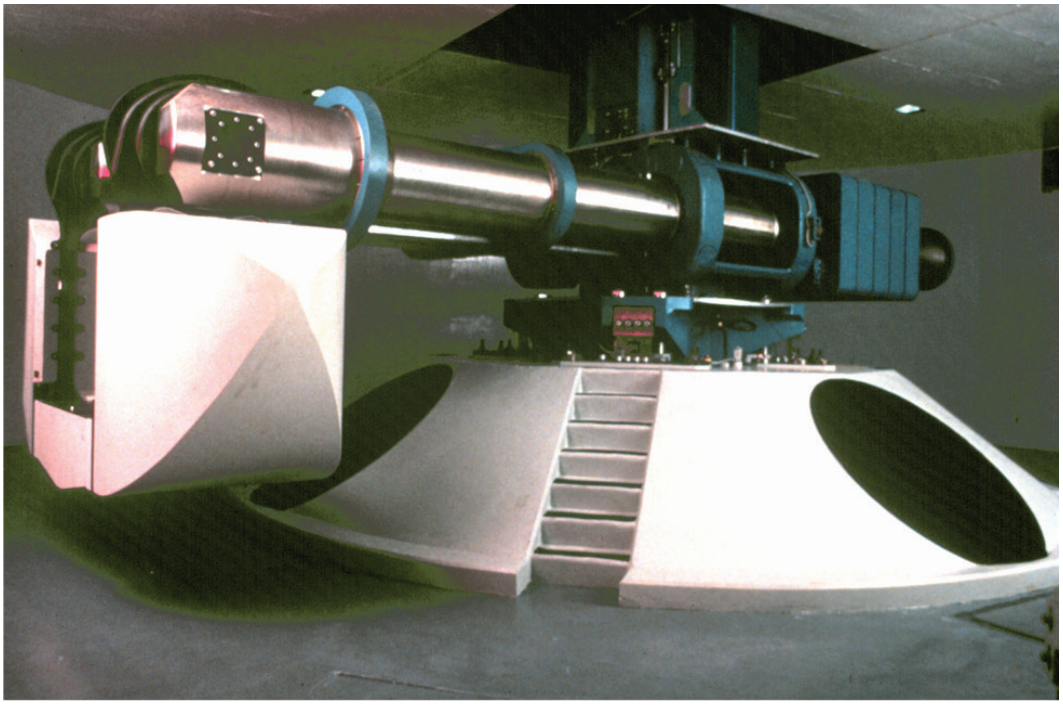

1.1 Research objectives

The general objectives of the centrifuge tests for this research were to model a realistic geologic prototype of a levee with a foundation containing a sand layer that is susceptible to an internal erosion/piping failure mechanism with objectives to initiate and monitor piping. Models 1 and 2 consisted of a clay embankment on clay substratum, both resistant to piping, overlaying a foundation sand that is susceptible to piping. The initiation of piping was affected by introduction of a pressure relief hole at the downstream toe of the embankment, allowing flow to exit the sand layer to the ground surface. The seepage flow was introduced directly from a reservoir into the foundation sands with the clay embankment providing only overburden stress conditions in the foundation sands. A clay top-stratum, which represents a common geologic setting for levees, also provided experimental control of the model's piping boundary conditions.

Boundary conditions are important considerations in scale-model testing with the constraint they provide a realistic full-scale model response. In this respect, the piping-susceptible foundation sand was fully contained within a piping-resistant clay box to preclude unwanted boundary effects of seepage along the sides of the model container. The model was constructed to support an overall seepage through foundation to a downstream free-field open face and drainage to maintain minimal tail water level at the piping exit point. After experience with tests on a single, piping-susceptible sand layer directly under the clay top-stratum, a two-layer foundation was constructed in Model 3 to force piping deeper within the foundation sand. The approach included adding a top clayey sand layer significantly more resistant to piping, but still highly susceptible compared to the clay top-stratum. This more piping-resistant clayey sand overlaying the much more susceptible uniform clean sand enabled piping to begin in the lower sand layer and prevented piping along the foundation clayey sand-clay interface. Tests were conducted in a general procedure of raising the reservoir height, monitoring the seepage and initiation of piping with sand boil formation, recording videos of changes in the model surface, and measuring pore pressure response in the foundation along the seepage path. A full description of the tests and their results are provided in the following chapters of the report.

1.2 Background

Physical modeling is a valuable approach for investigation of complex problems that are not easily solved or modeled numerically and provides a means to validate numerical models and theory. Physical modeling is also useful to develop parametric studies of synthetic field case histories with the advantage of inclusion and control of important parameters. Full-scale physical modeling, especially for investigation of failures, has limited practical use due to cost and safety. However, physical modeling using centrifuge testing enables use of a small-scale model of the full-scale (prototype) structure to mitigate these problems and enable its use (Ledbetter 1991).

The centrifuge has been found to be most useful for geotechnical engineering and soil mechanics research (Garnier et al. 1984, 2007; Joseph et al. 1988; Ledbetter 1991; Ng et al. 2001; van Beek et al. 2010). The basic principle of centrifuge modeling relies on exposing a scale model to a larger gravity field, N, than the normal (1 *g*) gravity of the earth. Many geotechnical mechanisms produce the response of the prototype that is effectively N times larger. Scaling relations between properties in the prototype and scale model have been developed, and most scale linearly (e.g., N, 1/N, N^2 etc.; where N × increase in gravity); however, "scale effects" not specifically addressed or even known will introduce modeling errors. One technique to evaluate the appropriateness of an application is "modeling of models," where a suite of different scaled prototypes are tested for the range of expected scaling to insure consistent results. Furthermore, the advantage of scaling down the real-world size problem has disadvantages. There are problems in working in the limited space of small models with resulting constraints of instrumentation and boundary conditions such that it is important to simplify the model to include only the necessary features to investigate the phenomena of interest. Therefore, with the probable loss of prototype detail and any unaccounted "scale effects," the concept that these small-scale model tests are exact replica tests is misleading, and its use should be realistically portrayed.

Centrifuge testing has been employed for investigation of internal erosion, specifically piping; however, this application has a relatively short history and concerns with appropriate scale factors and identification of "scale effects" are still a concern (van Beek et al. 2010; Le et al. 2010; Garnier et al. 1984). Considering that piping is a complex mechanism of coupled flow and particle transport, even the simpler precursor, the scaling of laminar flow

through soil, is a topic of some argument. Because this is a developing application for centrifuge testing, initial models that were developed to match the 1-*g* case may not include parameters that arise in scale-model testing at higher gravitational force (scale effects). A postulated example is that piping conditions generated in the scale model may introduce more turbulent flow not accounted for in a real-world empirical model (van Beek et al. 2010). Researchers investigated "scale effects" for the Sellmeijer critical gradient parameter (Sellmeijer and Koenders 1991) and found a dependence on gravitational level (van Beek et al. 2010). In spite of the current uncertainties in some aspects of centrifuge modeling of internal erosion piping failure modes, careful idealization and simplification of a model and conduction of scale-model tests at relatively low gravitational levels should alleviate scale effects and provide a useful research approach. Tests conducted at higher gravitational levels or where numerically quantitative precision is needed should include "modeling of models" in the test plan to investigate and quantify any scale effects.

2 Experimental Procedure

2.1 Soils tested

Materials used in the construction of the models were a premixed potter's clay of low plasticity, CL (Longhorn Red); a fine uniformly graded sand, SP (Nevada Sand); and a clayey sand, SC (from Fort Polk, Louisiana). The potter's clay was obtained from Armadillo Clay & Supply, Austin, Texas, and was received in 50-lb boxes with each box containing two 25-lb, 6.0-by-6.0-by-9.0-in. blocks. The premixed clay contained virtually no air voids and had the consistency of soft modeling clay. The clay had a smooth, silky surface and felt like talc when dried. When submerged in water or dried, the clay exhibited a volume change of less than 5%.

The clayey sand was received in 55-gal barrels and then air-dried and stored in sealed containers until needed for model construction. Soil parameters for each soil type are listed in Table 1, and the grain-size distributions are shown in Figure 2.

2.2 Centrifuge model container

A model container that was designed to withstand gravitational levels in excess of 150 *g* was used for all erosion/piping tests. Figure 3 shows a front view of the container as seen through the Plexiglas® face. The bottom and three sides of the container were constructed from 1-in.-thick aluminum plates with the fourth side made from 2-in.-thick Plexiglas®. The interior dimensions were 13 in. wide by 19 in. deep by 50 in. long. There were reservoirs at each end of the container with the upstream reservoir having dimensions of 13 in. wide by 19 in. deep and 6 in. long. The downstream reservoir had the same width and length but was 7 in. deep. The maximum model size that the container could hold was 13 in. wide by 19 in. deep by 38 in. long.

The upstream reservoir provided headwater for the model. Two 0.5-in.-diam holes provided a flow path for water into the model's sand foundation. These holes were located in the upstream reservoir face. They were spaced 5 in. apart and centered horizontally at a height of 3 in. above the base of the model container. After Models 1 and 2, the number of 0.5-in. holes was increased to 12, two rows of six holes, for Model 3 to reduce the magnitude

of the flow gradients at the flow holes. The holes were covered with finely meshed filter fabric to prevent the sand from entering the reservoir. The downstream reservoir was a collection point for the water being discharged from the model. A 0.5-in.-diam hole in the outside wall of the downstream reservoir spaced 5.5 in. from the base allowed water to drain from the reservoir, keeping water from backing up and flooding the surface of the model. The container's Plexiglas® face allowed viewing of the model during the test.

Table 1. Soil parameters for each soil type.

Soil Type	Atterberg Limits			Water Content (%)	Dry Density (lb/ft³)	Coefficient of Uniformity[a] (D_{60}/D_{10})
	Liquid Limit	Plasticity Index	Specific Gravity			
Longhorn Red Clay (CL)	39	27	2.80	28	97	
Nevada Sand (SP)			2.64		88.9 (min) 106.6 (max)	1.4
Clayey sand (SC)	28	11	2.70	14	88 (as-placed, estimated)	

[a] Various researchers have shown that as the Coefficient of Uniformity approaches 1, sand becomes more erodible (de Wit et al. 1981; Sellmeijer 1988).

Figure 2. Grain Size distribution for Longhorn red Clay (CL), Nevada Sand (SP), and Clayey Sand (SC).

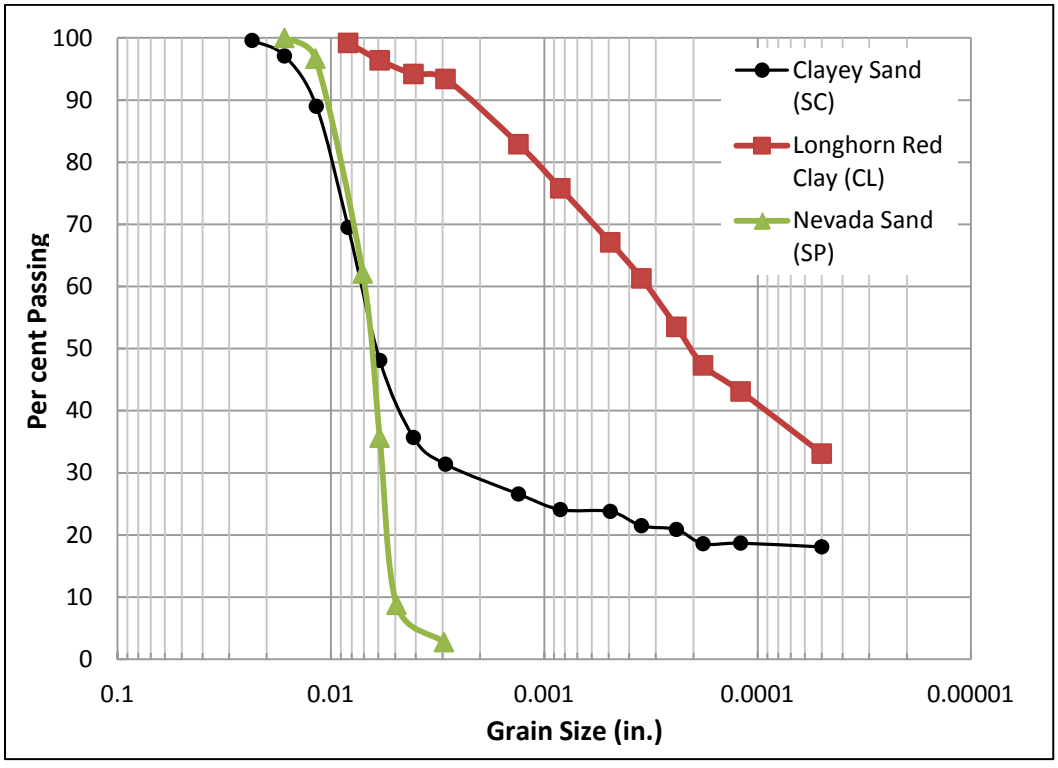

Figure 3. Front view through the Plexiglas® face of model container showing the reservoirs and flow holes.

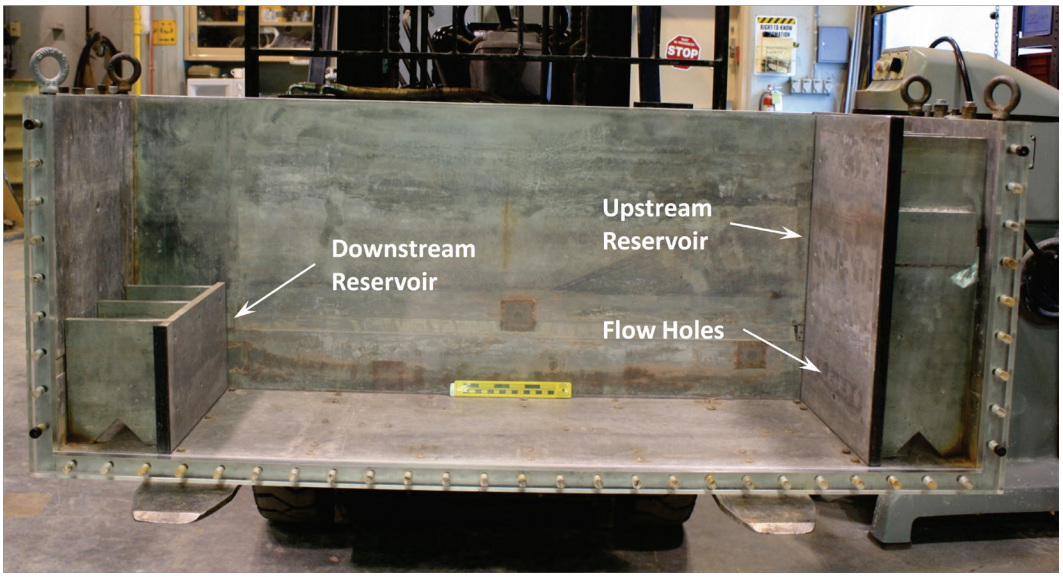

2.3 Model construction

Models 1 and 2 were constructed with the same number of layers. Model 3 had an additional foundation layer. Pore pressure transducers (PPTs) were installed in the foundation. A pictorial presentation of model construction is shown in Appendix A. A cross section of Models 1 and 2 is shown in Figure 4. The Longhorn Red clay was initially cut into 1.0-in.-thick slabs using a wire saw. The longitudinal boundaries of the model were lined with the slabs of the Longhorn Red clay to prevent the occurrence of erosion at these boundaries. It is well known that higher permeabilities and, therefore higher gradients, can occur along rigid surfaces (Richards and Reddy 2007). The edges of each clay slab were beveled to a 45-deg angle to provide a 1.0-in. overlap with each adjacent clay slab. This overlapping provided integrity of the walls, base, and top of the model.

The interior (between the upper and lower clay boundaries) of Models 1 and 2 contained Nevada Sand. The sand was pluviated through water until it was 5.0 in. deep and level with the top of the exterior clay walls. Any excess water was drained before the clay top was placed over the sand. Maintaining the sand in a saturated state minimized trapped air and ensured initial model permeability. The as-placed dry density of the sand was estimated to be 96 lb/ft^3 for Model 1 and 100 lb/ft^3 for Model 2.

Figure 4. Cross section of centrifuge Models 1 and 2 with pore pressure transducer (PPT) locations.

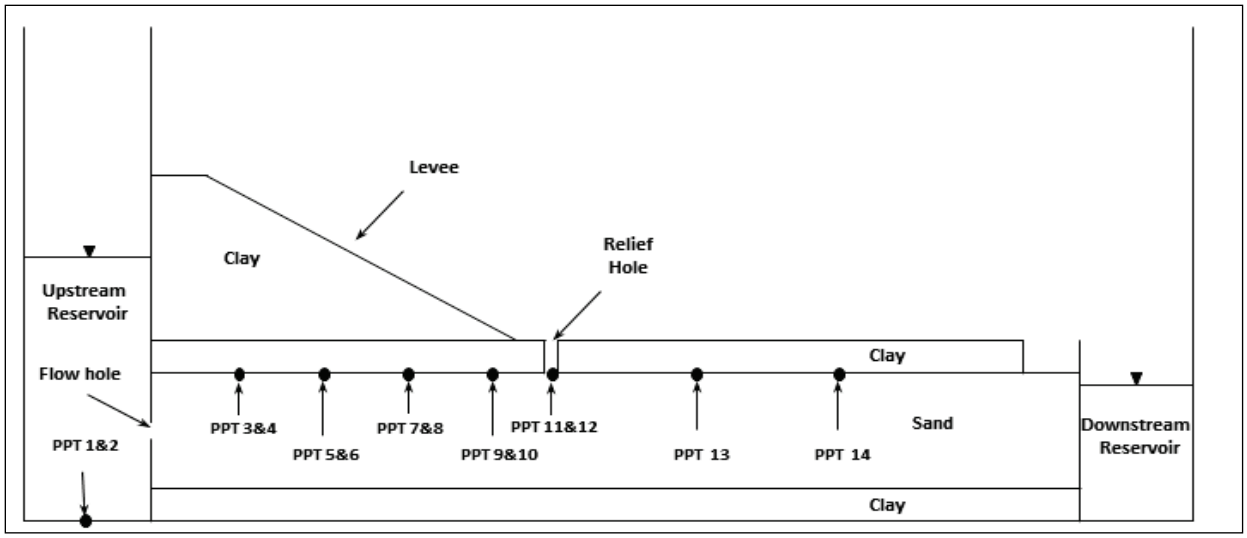

Model 2 differed from Model 1 only in the density of the Nevada Sand. After the post analysis of Model 1, the clay bottom and sides were left intact, and the Nevada Sand was replaced in a submerged condition. The model was left idle for about a month because of personnel and funding constraints.

When work began again on Model 2, the Nevada Sand was left undisturbed at the higher density. The construction procedures for Model 2 remained the same as Model 1 after placement of the sand.

The cross section of Model 3 is shown in Figure 5. The interior of Model 3 (between the upper and lower clay boundaries) contained 4.0 in. of Nevada Sand with a 1.0-in.-thick top layer of clayey sand. The Nevada Sand was pluviated through water until it was 4.0 in. deep. Any excess water was drained before the clayey sand layer was placed over the sand. The as-placed dry density of the Nevada Sand was estimated to be 96 lb/ft^3. The clayey sand layer was carefully placed on top of the sand layer and compacted using a pushing motion until it was level with the top of the exterior clay walls. The as-placed dry density of the clayey sand layer was estimated to be 88 lb/ft^3.

The same procedure was used to place the top clay layer for all three models. The top clay layer was beveled and placed on top of the sand or clayey sand layer and the exterior clay walls. The top clay layer was constructed from 6.0-by-9.0-in. clay pieces. The sequence of construction was to place two 6.0-in.-wide rows along the back wall of the model container. The final row (against the Plexiglas® face of the model

container) consisted of 4.0-by-9.0-in. clay pieces. A 2.0-in. gap that exposed the sand layer was formed adjacent to the downstream reservoir. The gap provided an exit for water flowing through the sand layer of the model. Water collected in the gap then spilled over into the downstream reservoir when the gap was full.

Figure 5. Cross section of the centrifuge Model 3 with pore pressure transducer (PPT) locations.

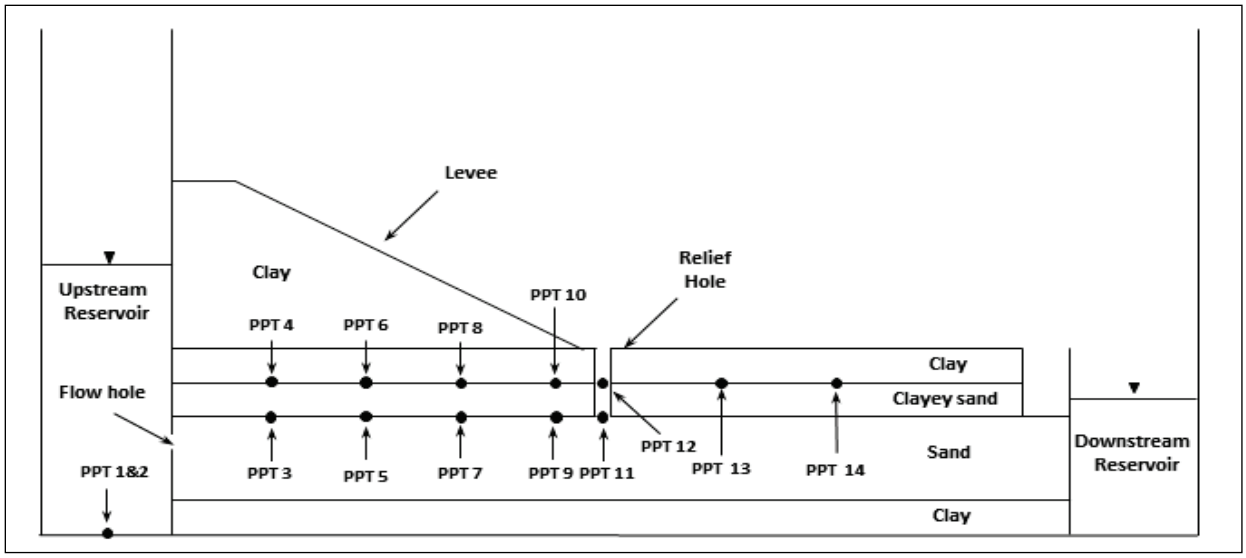

A levee was placed adjacent to the upstream reservoir. The levee dimensions were 13.0 in. wide, 6.0 in. high, and 17.0 in. long with a 2.0-in.-wide crest. The face of the levee had a slope of 2 on 5 and sloped from the downstream edge of the crest to the levee toe. The levee was constructed with six clay pieces that were wide enough to allow the PPT wires to be vertically sandwiched between the levee pieces. The four outside sections of the levee were approximately 3.5 in. wide with the two center sections being 6.0 in. wide. The first two outside pieces were placed against the back wall of the model. The two center sections were placed next with the last two placed against the Plexiglas® face of the model. The levee was smoothed and shaped after its construction.

2.4 Model instrumentation layout

Fourteen PPTs were used to monitor pore water pressure development and dissipation. Figure 6 shows a plan view of the models with the PPT locations. Each PPT had a maximum range of 15 psi and was approximately 0.25 in. in diameter and 0.5 in. long. The PPTs were numbered 1 through 14 with PPTs 1 and 2 located in the bottom of the upstream reservoir. These two PPTs measured the reservoir water height continually.

Figure 6. Plan view of the centrifuge models with pore pressure transducer (PPT) locations.

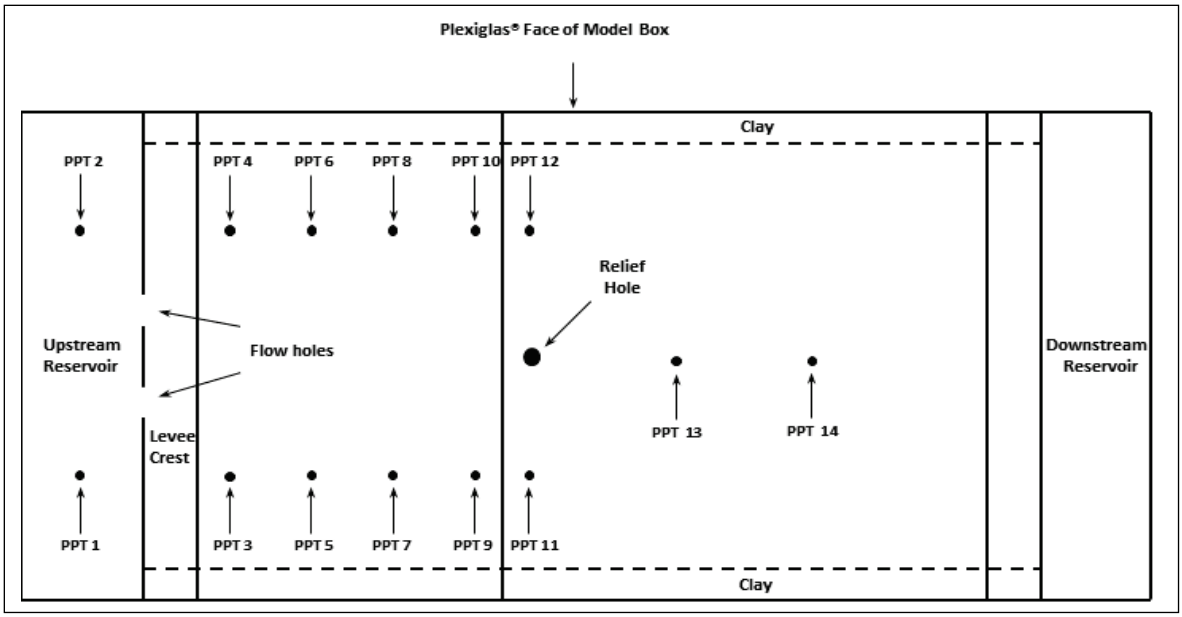

PPTs 3 through 14 were placed at the top of the sand-clay interface for Models 1 and 2 and provided pore pressure measurements along the top of the sand strata where piping/erosion was likely to occur. For Model 3, the odd-numbered PPTs (3 through 11) were placed at the sand-clayey sand interface with the even-numbered PPTs (4 through 12) and PPTs 13 and 14 placed at the clayey sand-clay interface (Figure 5).

PPTs 3-12 were positioned in pairs (e.g., PPTs 3 and 4, PPTs 5 and 6, etc.) and placed 3.5 in. from the outside boundaries (the back wall and the Plexiglas® face of the model). Opposing pairs were separated from each other by 6.0 in. PPTs 3-10 were located every 4.0 in. from the upstream reservoir face. Placing the PPTs in pairs not only gives a redundancy in readings at each downstream location, but also allows individual readings of both the right and left sides of the model. Placement of PPTs in this fashion gives complete coverage of the area under the levee and allows the effects of an erosion channel on the pore pressure to be measured. Any reduction in pore pressure may be an indication that a piping/erosion channel is forming in the area of the corresponding PPTs.

PPT 11 and 12 were located 1 in. beyond and parallel to the levee toe. PPTs 13 and 14 were located downstream of the levee toe in the center of the model and were spaced 6.0 in. and 11.0 in., respectively, from the levee toe to measure far-field pore pressures during model testing. These PPTs

were used to indicate water flow or pore water pressure development downstream of the relief hole.

2.5 Installation of model instrumentation

PPTs 3-14 were inserted vertically through the top clay layer to the sand-clay interface for Models 1 and 2. Initially, a PPT hole was formed by inserting a 0.20-in.-diam straw through the top layer(s) until contact was made with the underlying sand layer. The straw and the soil core were then slowly withdrawn from the hole. The soil core was checked to see if there was a thin film of sand at the base of the core. The film of sand indicated that the transducer would be in contact with the sand layer when placed. The PPT was then slowly pushed into the hole until resistance from the sand layer was felt. The undersized hole (0.2-in. straw hole versus 0.25-in. PPT diam) provided the PPT with a water-tight seal that minimized water leakage and pore pressure dissipation during testing. Small slivers of clay were then compacted into the cavity behind the PPT and around its connecting wire. The clay slivers helped seal the PPT and provided additional protection against pore water leakage and/or pore pressure dissipation.

Figure 7 shows the levee after the first two sections are placed with PPTs 3, 5, 7, and 9 positioned at the clay-sand interface with their wires extending vertically through the levee. The PPT wires were taped to the box walls after each PPT installation to keep them out of the way during the construction phase. Once construction of the levee was complete and all PPTs were installed, a small circular berm was placed around PPTs 11-14. Figure 8 shows these berms around PPTs 11, 12, and 13 that are downstream of the levee toe. These berms provide a third level of protection against pore water leakage and/or pore water pressure dissipation during the test.

While the horizontal locations of PPTs in Model 3 were the same, their vertical placement differed slightly from Models 1 and 2. In Model 3, odd-numbered PPTs 3-11 were placed at the sand-clayey sand interface and even-numbered PPTs 4-12, 13, and 14 were placed at the clayey sand-clay interface. The placement of the PPTs at both interfaces allowed monitoring of pore water pressures during the test. Therefore, pore water pressures would indicate the initiation of piping and the soil interface where it was occurring.

Figure 7. The first two sections of levee placed with PPTs inserted into top clay layer. PPT wires pass vertically through the levee and are sandwiched between levee sections.

Figure 8. The relief hole and berms that were placed around PPTs 11, 12, and 13 in Models 1, 2, and 3.

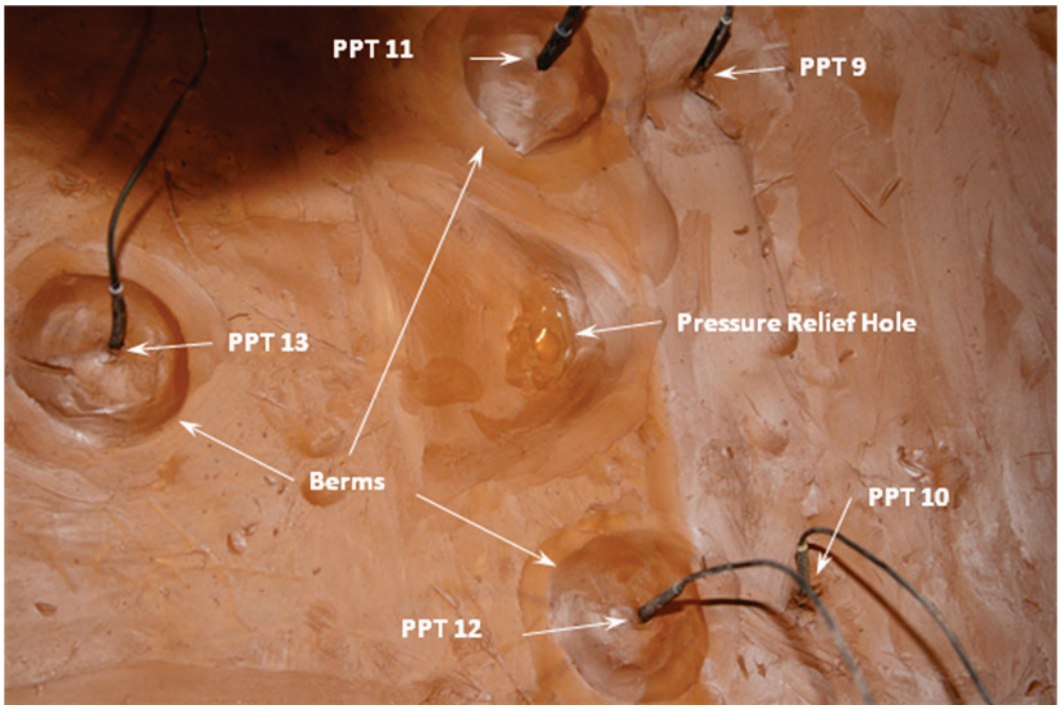

A relief hole was placed 1 in. downstream of the levee toe in line with PPTs 11 and 12 as seen in Figure 8. The relief hole was formed by inserting a 0.35-in.-diam straw through the top layer(s) until contact was made with the underlying Nevada Sand layer. The straw with the soil core was then slowly extracted. The area around the relief hole was scooped and tapered into a fan shape, having a width of about 0.5 in. around the relief hole (Figure 8). The fan area had a downstream length of about 2.0 in. and a width of about 3.0 in. with a maximum depth around the hole of approximately 0.75 in. The top clay layer at the location of the relief hole was approximately 0.25 in. thick. The scooped-out area provided a collection point for any eroded material and allowed visual detection of material movement.

Six video cameras were mounted at optimal vantage points both inside and outside the model box for viewing/recording model behavior during each test. The two cameras located inside the model box provided views of the upstream and downstream surfaces of the model. The upstream camera showed the levee, PPTs 3-12, and the relief hole. The downstream camera showed PPTs 13 and 14 and the downstream reservoir. Two of the four exterior cameras provided a view of the upstream and downstream sides of the model through the Plexiglas® face. The last two exterior cameras allowed monitoring of the water height in the upstream reservoir, water feed hose, and PPT cables going from the model box to the centrifuge platform. In addition, both of these cameras provided a view of the centrifuge platform, which was closely watched for water leakage during the in-flight testing phase.

3 Test Protocol

The overall testing protocol for Models 2 and 3 was developed from the behavior of Model 1. For Models 2 and 3, a test was performed without a relief hole to obtain overall pore pressure measurements as a basis for comparison. The need for a comparative run without a relief hole was not realized until the Model 1 results were analyzed. Therefore, data from numerical analyses, which are discussed in Chapter 6, were used as the basis for Model 1 comparisons.

Models 1 and 3 were each tested at a low and then a higher gravitational level. The models were not repaired between the different gravitational level runs. Therefore, any erosion/piping damage caused by the lower gravitational level added to the erosion/piping experienced at the higher gravitational level.

3.1 Model 1

The first model was tested at 10 *g* and 20 *g*. The reservoir water height for the 10-*g* test was not allowed to exceed the levee crest. The only way to increase the head pressure on the model was to increase the gravitational level.

Model permeability was checked at 1 *g* by slowly filling the upstream reservoir until the water was 1.0 in. above the base of the levee (8.0 in. from base of model). Almost immediately, water started to rise in the relief hole, and within 5 min, the gap adjacent to the downstream reservoir began filling with water. After about 10 min, the water in the reservoir stabilized at a height of about 6.7 in. (0.3 in. below the levee base).

All cameras and instrumentation were checked, and the PPTs were zeroed before the start of the test. The centrifuge was then incrementally brought up to the test gravitational level. Incremental gravity loading allows the model to settle and come to equilibrium slowly. The g-level increments for the 10-*g* test were 2 *g*, 5 *g*, and 10 *g* with the centrifuge staying at each level for several minutes. Once the centrifuge stabilized at 10 *g* for approximately 5 min, the reservoir height was raised in 1.0-in. increments every 5 min. The model was closely observed at each reservoir height for movement of sand

grains in the fan area of the relief hole or water discoloration in the relief hole. Either of these conditions would indicate the start of a piping event.

The same procedure was followed for the 20-*g* test except the increments were 2 *g*, 10 *g*, and 20 *g*. After the model stabilized at 20 *g* for about 5 min, the reservoir water height was raised in 0.5-in. increments every 5 min until a 3.0-in. head on the levee was reached. The water level was then raised in 0.25-in. increments every 5 min until a 6.0-in. head on the levee was attained. The upstream reservoir was recharged multiple times during the 5-min interval to maintain the appropriate water head. After the 6.0-in. head was attained, the flow through the model was high enough that the reservoir charge rate could be matched to the model flow rate, thereby keeping a constant 6.0-in. head on the levee until test completion.

3.2 Model 2

The second model was tested at 12 *g* both with and without a relief hole. The test without a relief hole allowed measurement of pore water pressures along the axis of the model as the reservoir head was increased without the influence of the relief hole. It was assumed that the head pressure used in this test was low enough so no model damage was caused. Model permeability was checked in the same way as Model 1. For the non-relief hole test, the PPTs were zeroed at a 6.0-in. reservoir water height (1.0 in. below the base of the levee) before the start of the test. The centrifuge was incrementally brought up to the test gravitational level with the centrifuge staying at each level (2 *g*, 5 *g*, and 12 *g*) for several minutes. Once the model stabilized at the 12-*g* level for about 5 min, the reservoir height was incrementally raised until a 2.0-in. head on the levee was reached. The flow rate was hard to maintain so the centrifuge test was stopped.

Modifications to the upstream reservoir were made by drilling three holes in the upstream reservoir at 9.0, 11.0, and 13.0 in. above the levee base. When the reservoir height reached a hole, the excess water would flow from the reservoir and onto the floor of the centrifuge chamber, thereby maintaining a constant reservoir height. After the model was run for an appropriate time at that constant reservoir height, the centrifuge was stopped and the hole at 9 in. was plugged. The centrifuge was then restarted, the test continued until the reservoir height reached the next hole, and the procedure was repeated until the test was completed.

A relief hole was installed 1.0 in. downstream of the levee toe in the center of the model. The centrifuge was again brought up to speed using the same gravitational-level increments. Once the model was at 12 *g* for about 5 min, the reservoir height was incrementally raised approximately every 5 min. The holes drilled in the outside wall of the reservoir were used to maintain a constant head at 2.0 in., 4.0 in., and 6.0 in. on the levee during the test.

3.3 Model 3

The third model was tested without a relief hole at 12 *g* and with the relief hole at both 12 *g* and 24 *g*. The head pressure on the levee was kept low (<2.0 in.) during the test without a relief hole. Again, it was assumed that this pressure was low enough to not cause model damage. Because the reservoir water height was not allowed to exceed the levee crest, the head on the levee could be increased only by raising the gravitational level to 24 *g*.

The model permeability was checked, and the water head set at the clayey sand-clay interface (6.0 in. above base of the upstream reservoir) before the start of each test sequence. The PPTs were zeroed, and the centrifuge was then brought up to speed in predetermined gravitational-level increments. The increments for the 12-*g* test were 2 *g*, 5 *g*, and 12 *g*, with the centrifuge staying at each level for several minutes. After the model stabilized at 12 *g* for about 5 min, the reservoir was slowly raised in 0.5-in. increments every 5 min. Once the reservoir water height reached 9.0 in. (2.0-in. head on the levee), the centrifuge was stopped.

The relief hole was placed in the center of the model 1.0 in. below the levee toe. The same startup procedure was followed as before. After the model was stabilized at 12 *g* for about 5 min, the reservoir height was raised in 0.5-in. increments every 5 min until a 2.0-in. head was attained. The holes in the reservoir were used to maintain a constant water head on the model. Once a 6.0-in. head was attained, the centrifuge was stopped and prepared for the 24-*g* test.

The same test procedure was followed for the 24-*g* test except the increments were 2 *g*, 5 *g*, 18 *g*, and 24 *g*. After the model was stabilized at 24 *g* for about 5 min, the reservoir height was raised in 0.5-in. increments every 5 min until a 2.0-in. head was reached. The holes in the reservoir were again used to maintain constant reservoir water levels during the test. Once the reservoir water height reached 13.0 in., the centrifuge was stopped.

4 Test Results and Discussion

Photographs of the post-analysis of the models are shown in Appendix A. All test data were tabularized and are in Appendix B. Data for each model run are shown in two tables where the first table contains the raw data and the second contains the analyzed data. Each PPT data point was taken at the start of a pressure increment. The analyzed data are presented and discussed during the discussion of each model run.

4.1 G-level scaling factor

Reservoir data from the 10-*g* and 20-*g* tests were compared to ensure the scaling factors were applied correctly. The reservoir water pressures that were measured during the 20-*g* tests were linearly scaled and compared to the 10-*g* data as shown in Figure 9. The data points represent incremental increases in the reservoir head pressure. The equations for each of the data curves are presented in Figure 9 and show close agreement. The results indicate that a linear scaling factor (measurement multiplied by the gravitational level) was applied correctly to compare the reservoir water heights at different gravitational levels.

Figure 9. Comparison of reservoir head pressures during 10-*g* versus 20-*g* tests (the 20-*g* test data were scaled for comparison purposes).

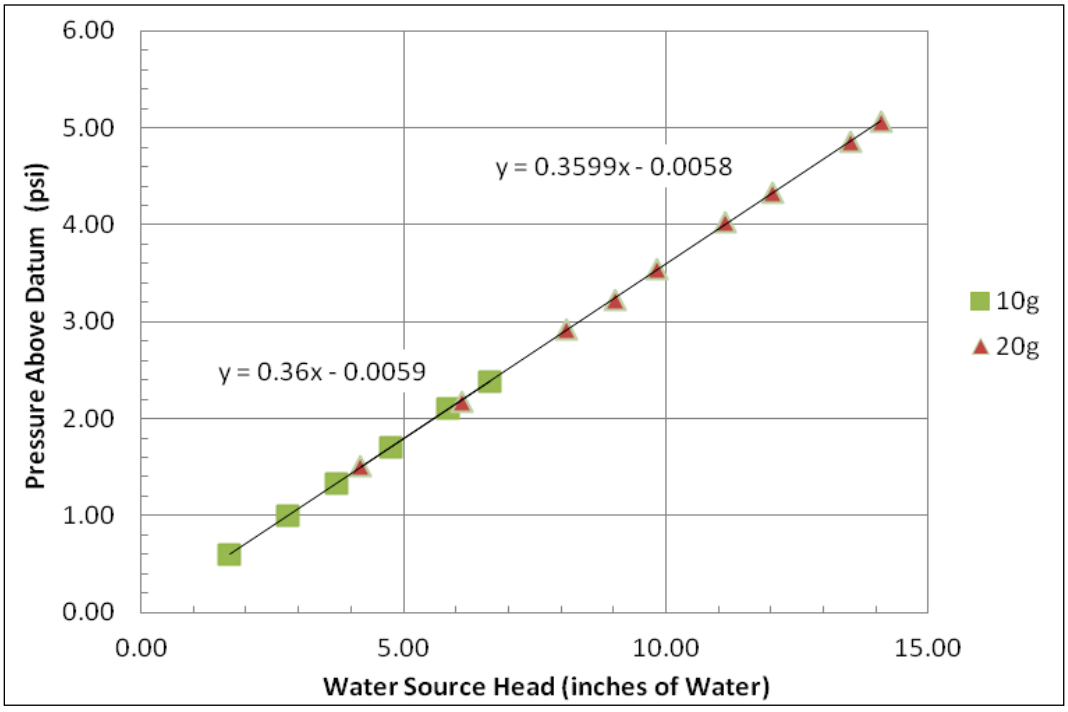

The influence of gravitational level on piping/erosion results are a concern (van Beek et al. 2010; Le et al. 2010; Garnier 1984). Even though the head pressure is known, the influence of gravitational level on piping results may not be known. Therefore, neither the results from Model 1 at 10 *g* and 20 *g* nor those from Model 3 at 12 *g* and 24 *g* were compared. Data from each test must be evaluated independently.

4.2 Model 1 at 10-*g* test

Figure 10 shows that as the upstream reservoir head pressure increases, the pore pressure measurement at each PPT decreases linearly as the downstream distance increases. PPTs 1 and 2 measured the reservoir water height as it was increased. For example, lower pore pressures were measured by PPT 5 and 6, which were 4.0 in. farther downstream than PPT 3 and 4. These lower pore pressures were caused by the loss in head pressure as the distance from the upstream reservoir increased. The magnitude of head pressure loss corresponds to a reduction in the measured pore pressure, thereby causing the slope of the PPT curves to flatten as their location downstream increases.

Figure 10. Response of pore pressure transducers (PPT) at top of sand layer versus increase in reservoir water head during the 10-*g* test.

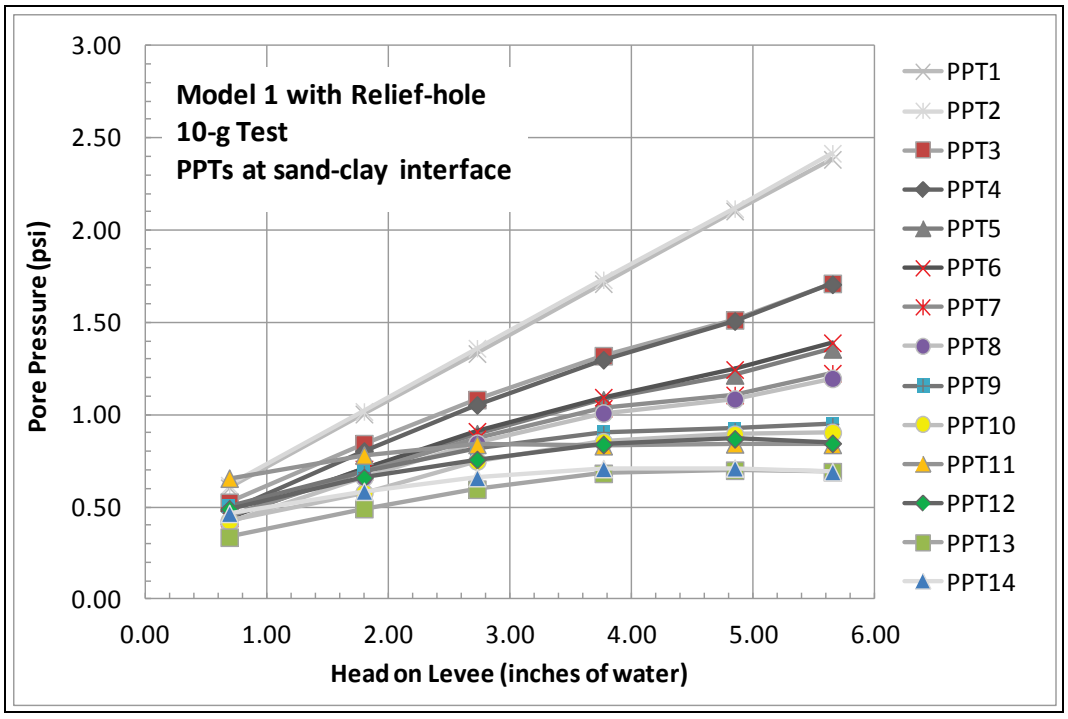

As long as the flow remains below the critical flow gradient, there is no particle movement, and the slope of the response curve remains linear. Once the gradient increased to a point at which a sand particle became buoyant and movement occurred, there was a corresponding slope change caused by a change in permeability and head loss at that location. Also, as piping progressed farther upstream under the levee, there was a change in pore pressure in the surrounding area recorded by the PPTs. The reduction in pore pressure was caused by the head pressure at the pressure relief hole being felt through the piped channel/area.

The first increment of head (0.7 in. on the levee) caused some sand particle movement in the relief hole. Particle movement was a result of the gradient being high enough to cause the surface particles to become buoyant. But the gradient was not high enough to cause sand particles that were locked into the matrix to move. The same particle movement occurred at a head of 2.0 in. on the levee but did not produce piping.

When the reservoir head was increased beyond about 2.7 in. on the levee, the slope of the response curves for PPTs 9-12 (Figure 10) tended to flatten, indicating a change in conditions. Note that PPTs 9 and 10 are 2.0 in. upstream of the relief hole. The slope change coincides with the appearance of sand in the fanned area of the relief hole. The amount of sand in the relief hole tended to accumulate to a point and then stop. The stoppage was because the reservoir head could not be kept at a constant level. The slope of other PPTs farther upstream started to flatten as the reservoir water level increased. The flattening in the slopes of the PPT response curves indicated that the gradient was high enough for piping to continue upstream under the levee. The slope of the response curves for PPTs 5-8 also showed a slope change when the head became greater than 3.7 in. on the levee. All PPT response curves flattened even more as the head is increased with the exception of PPTs 1, 2, 3, and 4. PPTs 1 and 2 were in the reservoir and unaffected by the piping event. In the case of PPTs 3 and 4, either the gradient was not high enough for the piping to progress to their location or the test was not run long enough for piping to reach them.

The response of PPT 9 is shown in Figure 11. When the head pressure at the sand-clay interface increased to 1 in., PPT 9 showed a corresponding increase in pore water pressure. The pore pressure continued to rise after the 1.0-in. head pressure was reached. The increasing PPT pressure with no head pressure increase indicated that the sand layer was either not fully saturated or the model was still consolidating under the 10-*g* force. Notice

that when the head pressure at the sand-clay interface increased to 2.0 in., the PPT was more responsive and correctly followed the decrease in reservoir water level. Also, note that the pore water pressure did not continue to increase linearly after the 2.0-in. head pressure but tended to flatten out. The slope of the response curve tended to remain constant after a 4.0-in. head was reached at the sand-clay interface. The flattening of the response curve indicated that piping/erosion may have started between the 2.0- and 3.0-in. head pressures but did not fully develop into a piping event until the 4.0-in. head pressure was recorded at the location of PPT 9, which was 1.0 in. upstream of the levee toe.

Figure 11. Pore pressure response to changes in *g*-level and upstream reservoir pressure levels (measured in inches of water) for PPT 9 (sand-clay interface) during 10-*g* test.

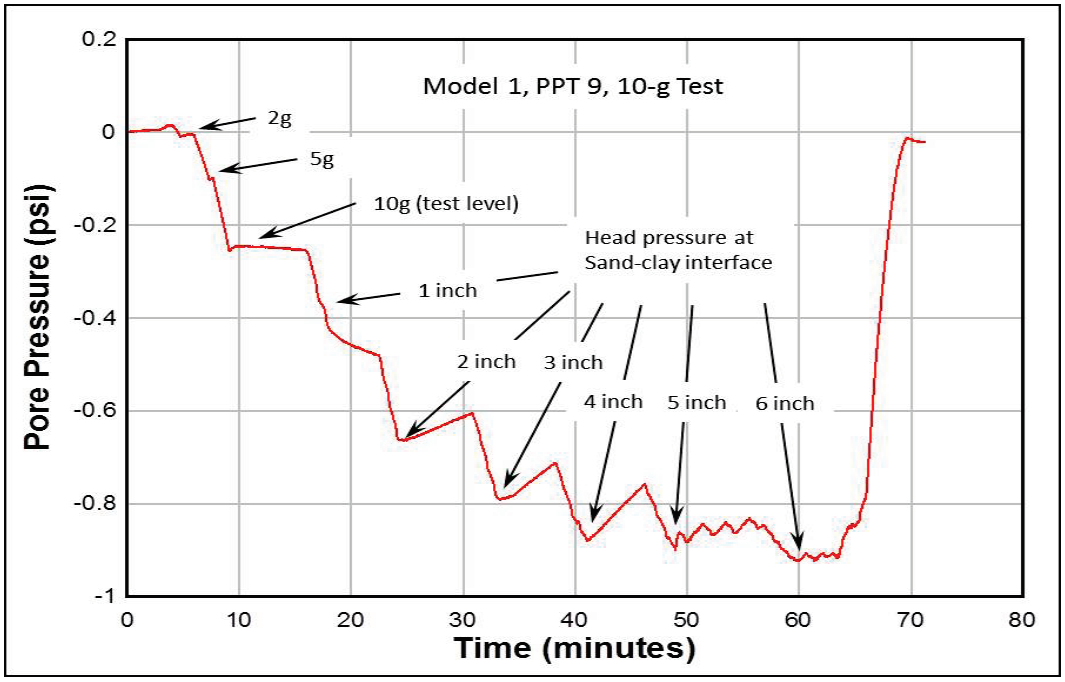

At the completion of the 10-*g* test, the centrifuge was stopped, and the model was checked for indications of piping. Figure 12 shows the accumulation of sand around the relief hole in the fanned depression area. Also note that sand particles collected on the top edge of the fanned depression area, indicating that flow was great enough to carry sand out of the depressed area away from the relief hole. The depressed area inside of the sand cone suggests that, as flow slowed down or stopped, the buoyant sand fell back into a void below the relief hole. In addition, the depression in the sand cone suggests that the relief hole grew in diameter. Based on the depression, the diameter of the relief hole appears to have eroded from its initial diameter of 0.35 in. to between 0.75 and 1.0 in. in diam.

Figure 12. Sand piped from the relief hole in Model 1 and collected in fanned area during the 10-*g* piping test. Photograph was taken at the end of the 10-*g* test.

Excess water tended to accumulate on the clay surface downstream of the relief hole, making in-flight observations difficult during the 10-*g* test. Figure 12 shows the water level on the downstream surface to be halfway up the clay berms of PPTs 11 and 12 (approximately 0.25 in.). Therefore, before conducting the 20-*g* test, two channels were formed in the clay surface downstream of the levee. Figure 13 shows the channels in the clay surface between the relief hole and the downstream reservoir. These channels provided a direct drainage path for water exiting the relief hole and thereby prevented the clay surface from being inundated during testing and obscuring view of the area around the relief hole.

4.3 Model 1 at 20-*g* test

The reservoir water height was lowered to the base of the levee (7.0 in. from the base of upstream reservoir) and allowed to come to equilibrium before conducting the 20-*g* test. The model was brought up to the 20-*g* level in stages to allow the model to come to equilibrium and to ensure that instrumentation was working correctly. Figure 14 shows that the PPTs in the reservoir increased linearly as the water level was raised. The first three head pressures were in 0.5-in. increments. The head pressure increment was then changed to 0.25 in. so model behavior could be observed under smaller head pressure changes.

Figure 13. The water drainage channels constructed from the relief hole to the downstream reservoir to prevent in-flight inundation of the downstream surface of the model. Photo was taken before the start of the 20-*g* test.

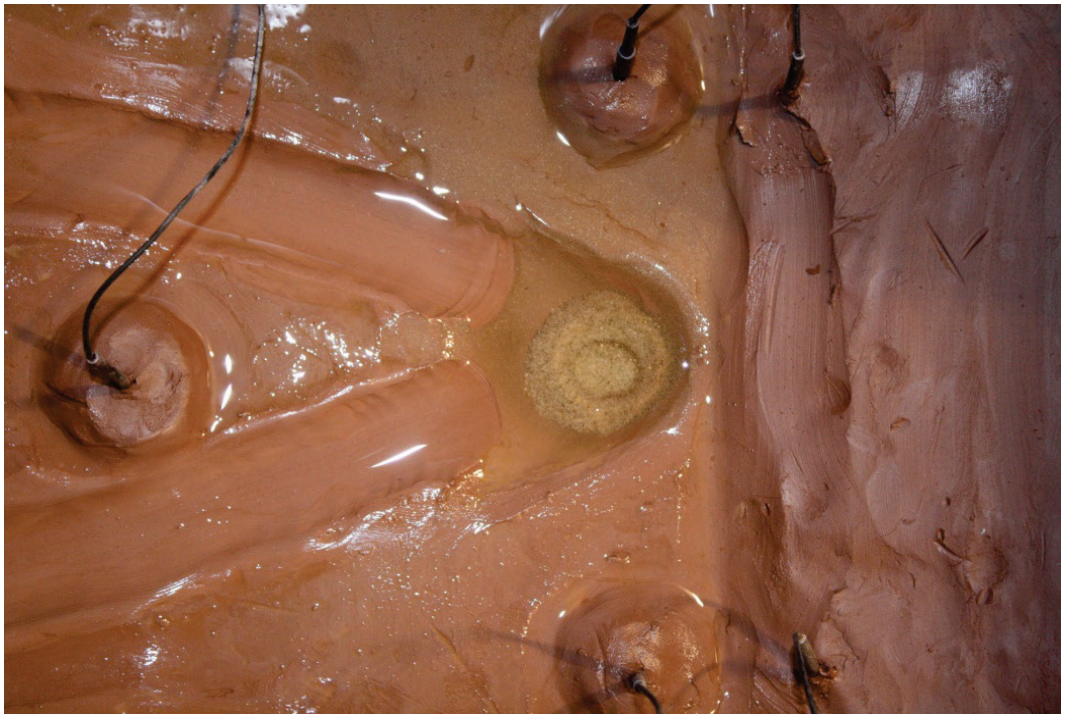

Figure 14. Pore Pressure response in upstream reservoir as reservoir head pressure is increased.

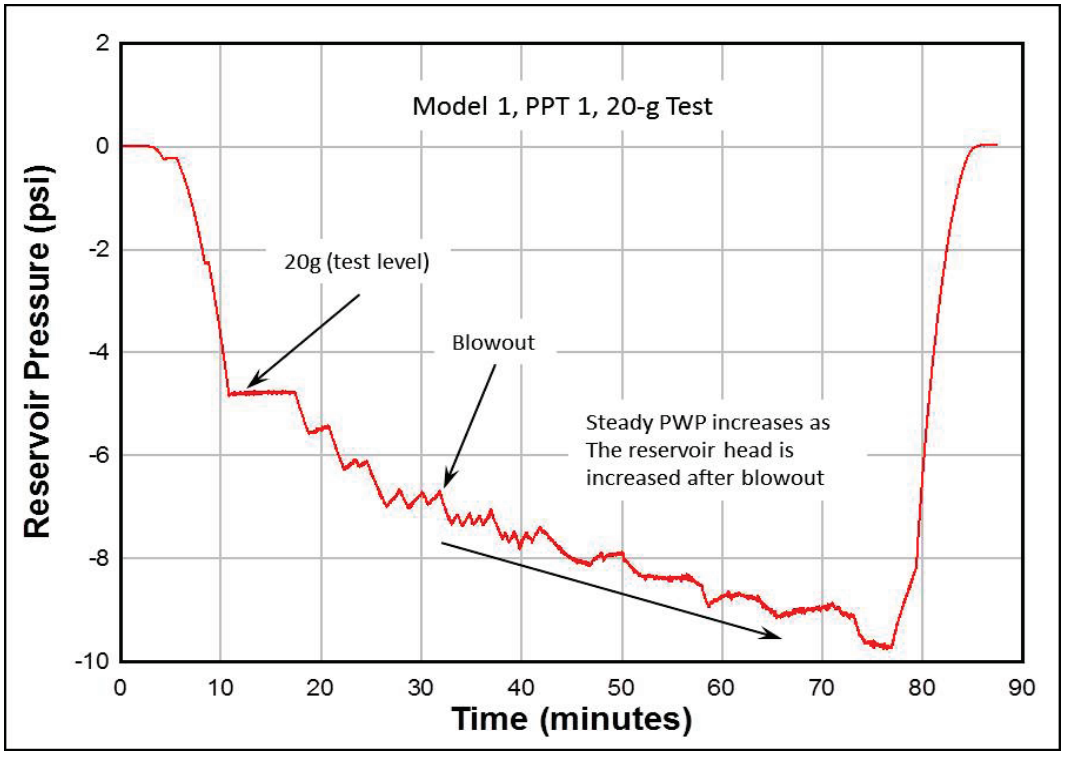

The flattening of the response curve for PPT 9 during the 10-*g* test was observed at about 2.5 in. of head pressure (Figure 10). Figure 15 shows that the response curve of PPT 7 plateaus at an equivalent head pressure of 3.5 in. The flattening of the curve corresponded to a blowout of clay and sand from the relief hole when the pressure head on the levee was increased to 3.5 in. The blowout also indicates that the piping channel reached PPT 7, which is 5.0 in. upstream of the levee toe and 6.0 in. upstream of the relief hole. Increasing the reservoir water height did not increase the pore pressure at the PPT 7 location.

Figure 15. Pore water pressure response at PPT 7 (sand-clay interface) location as upstream reservoir pressure head is increased during 20-*g* piping test.

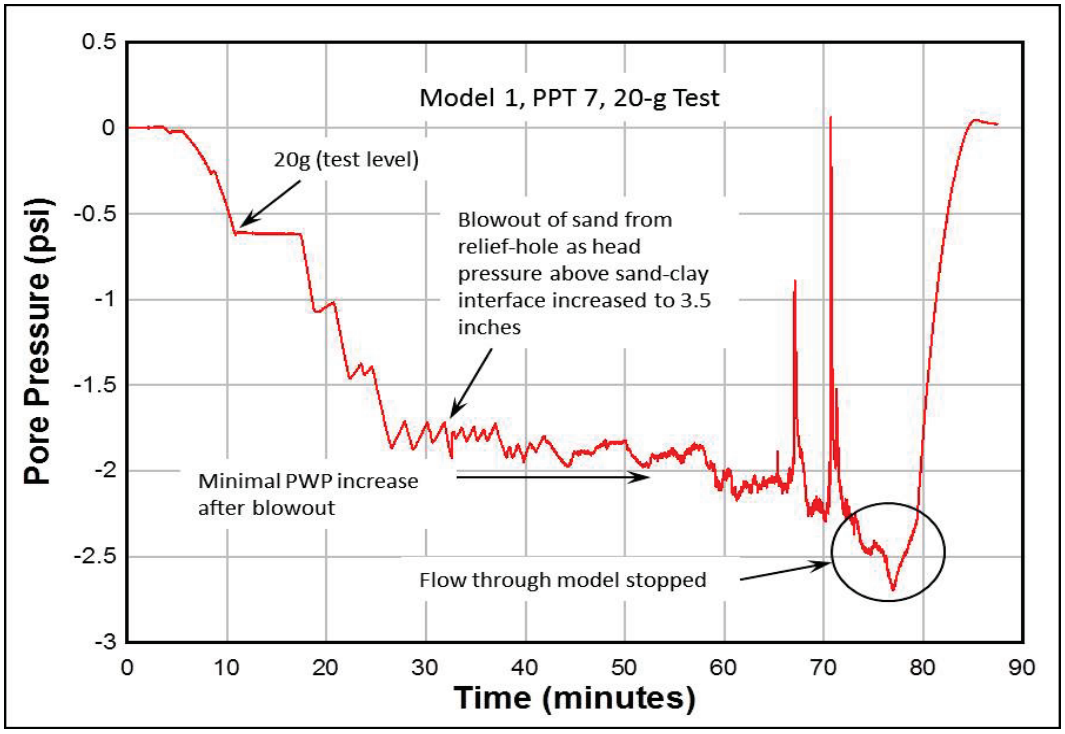

All PPT curves for the 20-*g* test are shown in Figure 16. The pore pressure response curves for PPTs 3-14 did not flatten until after a 3.0-in. head was felt on the levee -- the maximum head pressure felt on the model during the 10-*g* test.

More sand was seen being expelled from the relief hole as the water head on the levee was increased past 3.0 in. and continued until conclusion of the test. Figure 17 shows the expelled sand and the increased size of the sand depression in the relief hole. The sand depression had increased to about 1.5 in., and the sand now covered the relief hole and toe of the levee and extended past PPT 13.

Figure 16. Response of pore pressure transducers (PPT) at top of sand layer versus increasing reservoir water head during the 20-*g* test.

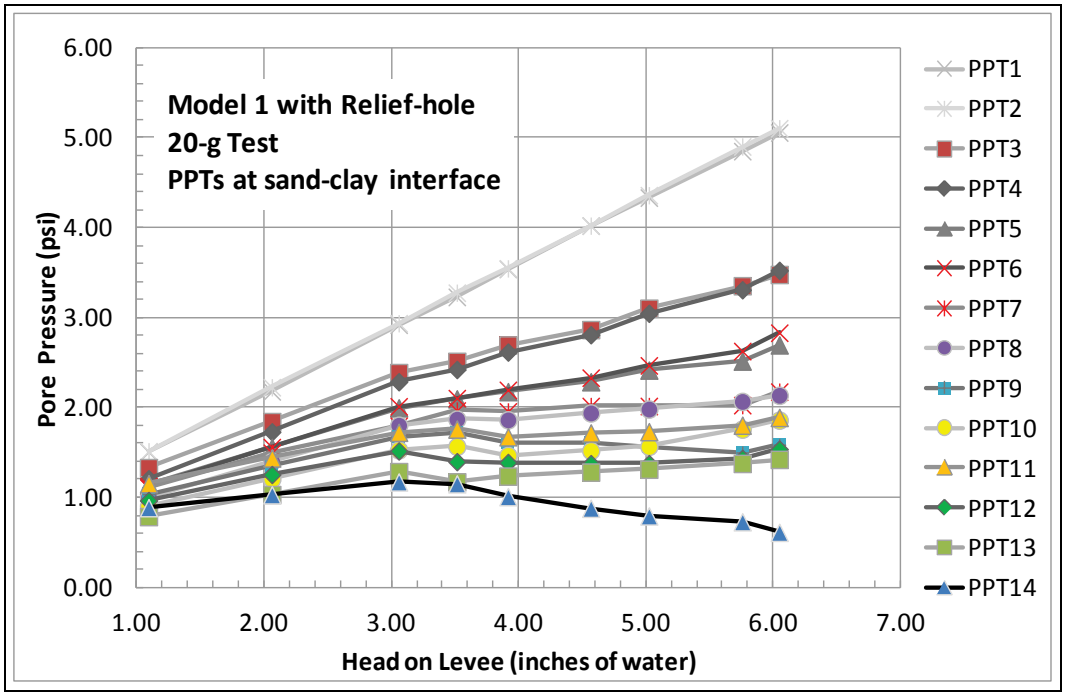

Figure 17. Sand piped from relief hole and overflowing fanned area after completion of the 20-*g* piping test for Model 1.

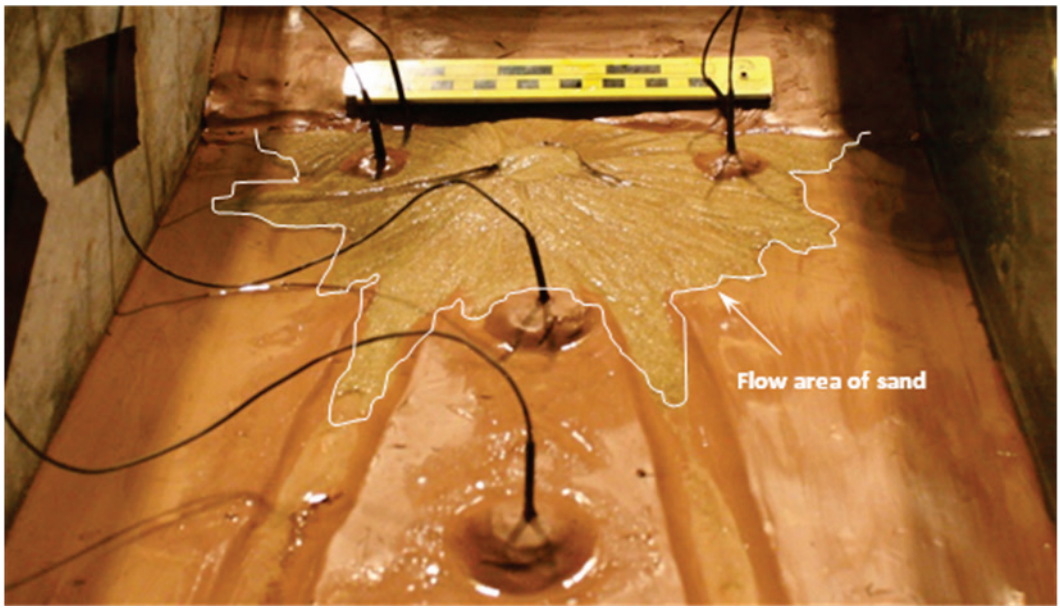

When the 6.0-in. head on the levee was reached, the flow through the model was high enough that the reservoir charge rate could be matched to the model flow rate, thereby keeping a constant 6.0-in. head until test completion. After about five minutes, all flow from the relief hole stopped (Figure 15).

4.4 Post analysis of Model 1

Figure 17 shows the large amount of sand that was expelled from the relief hole. The sand was carefully spooned from the surface of the model and placed in a tare can for drying. It was estimated that about 90% of the piped material was collected, dried, and weighed. The dried sand weighed 205 grams.

The model was carefully disassembled to see if ruminates of piping under the levee could be ascertained. The levee and all the PPTs were slowly removed, leaving the 1.0-in. clay layer covering the sand. The model's clay layer was then vertically sliced parallel to the upstream and downstream axis of the model. Each slice was about 3.0 in. wide and 12.0 in. long. Disturbance of the sand layer was checked during the removal of each slice. No sand seemed to adhere to the clay as it was removed. In some areas, the vertical cut through the clay layer penetrated into the sand layer, leaving a knife mark in the sand surface (Figure 18). Other than the knife cuts, there was minimal damage or disturbance of the sand-clay interface.

Figure 18. Erosion pattern at the sand-clay interface after the 20-*g* piping test.

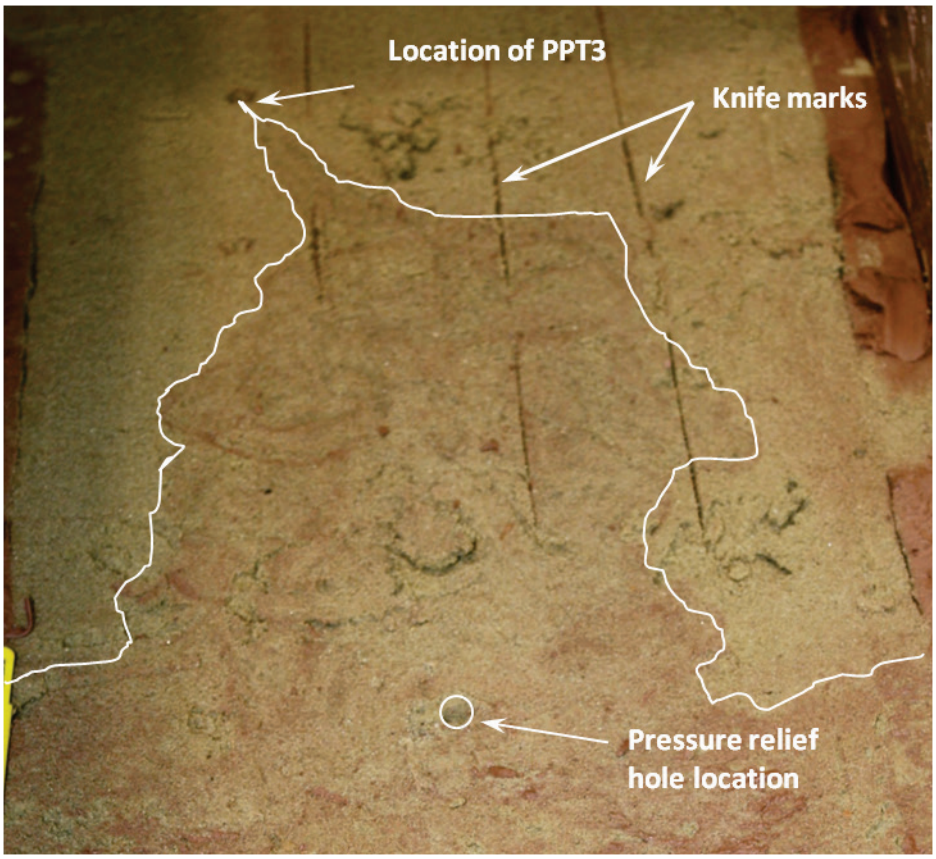

Inspection of the sand-clay interface showed that the red clay had stained the sand. It is thought that high flow rates from piping may have caused the clay under surface to erode, thereby staining the sand. The stained area and the relief hole are outlined in Figure 18. It is impossible to definitively state that there was a piping channel because the staining tends to be under a large area of the levee. However, piping/erosion would normally initiate at the relief hole and erode back toward the water source. If an eroded channel/pipe did exist, it would have traveled back toward the upstream reservoir. Once the erosion channel was fully formed, the channel could have slowly spread under the levee creating the eroded surface that was found. The erosion surface may have started in a channel that ended at or near PPT3. The amount of sand expelled through the relief hole must have come from a large surface area; otherwise, a channel would have been obvious.

The depth of the eroded surface can be estimated if it is assumed that the eroded area covered about half of the levee footprint (Figure 18) and by knowing the volume of material removed. An estimated volume can be calculated by using the initial dry density of the sand and the dry weight of sand removed. Based on this calculated volume, an estimated overall depth of the eroded surface was calculated to be 0.1 in. Based on this depth, it is easy to see why the eroded area could be hard to visualize and/or determine.

The final part of the post analysis was to identify if erosion occurred with depth in the sand layer. The sand was slowly removed in vertical slices that were perpendicular to the upstream and downstream axis of the model. Each slice was approximately 1.0 in. thick and about 6.0 in. wide, covering the center portion of the model where it is thought that erosion took place. After each slice, a photograph was taken of the sliced surface for documenttation and further analysis. Figure 19 shows no erosion occurring with depth.

The relief hole was removed from the model in a 4.0-by-4.0-in. section and examined for any obvious dimension changes. Figure 20 shows that the relief hole eroded to about triple its initial size (1.0 in. versus 0.35 in.). It can also be seen that the edges of the hole did not retain the initial circular feature but eroded into an irregular shape. An uneven gradient around the hole may have caused the non-uniform shape and could indicate where the erosion channel may have been concentrated.

Figure 19. Sand foundation of Model 1 vertically sliced to determine if there was any piping with depth.

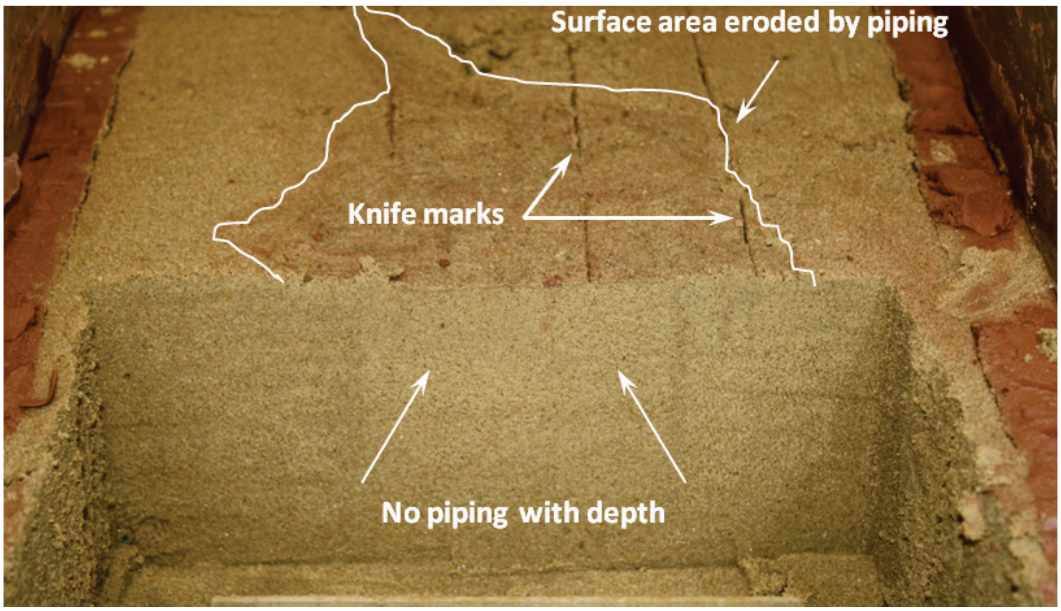

Figure 20. Pressure relief hole increased in size from 0.35 in. to approximately 1.0 in. after completion of the 20-*g* piping test of Model 1.

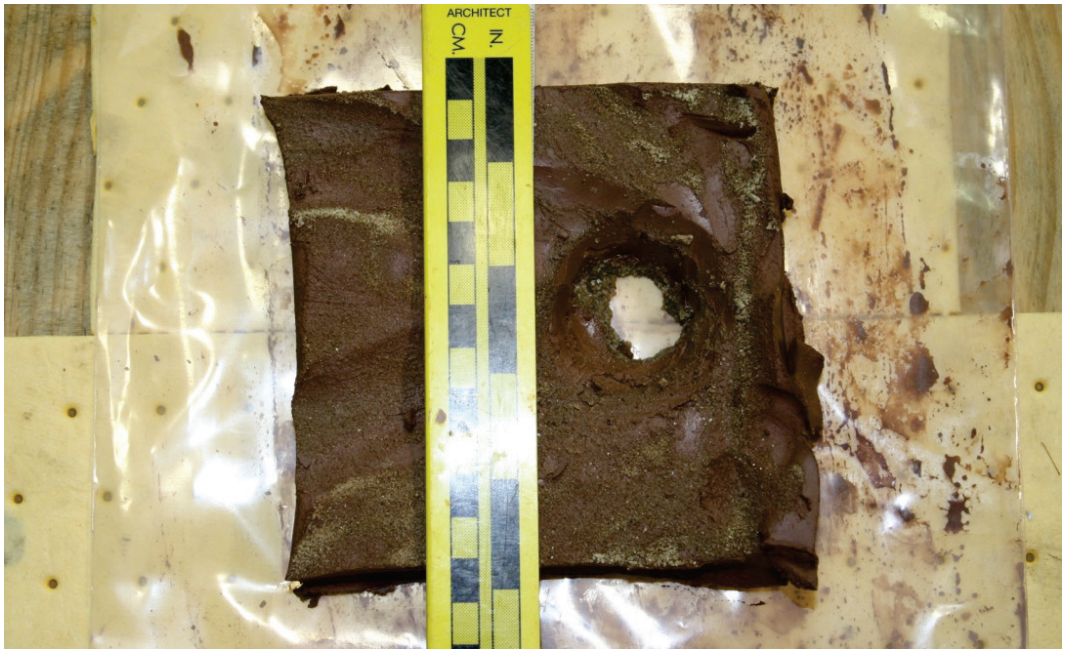

4.5 Model 2 at 12-*g* test

4.5.1 Test with no relief hole

Model 2 was first run without a pressure relief hole to evaluate its influence on the model. Figure 21 shows the response of PPT 2 to increases in the

gravitational level and reservoir water level. The response of PPT 2 to pressure changes is crisp and shows no sign of sluggishness. Figure 22, on the other hand, shows that PPT 7 responds immediately to a change in gravitational level but slowly loses some of the induced pore pressure. The reduction in pore pressure can be attributed to air trapped under the upper clay layer during model construction, which may have produced an unsaturated sample. Figure 22 also shows an increase in the responsiveness of PPT 7 as the gravitation level is increased. Increasing the gravitational level causes the model to consolidate, which reduces the unsaturated pore volume.

The initial reservoir water height was 6.0 in. It should be noted that flow through the model cannot occur until a reservoir water height of 7.0 in. is reached. Therefore, without flow through the model, the likelihood of air being in the gap between the sand and the upper clay layer is high. Figure 22 shows that PPT 7 reacts slowly to the 0.5-, 1.0-, and 1.5-in. head pressure increases. The slow response is another indication that the model is not completely saturated. However, once the head pressure reaches 1.5 in., a sharper response is seen indicating that the model achieved a higher saturation at the PPT 7 location.

Figure 21. Reservoir head pressure at sand-clay interface (measured in inches of water) response to increasing gravitational level and changes in upstream reservoir water level.

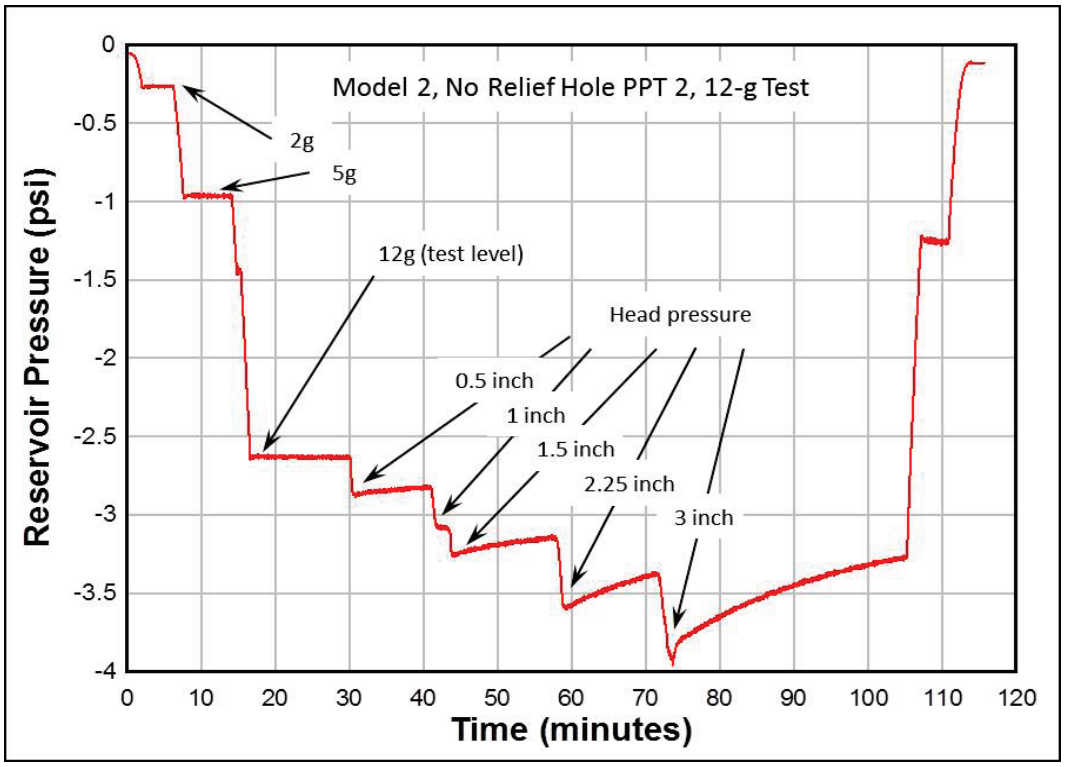

Figure 22. Measured pore pressure at PPT 7 (sand-clay interface) when the upstream reservoir water level is increased.

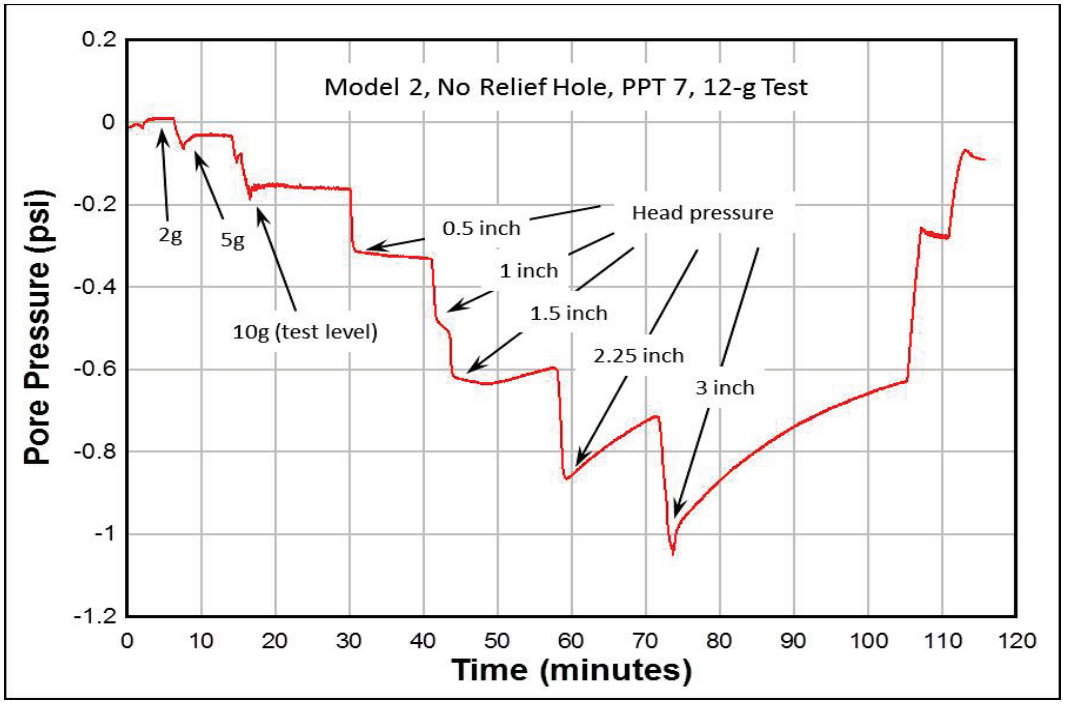

Figure 23 compares the reservoir PPTs to the response of PPTs downstream. The downstream PPTs have the same slope as PPT 1 and 2 below a head pressure of approximately 1.5 in. Theoretically, the downstream PPTs should have a different slope once flow through the model occurs (shown in Chapter 6). Because the model was only run for 15 min between the 1.0- and 2.25-in. increments, there may have been insufficient time for steady-state flow to develop.

4.5.2 Test with relief hole

A pressure relief hole was inserted into the model at the end of the first centrifuge run. The hole was placed in the center of the model 1 in. downstream of the levee toe. The area around the relief hole was scraped out in the shape of a fan to a depth of about 0.75 in. Two channels were scraped into the clay top layer from the relief hole to the downstream reservoir. These channels were located on both sides of PPTs 13 and 14.

Not being able to maintain a constant reservoir water height during the running of Model 1 and the initial run of Model 2 made interpretation of the test data difficult. Therefore, two holes were drilled into the outside of the upstream reservoir, one at 9.0 in. and the other at 11.0 in. above the base of the model allowing for a constant water head on the levee at

Figure 23. Response of pore pressure transducers (PPT) at top of sand layer with increasing reservoir water level without influence of relief hole during the 12-*g* test.

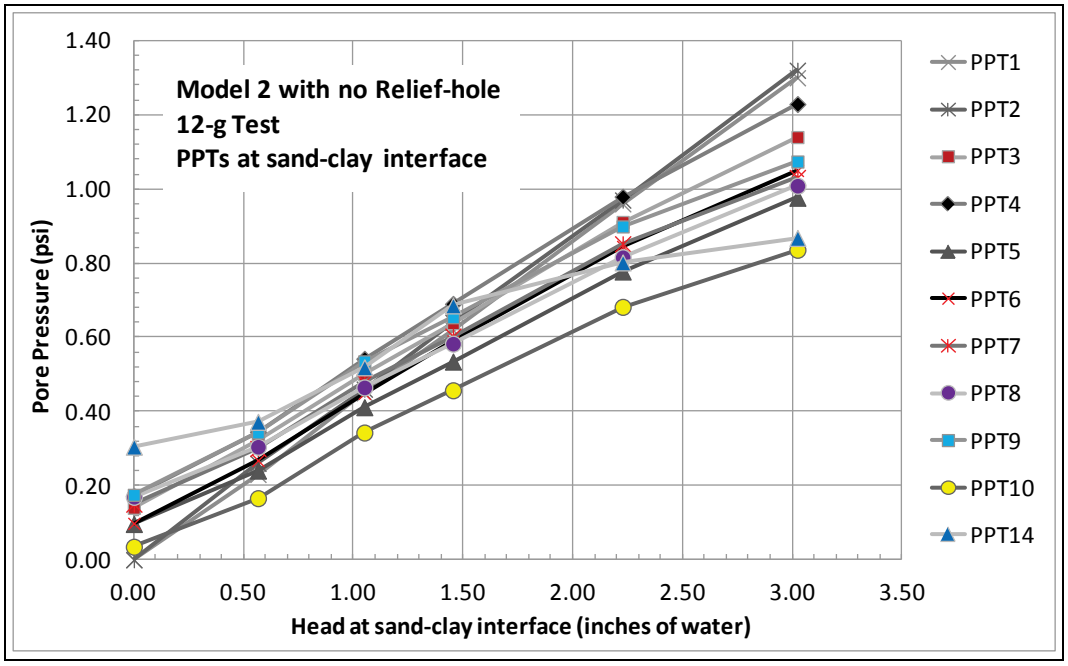

heights of 2.0 and 4.0 in., respectively. The reservoir water height was set at the sand-clay interface (6.0 in. from base of model), and the PPTs were zeroed. The model was incrementally brought up to the 12-*g* level and allowed to stabilize for 5 min before the reservoir height was raised.

The relief hole was closely monitored for any sand movement as the reservoir height was increased to a 2.0-in. head on the levee (9.0 in. from base of model). The hole that was placed in the reservoir at the 9.0-in. level allowed a constant pressure head on the model. No sand movement was observed while the pressure head was held constant for 10 min. After the 10-min interval, the centrifuge was shut down, and the hole at the 9.0-in. level was plugged. The reservoir level could now be raised to the 11.0-in. level. Each time the centrifuge was stopped, the reservoir height was brought back to 6.0 in., and all downstream PPTs were re-zeroed.

The centrifuge was brought back up to the 12-*g* level after plugging the reservoir hole at the 9.0-in. level and stabilized for 5 min. The reservoir height was then raised in 0.5-in. increments while the relief hole was monitored for sand movement. A small amount of sand movement was observed at a 3.0-in. head on the levee (10.0 in. from the base of the model). It was observed that sand movement would stop as the head pressure slowly fell below this level and would begin each time this

pressure head was reached. When the head reached 4.0 in. above the levee (11.0 in. from the model base), the hole in the reservoir wall allowed the head pressure to be held constant. The constant head pressure was maintained for 30 min. Figure 24 shows a decrease in the pore pressure at PPT 7 even though the head pressure remains constant. The decrease in pore pressure may indicate the occurrence of piping in the foundation and the formation of a channel under the levee. After 30 min, the centrifuge was stopped and the reservoir hole at the 11.0-in. level was plugged. An additional hole was drilled at the 13.0-in. level so that a constant head could be maintained at that level.

Figure 24. Measured pore pressure at PPT 7 (sand-clay interface) when the upstream reservoir water level was increased to constant heads of 2.0 and 4.0 in. on the levee.

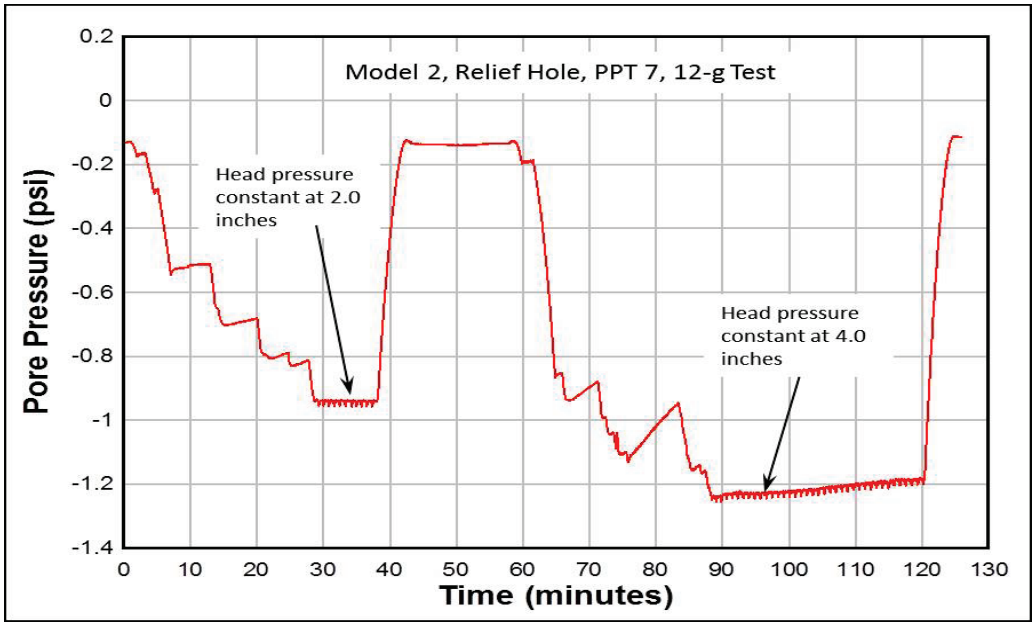

The centrifuge was brought back up to the 12-*g* level and allowed to stabilize for 5 min. The reservoir height was then increased in 0.5-in. increments while the relief hole was monitored for sand movement. It was visually observed that sand movement resumed when the head on the levee reached 3.0 in. PPT 7 showed virtually no increase in pore pressure after a 4.0-in. head on the levee was reached (Figure 25). The lack of pore pressure at PPT 7 may suggest that a seepage channel has reached this location under the levee.

The reservoir was brought up to a head pressure of 6.0 in. (13.0 in. from the base of the model). Piping (sand movement) continued as the reservoir water level was raised. Figure 25 also shows a noticeable drop in the pore

pressure at PPT 7 when a 6.0-in. head on the levee was reached. The pore pressure drop could mean that the piping channel has completely developed. After the initial drop, the pore pressure at PPT 7 remains relatively constant until the test ended. Other PPTs under the levee showed a similar response (Figure 26), which supports the conclusion that a piping channel developed.

Figure 25. Measured pore pressure at PPT 7 (sand-clay interface) when the upstream reservoir water level is increased to 6 in. on the levee.

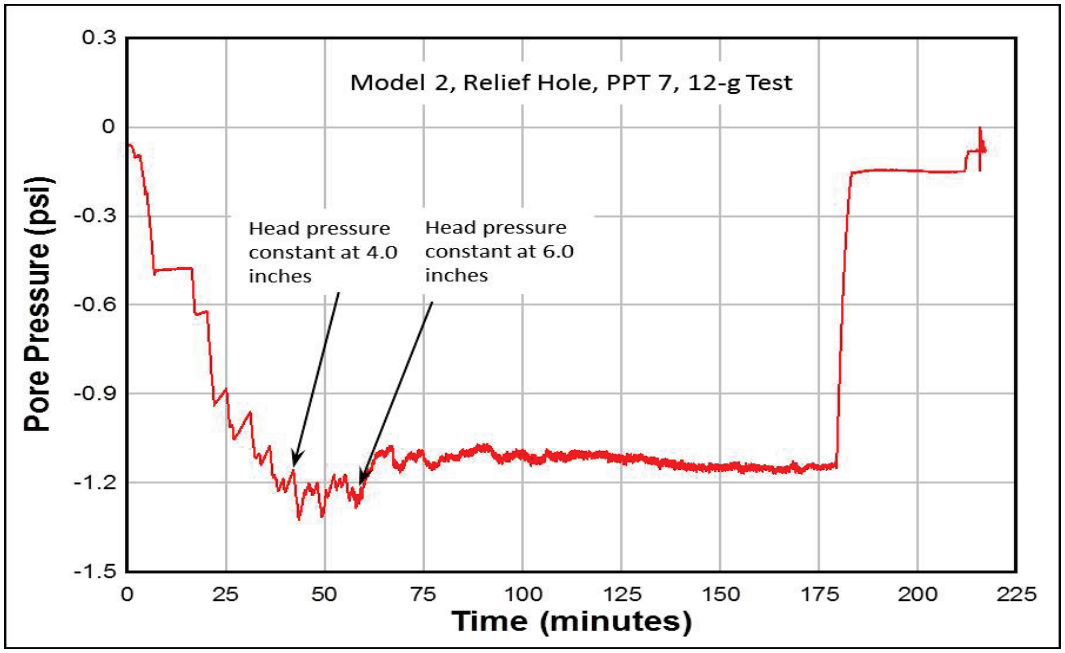

Figure 26. Response of Pore Pressure Transducers (PPT) at top of sand layer with increasing reservoir water head during the 12-*g* test.

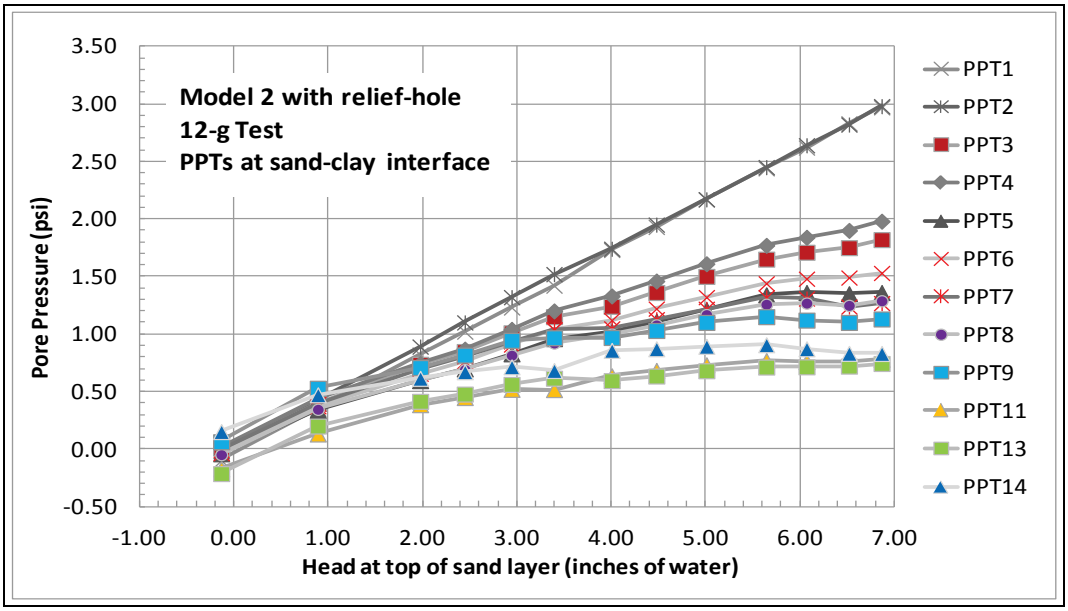

Figure 27 shows the relief hole at the conclusion of the Model 2 test. Sand has flowed from the relief hole and covered an area down to PPT 13. The sand in the hole had collapsed back into a subsurface void under the top clay layer. In addition, the hole appears to have increased from 0.35-in. diam to 1.0-in. diam.

Figure 27. Sand piped from relief hole and a view of an overflowing fanned area after testing Model 2 at 12 *g*.

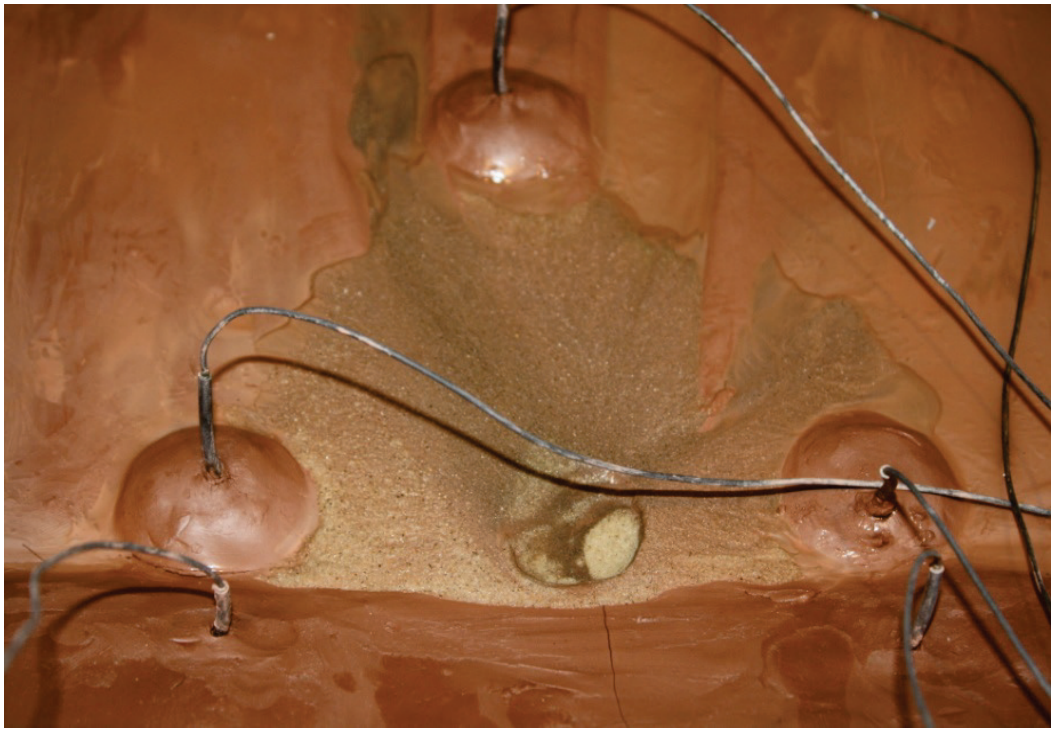

4.6 Post analysis of Model 2

Model 2 was carefully disassembled at the completion of the test to see if evidence of a piping channel could be found. The levee and all the PPTs were carefully removed leaving the 1.0-in. clay layer covering the sand. The model's top clay layer was sliced and removed as was for Model 1. Care was taken to ensure that the knife blade did not penetrate the clay layer as it did on Model 1 (Figures 18 and 19). The sand layer was checked for disturbance during the removal of each clay slice. No sand seemed to adhere to the clay, making its removal easy. Figure 28 shows ridges in the sand that indicate the junction between each clay piece used to form the top clay layer of the model. These ridges did not appear in Model 1 and could be caused by excess water on the sand surface when the clay layer was placed.

Figure 28. Erosion patterns are visible along with ridges in the sand. The ridges were formed at the intersection of clay pieces that form the top clay layer of the foundation.

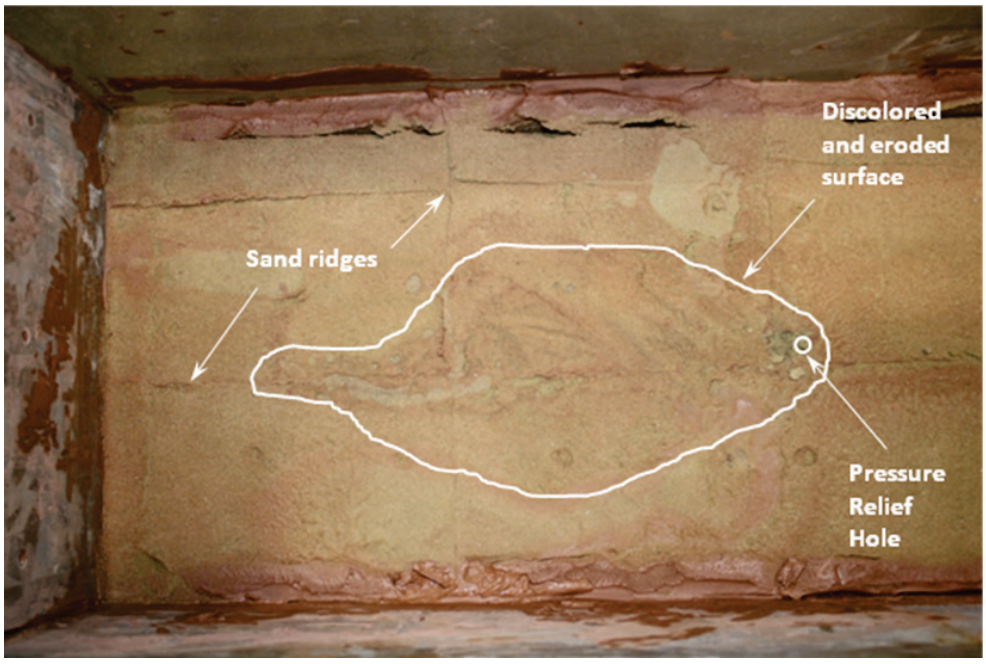

Further inspection of the sand-clay interface showed that the red clay had stained the sand in high flow areas. Similar staining of the sand was seen in Model 1. The flow rates were lower relative to those in Model 1, but the sand was stained never the less. The stained area and the relief hole were outlined for easier identification in Figures 28 and 29. There were multiple erosion patterns visible on the sand surface, but not all areas outlined showed the formation of an erosion channel (Figure 29). The center area contained a possible erosion channel that seemed to follow one of the clay edge junctions. There may have been a small gap at the sand-clay interface allowing water to flow through this gap. The denser sand foundation and the possible gap at the interface may have contributed to the higher head needed to cause movement/piping of the sand. After inspection of the sand-clay interface, the sand was slowly removed in vertical slices, as in Model 1, from the downstream reservoir in the upstream direction. Each slice was approximately 1.0 in. thick and about 6.0 in. wide, covering the center portion of the model. After each slice, a photograph was taken of the sliced surface for documentation and further analysis. Figure 30 shows a visible erosion channel in the top of the sand layer. The channel appeared to be about 0.125 to 0.25 in. deep. Close examination of the slices taken from the foundation showed that no erosion/piping occurred with depth.

Figure 29. Erosion patterns at the sand-clay interface after testing Model 2 at 12 *g*.

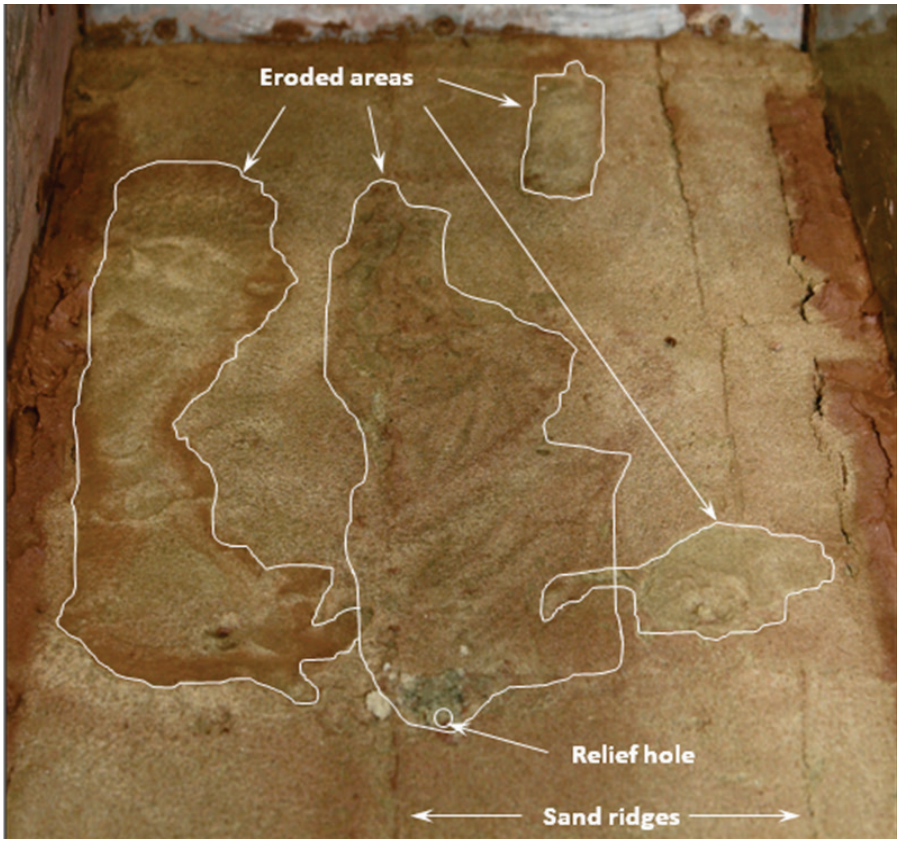

Figure 30. Sand foundation of Model 2 vertically sliced to determine if there is any piping with depth.

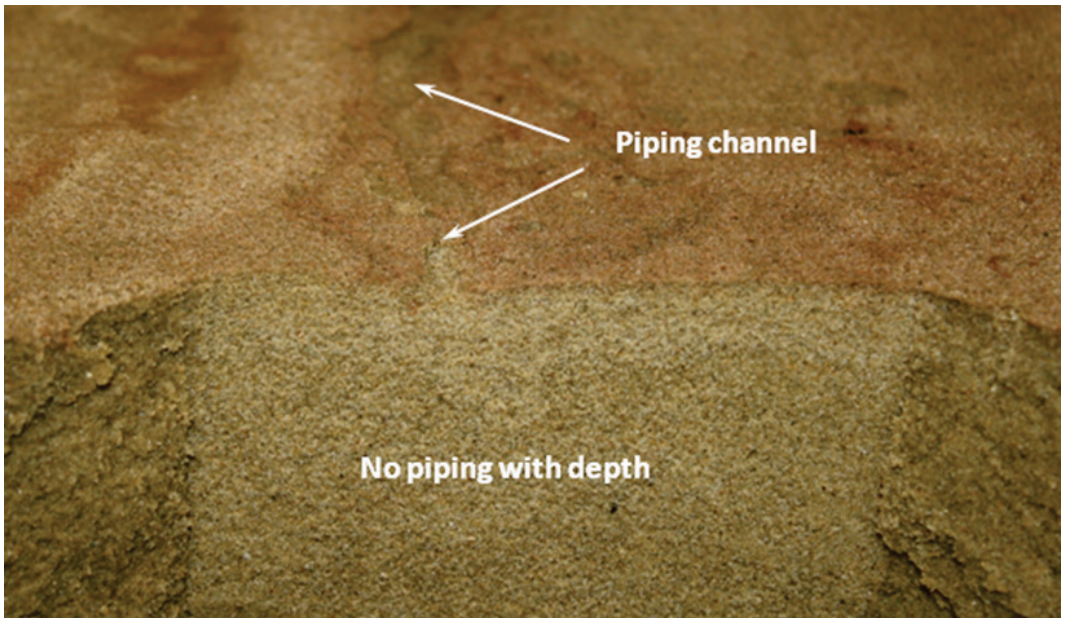

The relief hole was removed from the model in a 4.0-in.-by-5.0-in. section and examined for any obvious dimension changes. Figure 31 shows that the relief hole eroded irregularly and elongated in the downstream direction. The hole measured about 1.0 in. wide by 1.3 in. long versus the original 0.35-in. diam. The elongation of the hole in the downstream direction may indicate that flow from the hole may have been greater than initially thought.

Figure 31. Pressure relief hole increased in size of from 0.35 in. to approximately 1.25 in. after testing Model 2 at 12 *g*.

4.7 Model 3 at 12-*g* test

4.7.1 Test with no relief hole

The initial water height in the upstream reservoir was set at 6.0 in. and all downstream PPTs were zeroed. PPTs 3, 5, 7, 9, and 11 were located at the sand-clayey sand interface, which is 5.0 in. from the base of the model.

PPTs 4, 6, 8, 10, and 12-14 were located at the clayey sand-clay interface at 6.0 in. from the base of the model. It should be noted that flow through the model cannot occur until a reservoir water height of 7.0 in. is reached. Therefore, without flow through the model, the likelihood of trapped air in the sand-clayey sand and clayey sand-clay interfaces is high.

Model 3 was first run without a pressure relief hole to evaluate its influence on pore pressure response in the model. Figure 32 shows the response of PPT 1 to increases in the gravitational level and reservoir level.

Figure 32. Reservoir head pressure response to increasing gravitational level and changes in upstream reservoir water level.

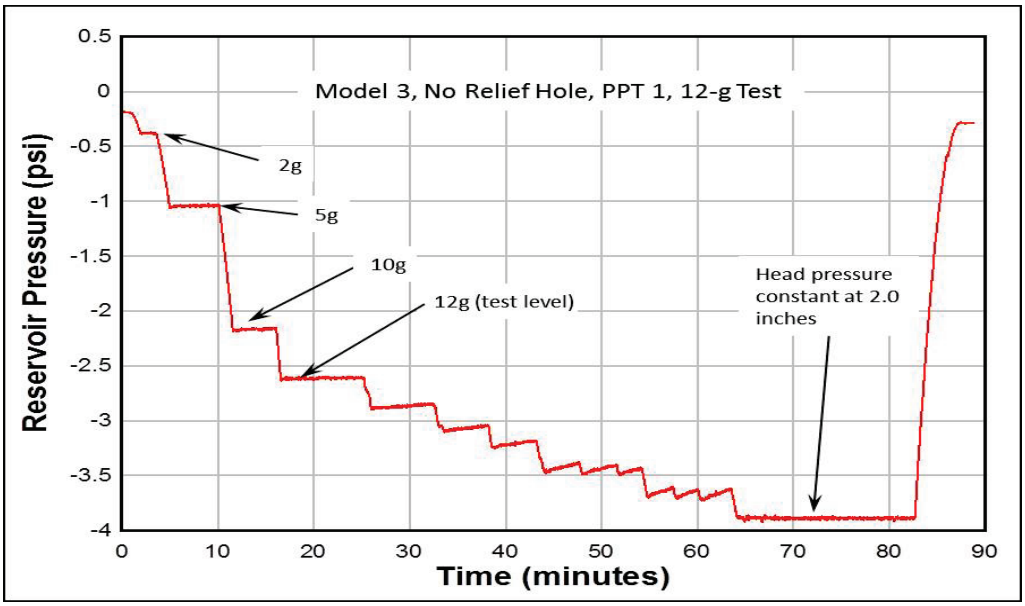

The response to both gravitational level and changes in water level are sharp and show no signs of sluggishness. Figure 33, on the other hand, shows that PPT 7 responds immediately to a change in gravitational level but slowly loses some of the induced pore pressure. The reduction in pore pressure could be attributed to an unsaturated model. This supports the idea that air may have been trapped in the soil interfaces during model construction. Figure 33 also shows an increase in the responsiveness of PPT 7 with increasing gravitational level. Increasing the gravitational level causes the model to consolidate, thereby reducing the unsaturated pore volume.

Figure 33 also shows that PPT 7 reacts slowly when the reservoir water level was changed from 6.5, 7.0, and 7.5 in. The slow response is another indication that the model was not completely saturated. However, once the water level reaches 7.5 in., a sharper response is observed indicating that the model has achieved a higher saturation at the PPT 7 location.

Figures 34 and 35 compare the reservoir PPTs to the response of PPTs downstream. The PPTs shown in Figure 34 are located at the sand-clayey sand interface, which is 5.0 in. above the model base. The PPTs shown in Figure 35 are located at the clayey sand-clay interface, which is at 6.0 in.

above the model base. The downstream PPTs have the same slope as PPT 1 for heads below 2.0 in. but deviate from this slope as the head is increased. Theoretically, this makes sense because flow through the model does not start until the reservoir water level exceeds 7.0 in. (2.0-in. head on the levee). The PPTs show a linear decrease in pore pressure measurements as their downstream location increases because of head loss.

Figure 33. Measured pore pressure at PPT 7 (sand-clayey sand interface) when the upstream reservoir water level is increased to a constant head of 2 in. on the levee.

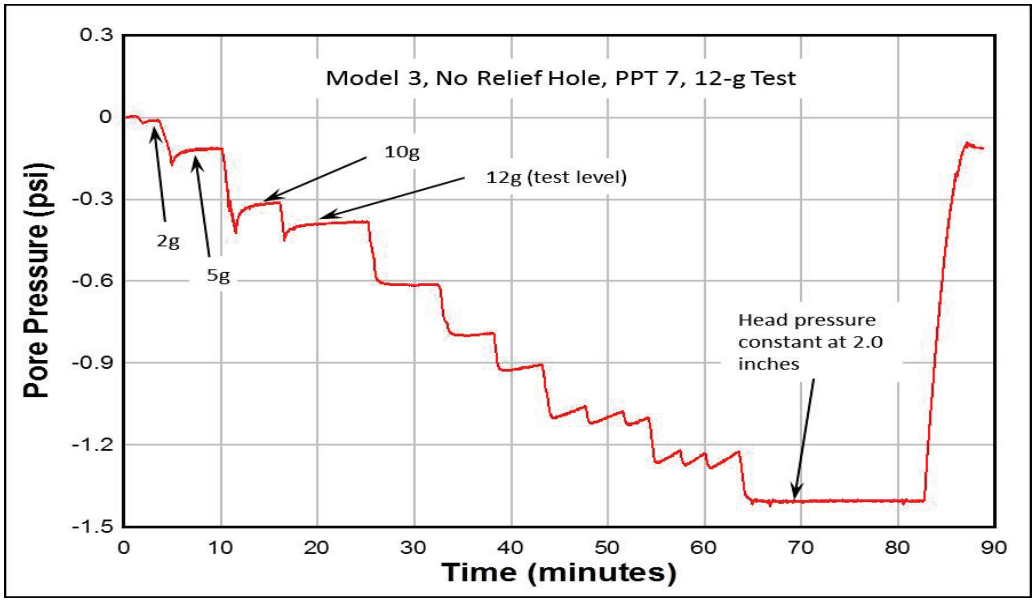

Figure 34. Response of pore pressure transducers (PPTs) at sand-clayey sand interface to increasing water level in the upstream reservoir without presence of relief hole at 12 *g*.

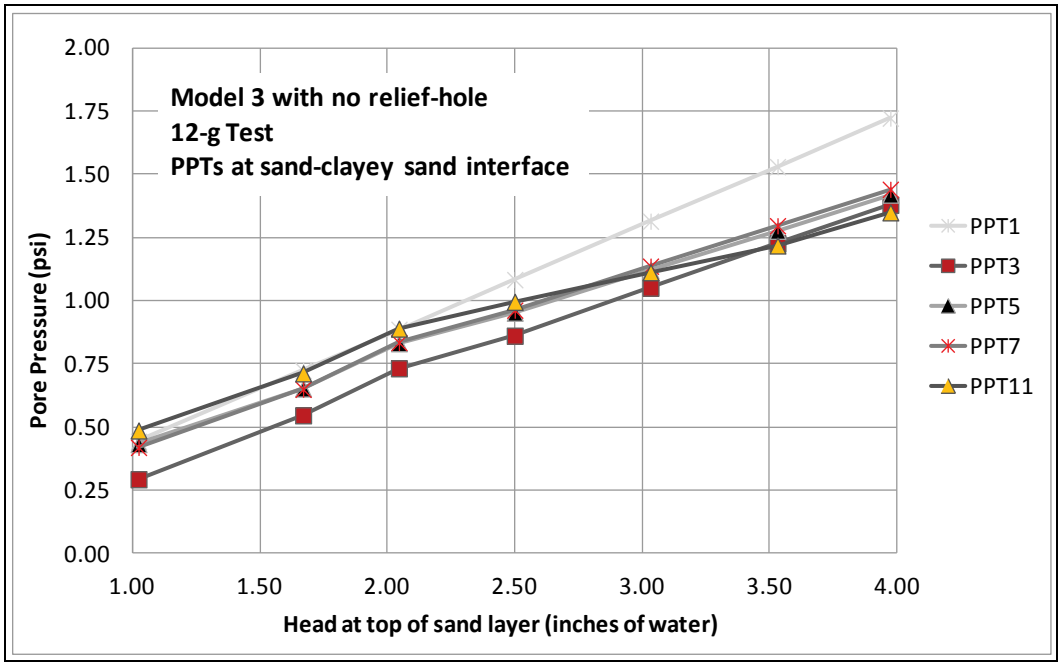

Figure 35. Response of pore pressure transducers (PPTs) at clayey sand-clay interface to increasing water level in the upstream reservoir without presence of relief hole at 12 *g*.

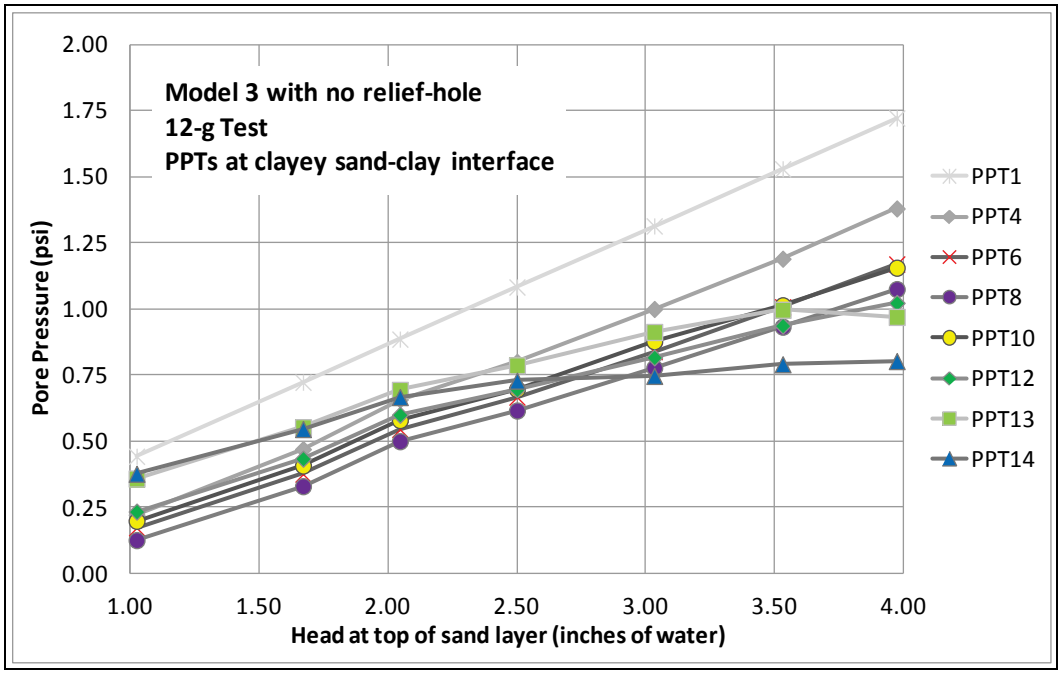

Flow through the model occurred during the 50-min run time between the 7.0- and 9.0-in. increments. Figures 34 and 35 show that the slopes of the PPTs farther downstream change when the reservoir water height is increased above 7.0 in. (2.0 in. above the sand layer). The slopes of PPTs 12-14 continue to flatten as the reservoir water height is increased. The flattening may be caused by unsaturated interfaces at their respective PPT locations.

4.7.2 Test with relief hole

Model 3 was modified after the initial test by inserting a pressure relief hole 1.0 in. downstream of the levee toe centered between the outside walls. Some of the soil around the relief hole was removed, and the area was formed into a fan that was about 0.75 in. deep. Two channels about 0.5 in. deep were scraped into the top clay layer. The channels extended from the relief hole to the downstream reservoir and were located on either side of PPT 13 and PPT 14.

Three holes in the outside of the upstream reservoir were used to maintain a constant water height. These holes allowed excess reservoir water to drain from the reservoir when the water height reached 9.0, 11.0, and 13.0 in. (the lower holes were plugged to attain the higher water heights).

All downstream PPTs were zeroed before each run when the reservoir height was at the clayey sand-clay interface (6.0 in. from base of model). The model was then incrementally brought up to the 12-*g* level and allowed to stabilize for 5 min before the reservoir height was raised.

The relief hole was closely monitored for sand movement as the reservoir height was raised in 0.5-in. increments to a 3.0-in. head on the levee (9.0 in. from base of model). The constant pressure head at the 9.0-in. level was maintained for 12 min. No sand movement was observed during the 12-min interval. The centrifuge was shut down, and the hole at the 9.0-in. level was plugged.

No sand movement was noted during the centrifuge run when the reservoir height was increased to 11.0 in. The centrifuge was again shut down, and the hole at the 11.0-in. level was plugged.

The centrifuge was then brought up to the 12-*g* level and allowed to stabilize for 1 min. The reservoir height was raised in 0.5-in. increments while the relief hole was monitored for sand movement. No sand movement was observed during the transition to a head pressure of 6.0 in. (13.0 in. from the base of the model). This constant pressure head was maintained for 11 min. Some minor sand movement was observed during the 11-min interval. After 11 min, the water feed to the reservoir was raised to its maximum capacity in an attempt to overcome the volume of water being released from the hole at the 13.0-in. level. The maximum reservoir height that could be achieved was 13.5 in. The 13.5-in. level was maintained for 3 min with no increase in sand movement at the relief hole. The centrifuge was stopped and prepared for the 24-*g* run.

Valuable information was gained during the 12-*g* test even though no substantial sand movement was observed. Figures 36 and 37 show that PPTs 3-8 increase linearly as the reservoir water level increased, whereas PPTs 9-14 tend to flatten. Figure 6 shows that PPTs 9-12 are relatively close to the relief hole, and PPTs 13 and 14 are downstream of it. The flattening may be caused by one or both of two possibilities, i.e., the influence of the relief hole or the interfaces not being completely saturated. Unfortunately, there was no way of determining the cause.

Figure 36. Response of pore pressure transducers (PPTs) at sand-clayey sand interface to increasing water level in upstream reservoir with presence of relief hole at 12 *g*.

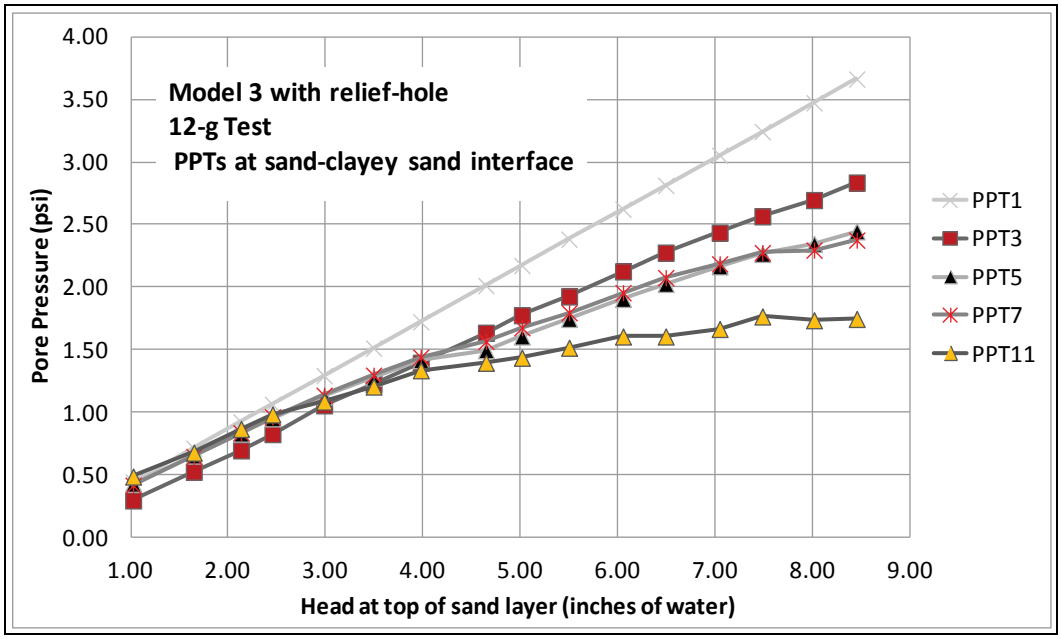

Figure 37. Response of pore pressure transducers (PPTs) at clayey sand-clay interface to increasing water level in upstream reservoir with presence of relief hole at 12 *g*.

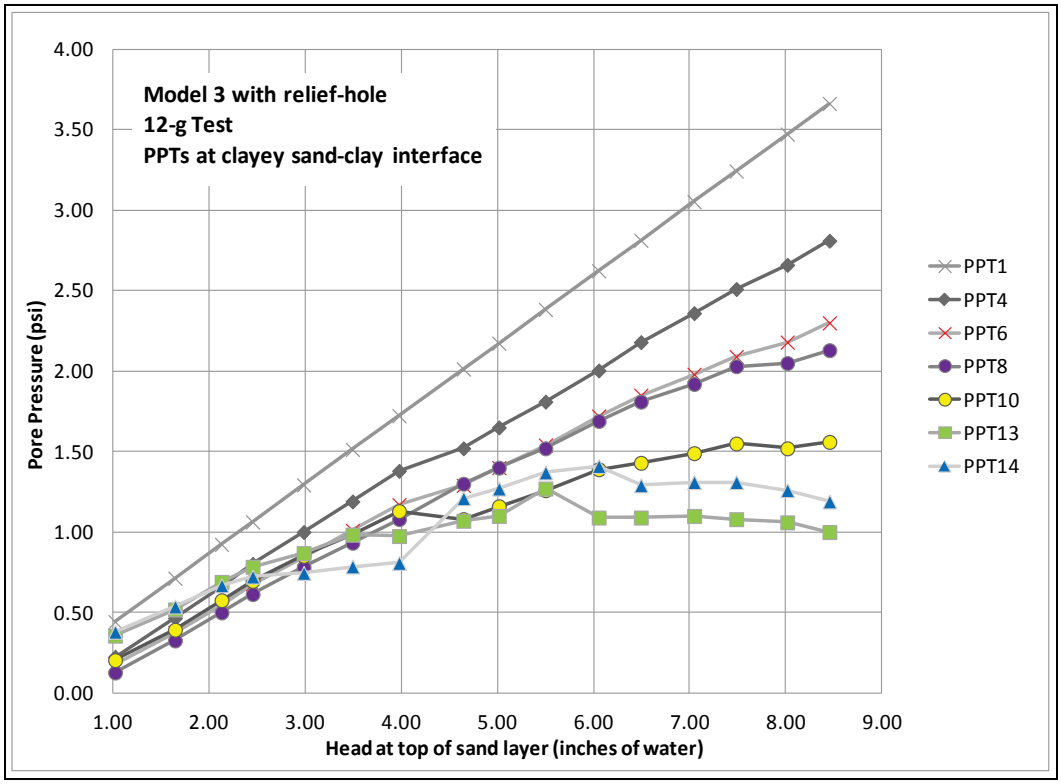

4.8 Model 3 at 24-*g* test

The same testing protocol used for the 12-*g* test was also used for the 24-*g* test. Plugs were removed from the reservoir before the initial run, and all downstream PPTs were zeroed when the reservoir height was at the clayey sand-clay interface. The model was then incrementally brought up to the 24-*g* level and allowed to stabilize for 5 min before the reservoir height was raised. Neither the 9.0-in. nor the 11.0-in. reservoir heights produced any sand movement. The centrifuge was shut down, and the respective holes were plugged.

The model was incrementally brought up to the 24-*g* level and allowed to stabilize for 5 min before the reservoir height was raised. The relief hole was closely monitored for sand movement as the reservoir level was raised in 0.5-in. increments to a 6.0-in. head on the levee (13.0 in. from base of model). No sand movement was observed at the 13.0 in. level after 5 min. The water feed to the reservoir was raised to its maximum capacity in an attempt to overcome the volume of water being released from the hole at the 13.0-in. level. The maximum level that could be achieved was about 14.75 in., which is 1.75 in. above the levee crest. Though this is an unrealistic event, test was continued at this reservoir height to force or initiate sand movement.

Sand started flowing from the relief hole once the reservoir water height was above 13.75 in. Sand continued to flow from the relief hole as the reservoir height increased to 14.75 in. The color of the discharged soil was white, which matched the color of sand. The reservoir height held at 14.75 in. for a minute and then dropped back to the 13.0-in. level. This indicated that the quantity of flow through the model foundation increased as a result of the enlarged subsurface erosion channel dimensions. The discharged soil color remained white, and piping in the sand continued for 12 min at a constant reservoir level of 13 in. After 12 min, the discharged soil color turned red, indicative of a mixture of white sand and red clayey sand. The red soil mixture continued to flow for about a minute until the discharge from the relief hole suddenly increased dramatically, and the reservoir level dropped to a height of 7.5 in., indicating a “blow out.” Not being able to maintain the reservoir water level caused the test to be concluded, and the centrifuge was stopped.

Figures 38 and 39 show that PPTs 3-7 increased linearly as the reservoir head pressure was increased, whereas PPTs 10, 11, and 13 tended to flatten

as the reservoir head was increased. Like the 12-*g* test, the flattening of the response curves could be the influence of the relief hole or the interfaces not being completely saturated at the PPT locations. The last data points on the response curves for PPTs 3-7 show a small decrease in pore pressure. This decrease could be caused by the formation of a piped channel under the levee.

4.9 Post analysis of Model 3

The post analysis of Model 3 was similar to those performed for Models 1 and 2. The only major difference involved the clayey sand layer that was constructed on top of the sand layer. Care had to be taken to ensure that there was minimal disturbance to it, and the underlying sand layer as each successive top layer was removed.

Figure 40 shows the relief hole at the end of the test. The size of the hole had enlarged from its initial size of 0.35 in. to about 0.6 in. The sand that collected on the surface around the hole was about 0.5 in. deep and covered the surface down to PPT 14. Also, notice the depth of the relief hole and its hollowed out appearance. The clayey sand under the top clay layer eroded

Figure 38. Response of pore pressure transducers (PPTs) at sand-clayey sand interface to increasing water level in upstream reservoir with presence of relief hole at 24 *g*.

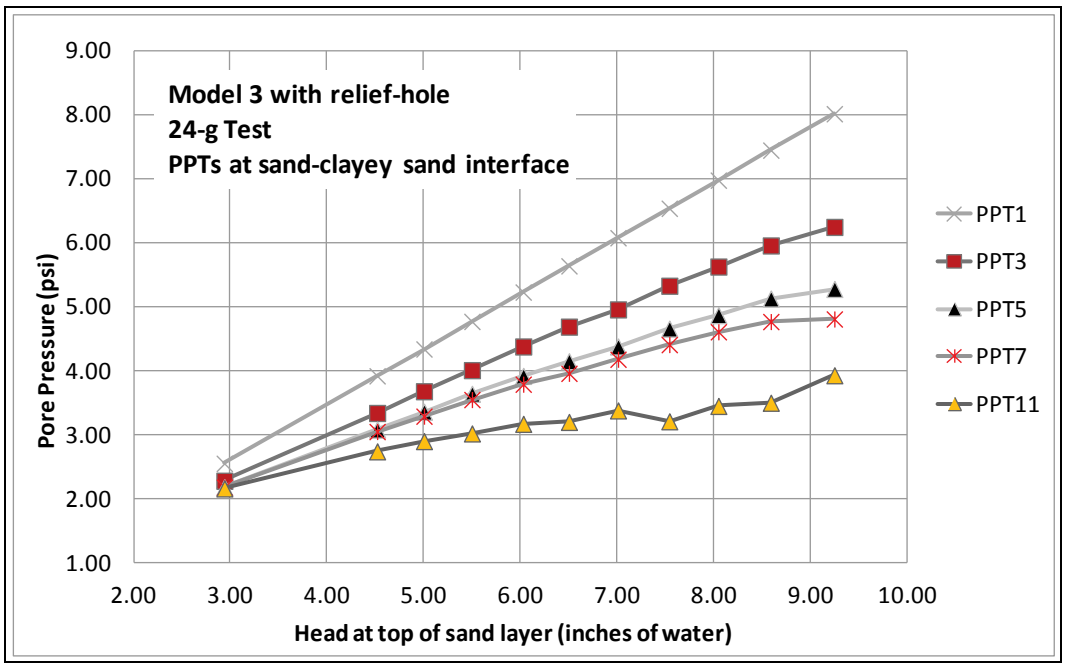

Figure 39. Response of pore pressure transducers (PPTs) at clayey sand-clay interface to increasing water level in upstream reservoir with presence of relief hole at 24 *g*.

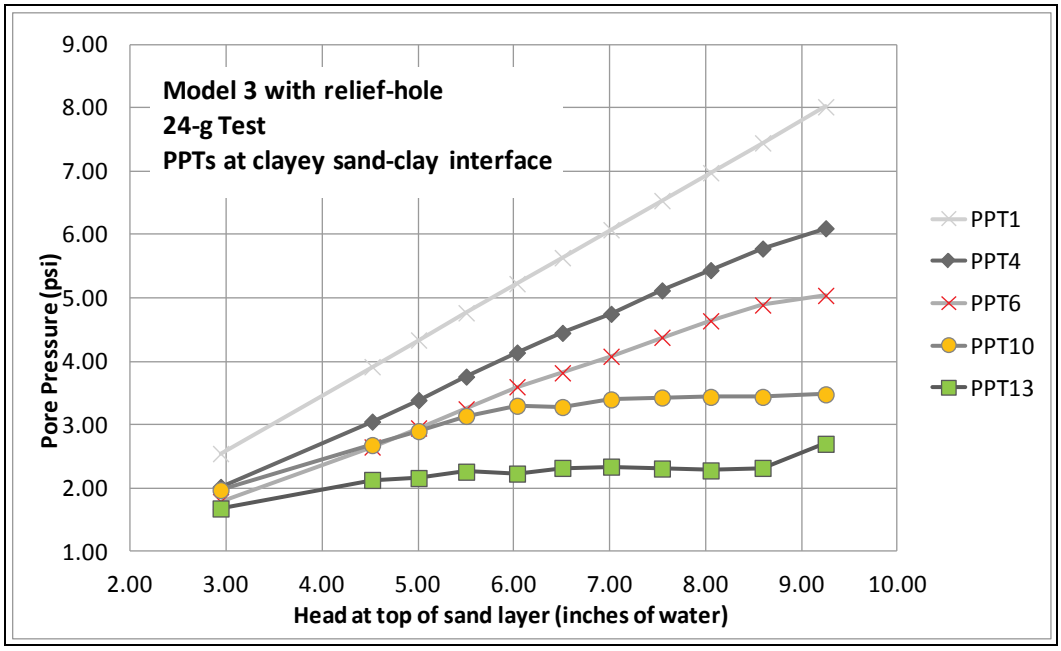

Figure 40. The relief hole with an eroded mixture of white sand and red clayey sand after the completion of the Model 3 test.

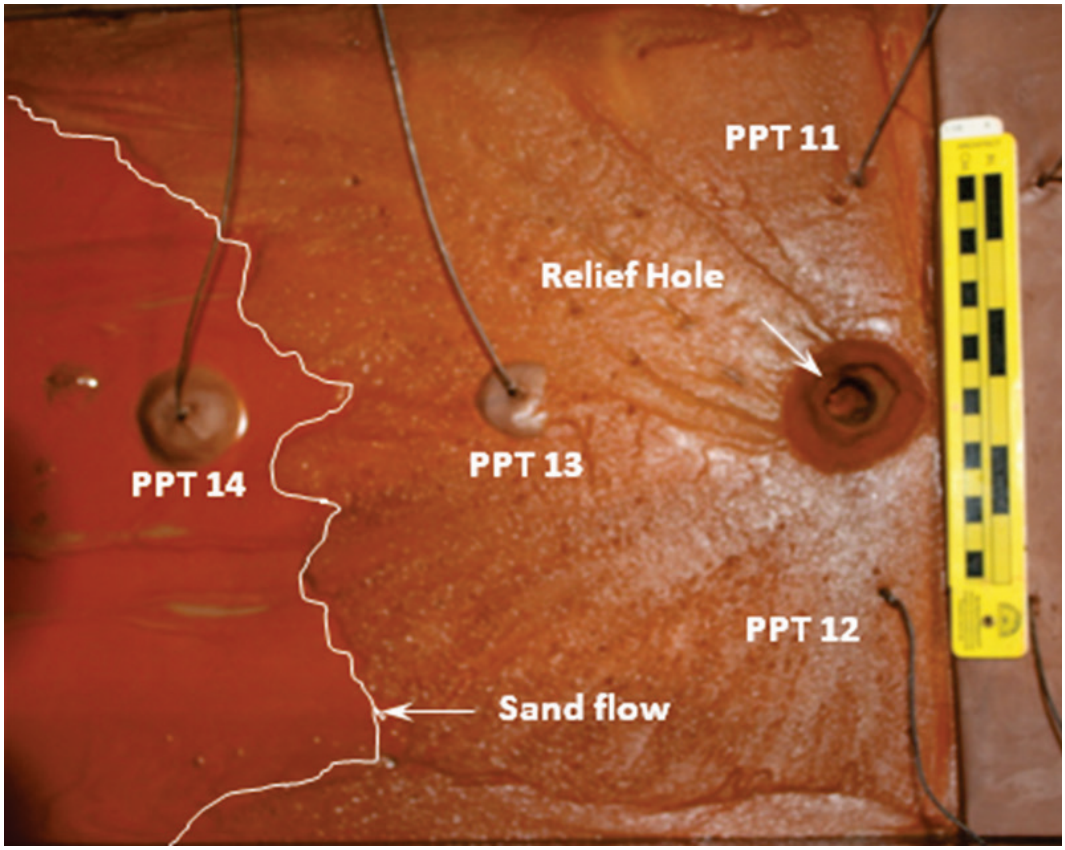

away, and a small cavity formed at the bottom of the hole. Models 1 and 2 had recessed sand in the relief hole and lacked the hollowed out appearance. The cavity and lack of sand in the relief hole could be caused by the high flow rates in Model 3 before the test was ended.

The PPTs and clay levee were carefully removed to fully expose the top clay layer. The clay layer was removed from the downstream reservoir to where the levee toe had been. The section containing the relief hole was cut out in a 4.0-by-6.0-in. section for closer examination. The remaining clay layer was then sliced parallel to the axis of the model in an attempt to remove it in one piece. Some of the clayey sand adhered to the bottom surface of the clay, leaving an outline of the piped channel that formed in the clayey sand (Figure 41). Figure 42 shows a top view of the piped channel in the clayey sand layer. The depth of the channel was about 0.25 in. and extended almost to the sand layer. The channel started at the relief hole and meandered toward the left side of the model, then back to where the reservoir flow holes were located.

The clayey sand was carefully removed from the sand. The clayey sand did not stick to the sand, which made for easy removal. Figure 43 shows a piped channel in the sand layer that is partially filled with the red clayey sand. The size of the eroded channel, and because it is partially filled with the clayey sand, indicates that the sand channel was the first to form. It is hypothesized that, as the sand channel increased in size, the clayey sand layer collapsed into the sand channel, blocking flow and allowing the clayey sand channel to form. After the clayey sand channel formed, the flow volume increased to the point that the reservoir level could not be maintained. This high flow rate pushed so much soil from the foundation that a subsurface cavity under the relief hole formed. When flow was diverted from the sand layer to the clayey sand layer, the clayey sand material partially filled the cavity below the clayey sand layer.

Figure 44 shows high-resolution 3D scans of the eroded channels that formed in the sand and clayey sand layers and their relative location in the model. The eroded channels are color-enhanced to indicate the depth of the channels. The average depth of both channels was in the 0.4-in. range with the area near the reservoir in the clayey sand channel being as deep as 1.0 in. near the reservoir wall. The orange and green lines in the cross section of the model indicate the erosion channels that occurred in the respective layers. The erosion channel in the clayey sand occurred only in

the upper third of the layer, with the remaining two-thirds of the channel being a mixture of white sand and red clayey sand. The area of mixed soils could be a combination of the two erosion channels.

Figure 41. Exposure of a piped channel in the clayey sand at the clayey sand-clay interface.

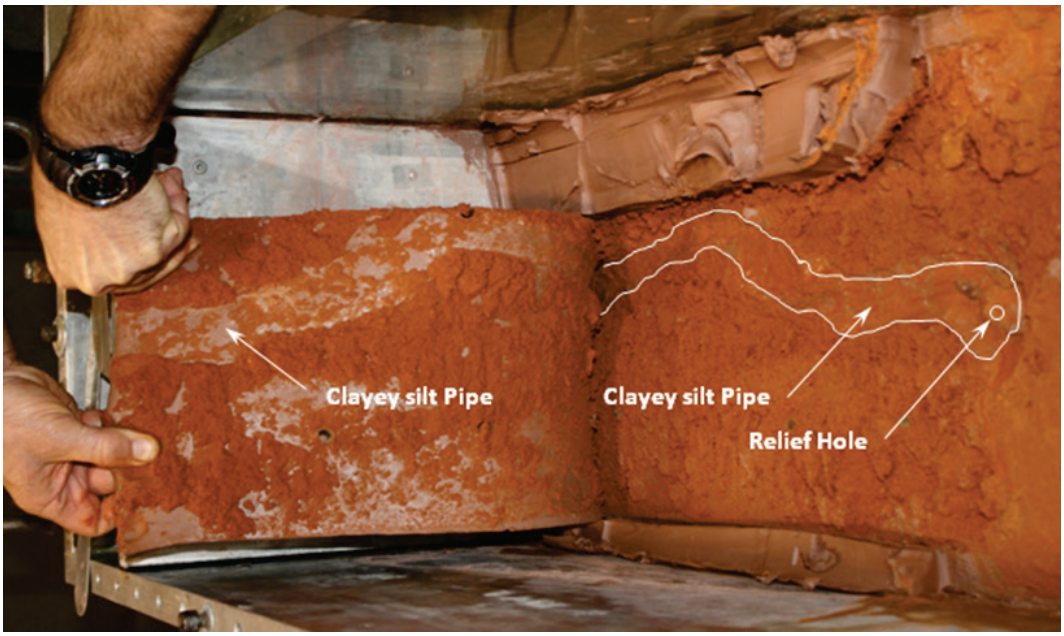

Figure 42. Plan view of piped channel in the clayey sand layer at the clayey sand-clay interface.

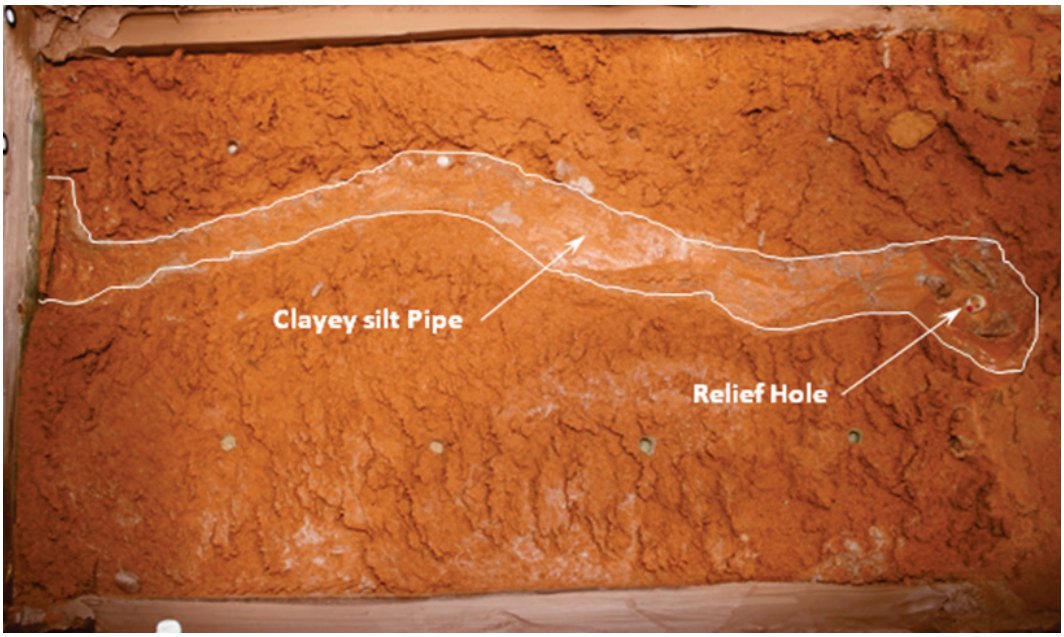

Figure 43. Top view of piped channel in the sand layer at the sand-clayey sand interface. The channel that formed in the sand layer is partially filled with clayey sand.

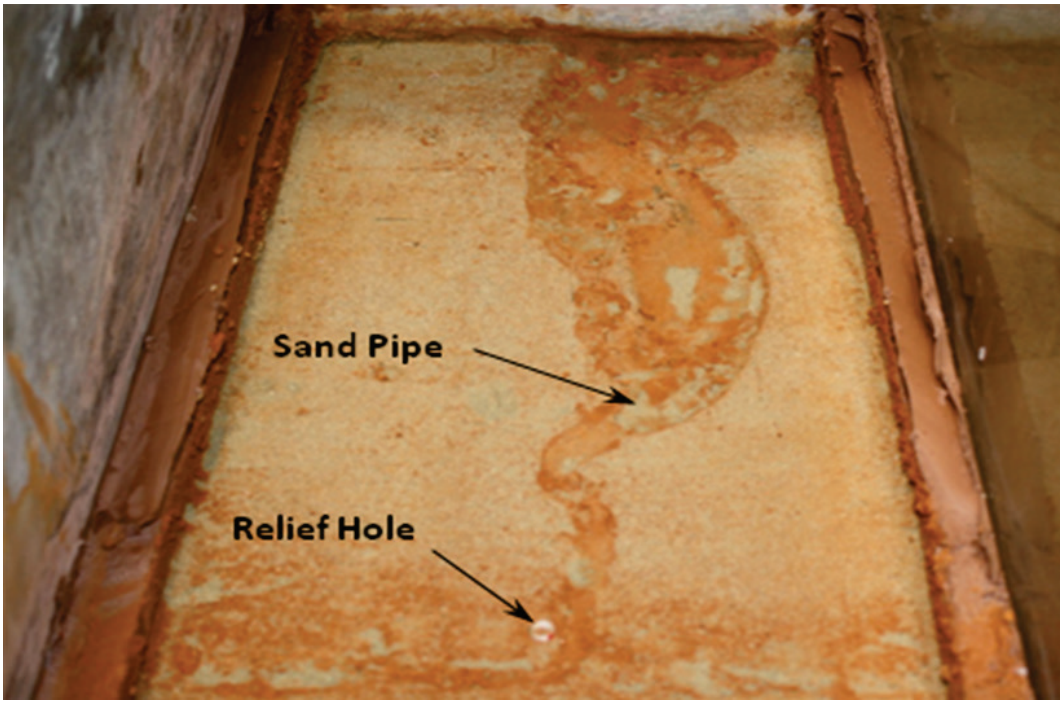

Figure 44. Cross section with pore pressure transducer (PPT) locations and 3D surface scans of resulting internal erosion (piping) during centrifuge test of two piping-susceptible layers (Model 3). Piping locations are highlighted by orange and green lines. Scanned surface color indicates increasing depth from blue to green.

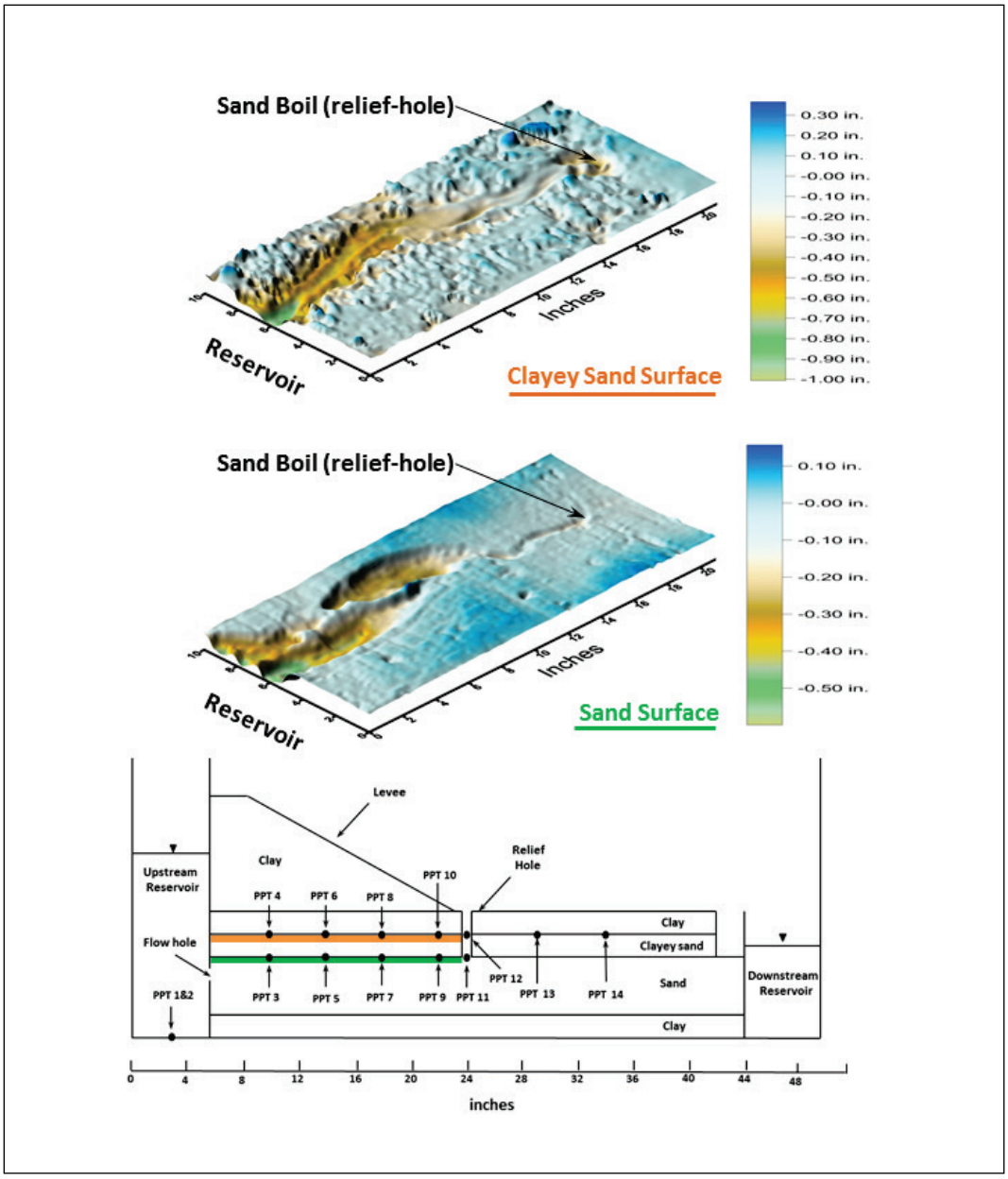

5 Numerical Computer Models of Centrifuge Tests

A two-dimensional (2D) numerical computer model was developed using SEEP/W© 2007 software from GEO-SLOPE International Ltd. to investigate the theoretical pore water pressure response under different upstream water heads in the centrifuge erosion/piping models. SEEP/W© is a 2D finite element groundwater seepage analysis code. The code is capable of modeling nonlinear multilayer subsurface seepage problems like those proposed in this study. Figure 45 shows the cross section of centrifuge Model 1 and the downstream locations of PPTs where data were obtained. This model consisted of a clay levee on a three-layer foundation that included a 5.0-in. sand layer sandwiched between two 1.0-in. clay layers.

Figure 45. A cross section of Model 1 and the location of the pore pressure transducers (PPTs).

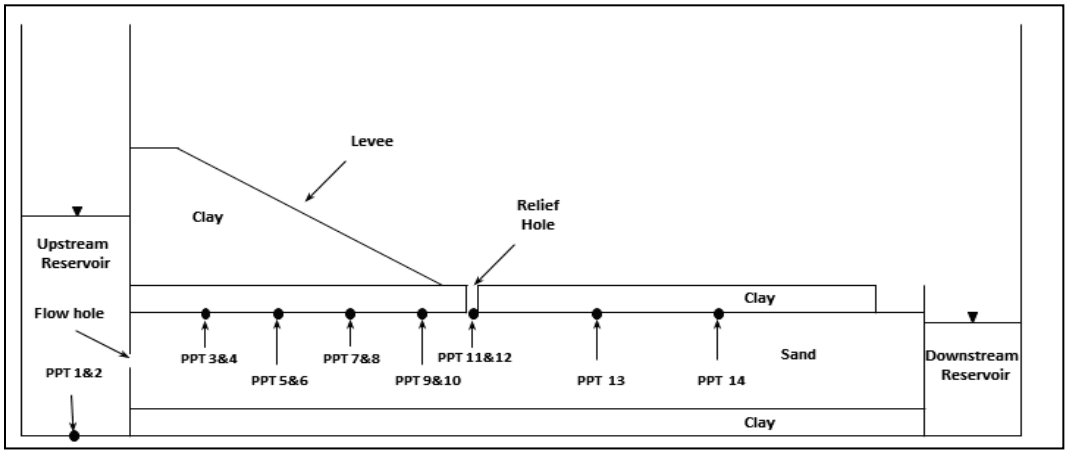

Figure 46 shows a cross section of Model 3 and the downstream locations of all PPTs where pore pressure data were measured. Model 3 has a clay levee founded on two 1.0-in. layers of clay and clayey-sand, a 4.0-in. layer of sand, and a 1.0-in. bottom layer of clay. The complicated foundation of Model 3 required pore pressure information at the sand-clayey sand and clayey sand-clay interfaces. Water entered the sand layer of each model from the upstream reservoir and was collected in the downstream reservoir after it exited the model. The spillover elevation of the downstream reservoir is the same as the levee base elevation. Therefore, no flow can occur until the upstream reservoir level is above the base of the levee. Both models were analyzed with and without the presence of a pressure relief hole.

Figure 46. A cross section of Model 3 and the location of the pore pressure transducers (PPTs).

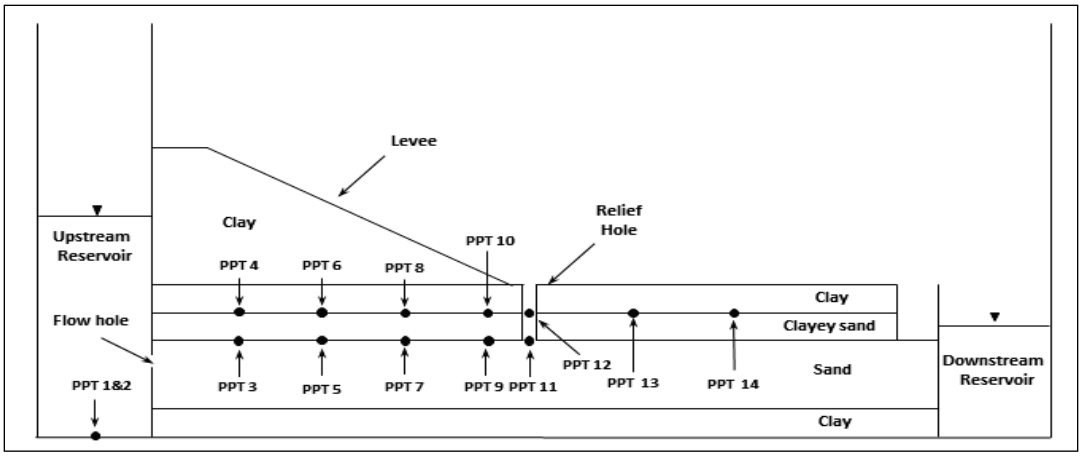

Performing an analysis on the model without a pressure relief hole provided a distribution of pore pressures in the model without relief hole influence. The placement of a pressure relief hole downstream of the levee toe allowed its influence to be characterized. Data from these two numerical analyses provide a theoretical basis from which the centrifuge data can be compared and analyzed.

5.1 Model 1

Three numerical analyses were made on Model 1 to simulate the centrifuge test runs. The first analysis was at 10 g's without a relief hole. The second and third analyses were at 10 g's and 20 g's with the addition of a pressure relief hole. Permeabilities used in the analysis were 10^{-7} cm/sec for the clay and 10^{-3} cm/sec for the sand. Figure 47 shows the results of the first analysis when the reservoir level is at the top of the levee. The colors represent the change in head pressure throughout the model. The flow vectors in the foundation show the magnitude of water flowing through the model when there is no pressure relief hole. The flow vectors at the reservoir flow holes indicate the size of the holes might be too small in the centrifuge model; therefore, additional holes were added in the centrifuge model to decrease the size of the flow vectors. However, the flow appears to be uniform and evenly distributed throughout the sand foundation.

Figure 48 shows the results of pore pressure calculations at the sand-clay interface for different downstream locations. Pore pressures along the interface at each PPT location increase linearly with reservoir head pressure, which is represented by PPT 1 and 2. The pore pressures in Figure 49 shows the numerical results of Model 1 after a relief hole is added 1.0 in.

downstream of the levee toe. The only difference between Figures 47 and 49 is that Figure 49 contains a pressure relief hole. Comparing Figures 47 and 49 shows a change in flow patterns. The presence of a pressure relief hole diverts most of the flow to the relief hole with very little flow going to the downstream outlet. The diversion concentrates the pressure drops between the upstream reservoir and the relief hole, thereby increasing the gradient under the levee.

Figure 47. Pore pressure distribution and flow vectors for Model 1 at 10 *g* with no pressure relief hole. The head pressure is indicated by the number at the intersection of colors.

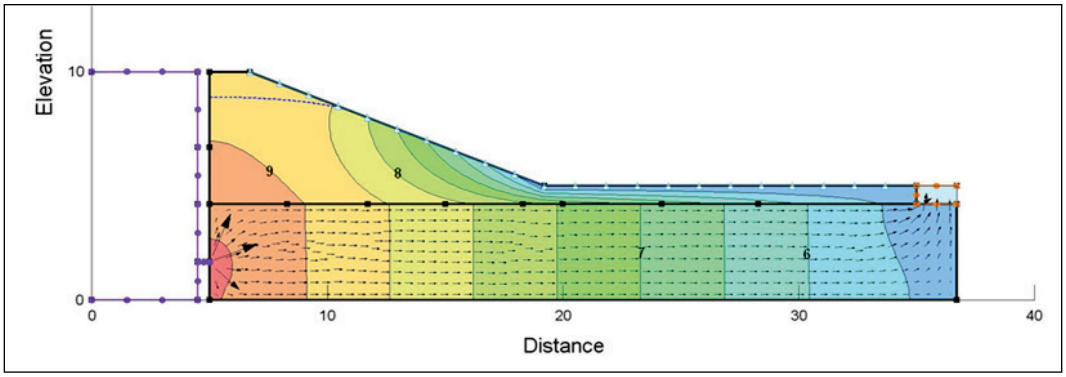

Figure 48. Pore pressure transducer (PPT) responses at sand-clay interface versus increasing upstream reservoir head above base of levee with no pressure relief hole downstream of levee for Model 1 at 10 *g*.

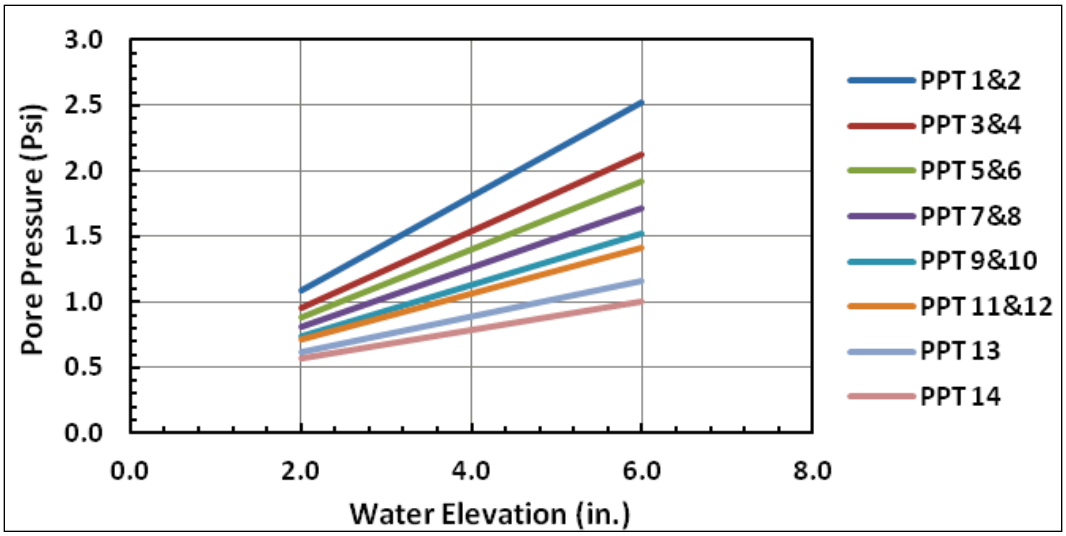

Figure 49. Pore pressure distribution and flow vectors for Model 1 at 10 *g* with pressure relief hole. The head pressure is indicated by the number at the intersection of colors.

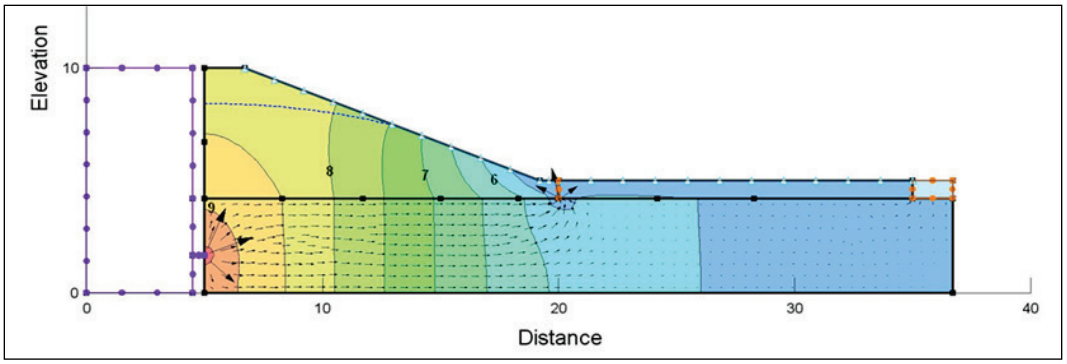

Figure 50 shows graphically that the pore pressure at each location increases linearly with an increase in head pressure except at the relief hole. The main difference between Figures 48 and 50 is the flatter slopes in the response curves with the pore pressures downstream of the relief hole showing little pore pressure response. The flatter slopes in the pore pressure curves between the two analyses translate into a pore pressure decrease at the downstream locations. The pore pressure decrease ranges from 15% to 50% depending on the location of the PPT. The farther downstream the PPT, the larger the drop in pore pressure.

Figure 50. Pore pressure transducer (PPT) responses at sand-clay interface versus increasing upstream reservoir head above base of levee with pressure relief hole downstream of levee for Model 1 at 10 *g*.

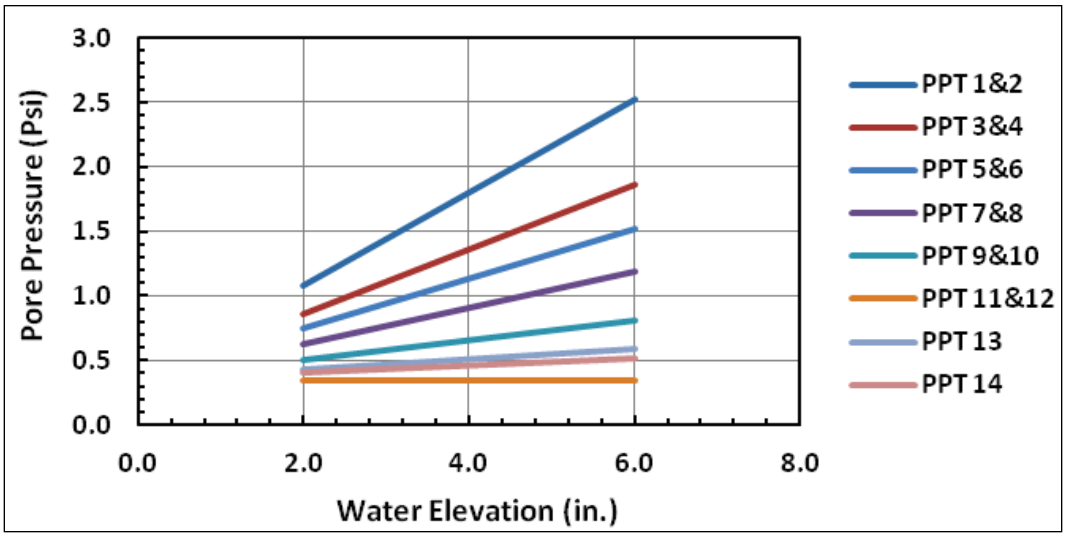

The third analysis shows the results of calculations in a 20-*g* environment (Figure 51). The only difference between the results of 10-*g* and 20-*g* analyses is the magnitude in the pore pressures. The 20-*g* analysis shows pore pressures that are double those of the 10-*g* analysis.

Figure 51. Pore pressure transducer (PPT) responses at sand-clay interface versus increasing upstream reservoir head above base of levee with pressure relief hole downstream of levee for Model 1 at 20 *g*.

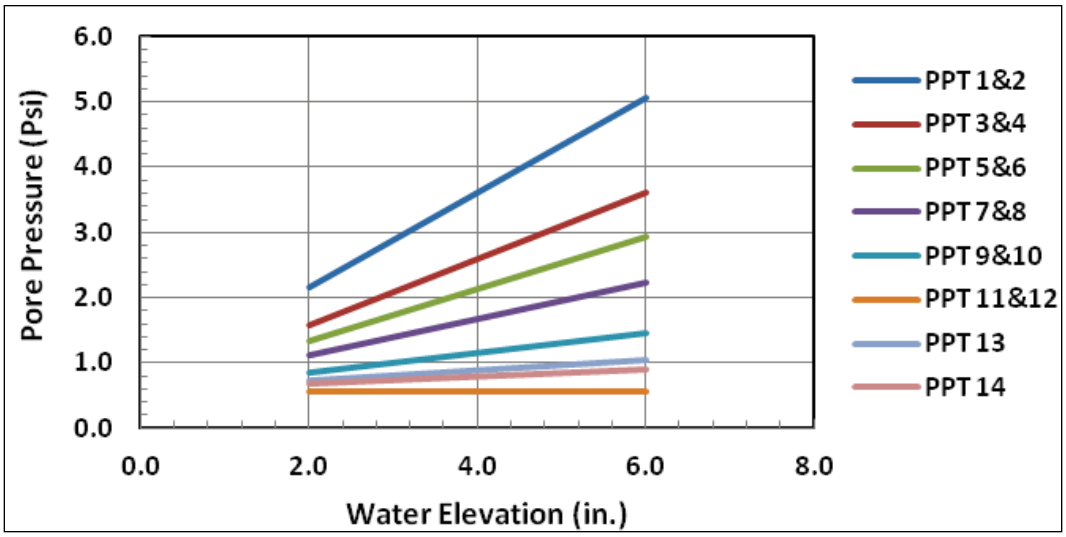

5.2 Model 3

Three numerical analyses were performed on the third model. The first analysis was at 12 *g* without a relief hole. This analysis gives the pore pressure response for increases in the reservoir head pressure without the influence of a relief hole. The second and third analyses were with a relief hole at 12 *g* and 24 *g*. The permeabilities used were 10^{-7} cm/sec for the clay, 10^{-4} cm/sec for the clayey sand, and 10^{-3} cm/sec for the sand.

Figure 52 shows the results of the first analysis of Model 1 when the reservoir level is at the top of the levee. The colors represent the changes in head pressure as the distance downstream increases. The flow vectors show the magnitude of water flowing through the sand and clayey sand foundation when there is no pressure relief hole. The number of flow holes between the reservoir and the foundation soils was increased in the centrifuge model to reduce the energy lost at these holes. The flow vectors at these holes are now more reasonable and appear to be relatively uniform and evenly distributed throughout the sand foundation. Flow through the clayey sand is small as compared to the sand with virtually no flow through the clay levee.

Figure 52. Pore pressure distribution and flow vectors for Model 3 at 12 *g* with no pressure relief hole. The head pressure is indicated by the number at the intersection of colors.

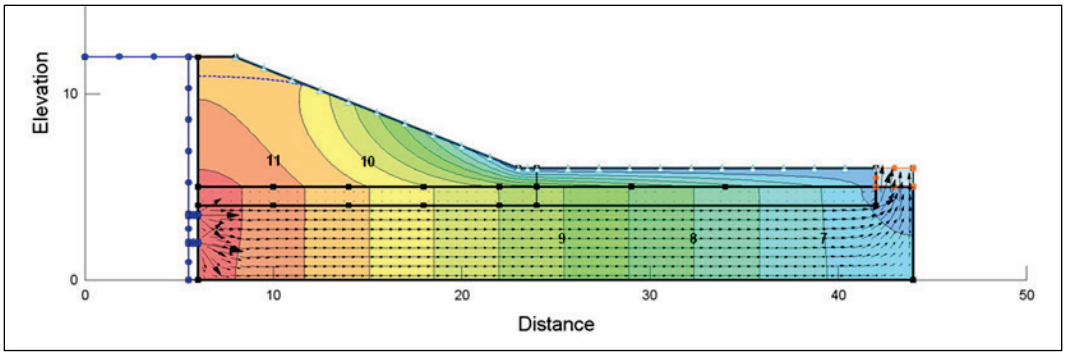

Figures 53 (clayey sand-clay interface) and 54 (sand-clayey sand interface) show that pore pressures at each location along these interfaces increase linearly with reservoir head pressure. Pore pressures plotted in Figure 53 at the clayey sand-clay interface are lower than those in Figure 54 because the PPTs at the sand-clayey sand interface are located 1.0 in. deeper. Also, the PPT response curves in each figure have similar trends in that their slopes decrease as the distance from the upstream reservoir increases. This response is as expected because the head loss increases the farther the measurement point is from the upstream reservoir.

Figure 55 shows the results of the second run when a relief hole is added to the model. The only difference between Figures 55 and 52 is that Figure 55 contains a pressure relief hole. A comparison of Figures 55 and 52 shows a change in the flow patterns. The presence of a pressure relief hole diverts most of the flow to the relief hole with very little flow going to the downstream outlet. The diversion concentrates the pressure drops between the upstream reservoir and the relief hole, thereby increasing the gradient under the levee. Also, note the flow through the clayey sand layer continues to remain low.

Both Figures 56 and 57 show graphical results of the second analysis of Model 3 when the reservoir level is at the top of the levee. The effect of the relief hole is similar to that of Model 1 and can be seen by comparing Figures 53 and 54 to Figures 56 and 57, respectively. The main difference between Figures 53 and 56 is the flatter slopes in the response curves with the pore pressures downstream of the relief hole showing little pore pressure response. The same type of response is found when comparing Figures 54 and 57. The flatter slopes in the pore pressure curves between the analyses translate into a decrease in pore pressure at the downstream

locations when a relief hole is present. The pore pressure decrease ranges from 15% to 50% depending on the location of the PPT. The farther downstream the PPT is, the larger the drop in pore pressure.

Figure 53. Pore pressure transducer (PPT) responses at clayey sand-clay interface versus increasing upstream reservoir head above base of levee with no pressure relief hole downstream of levee for Model 3 at 12 *g*.

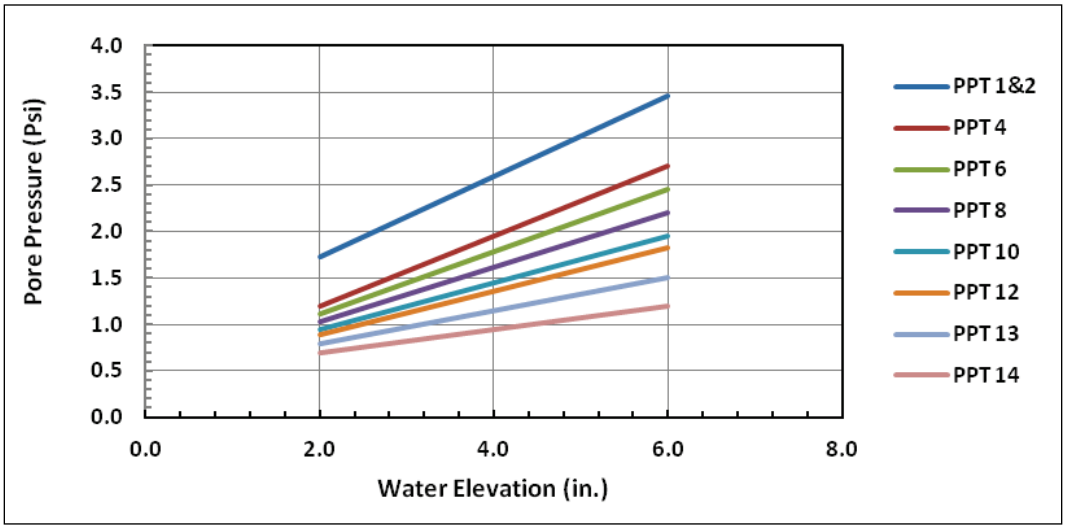

Figure 54. Pore pressure transducer (PPT) responses at sand-clayey sand interface versus increasing upstream reservoir head above base of levee with no pressure relief hole downstream of levee for Model 3 at 12 *g*.

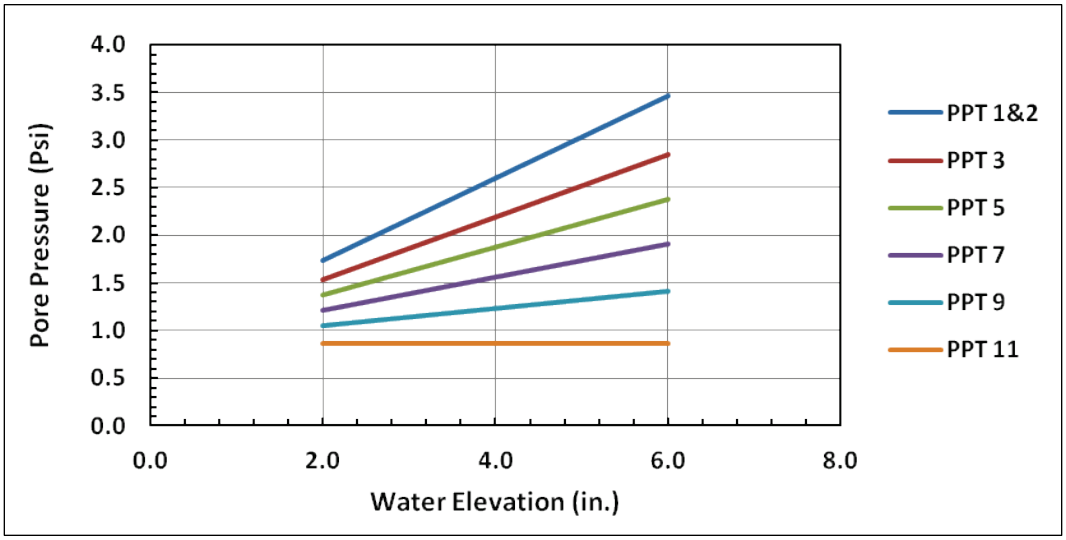

Figure 55. Pore pressure distribution and flow vectors for Model 3 at 12 *g* with pressure relief hole. The head pressure is indicated by the number at the intersection of colors.

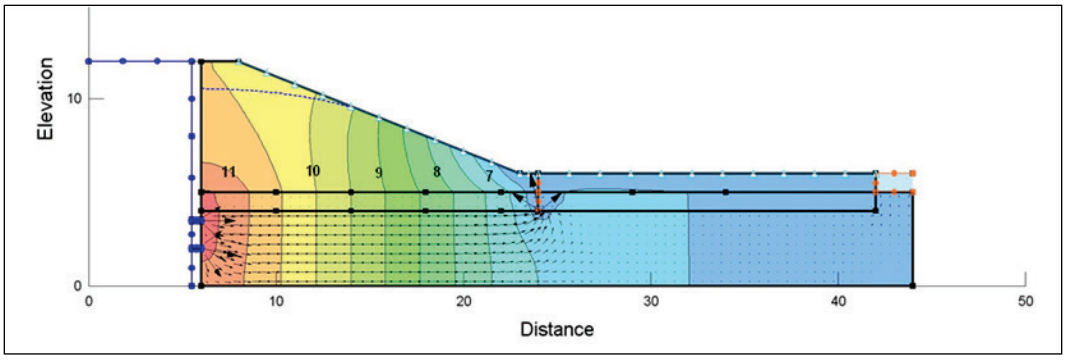

Figure 56. Pore pressure transducer (PPT) responses at clayey sand-clay interface versus increasing upstream reservoir head above base of levee with a pressure relief hole downstream of levee for Model 3 at 12 *g*.

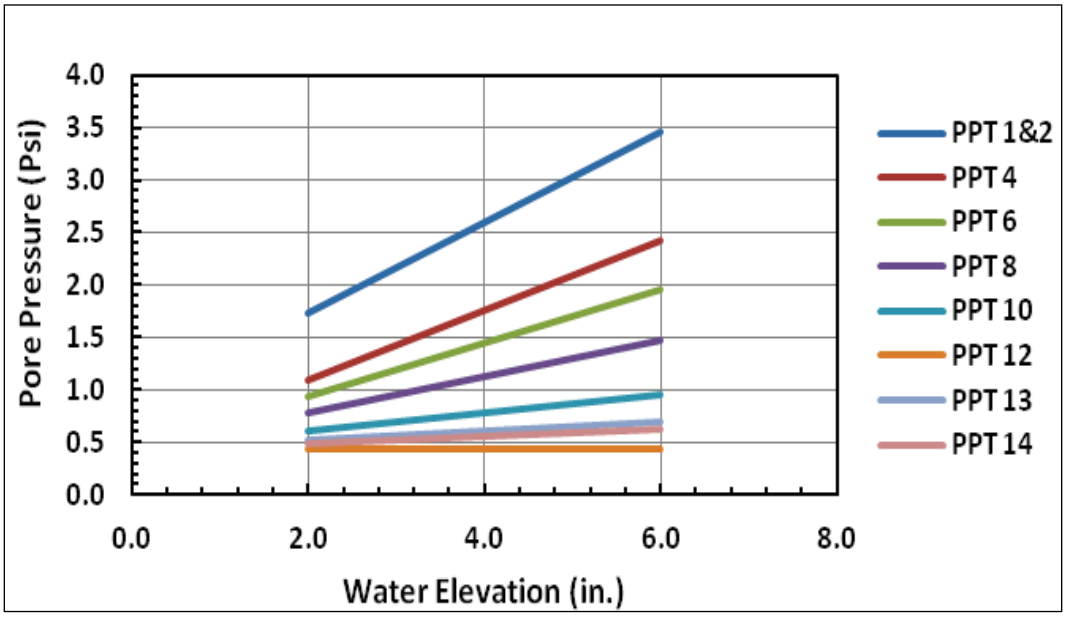

Pore pressures downstream of the relief hole decrease dramatically, indicating that most of the flow is being diverted to the relief hole. PPT 12 (Figure 56) is located at the relief hole and shows no response to an increase in reservoir level. The response curves of PPT 13 and 14 show a small amount of pore pressure increase with reservoir level. Their locations downstream of the relief hole put them outside the range of flow influence. The third analysis shows a similar response to that of the second analysis (see Figures 58 and 59 compared to Figures 56 and 57, respectively). The major difference between the two analyses is that the third analysis has larger pore pressures because of the higher gravitational level.

Figure 57. Pore pressure transducer (PPT) responses at sand-clayey sand interface versus increasing upstream reservoir head above base of levee with a pressure relief hole downstream of levee for Model 3 at 12 *g*.

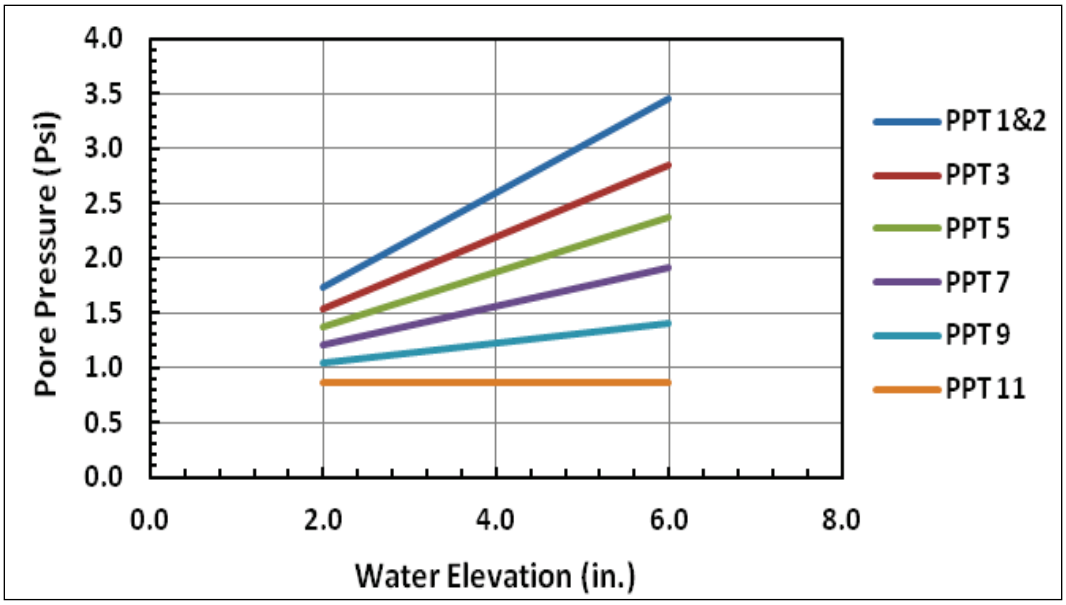

Figure 58. Pore pressure transducer (PPT) responses at clayey sand-clay interface versus increasing upstream reservoir head above base of levee with a pressure relief hole downstream of levee for Model 3 at 24 *g*.

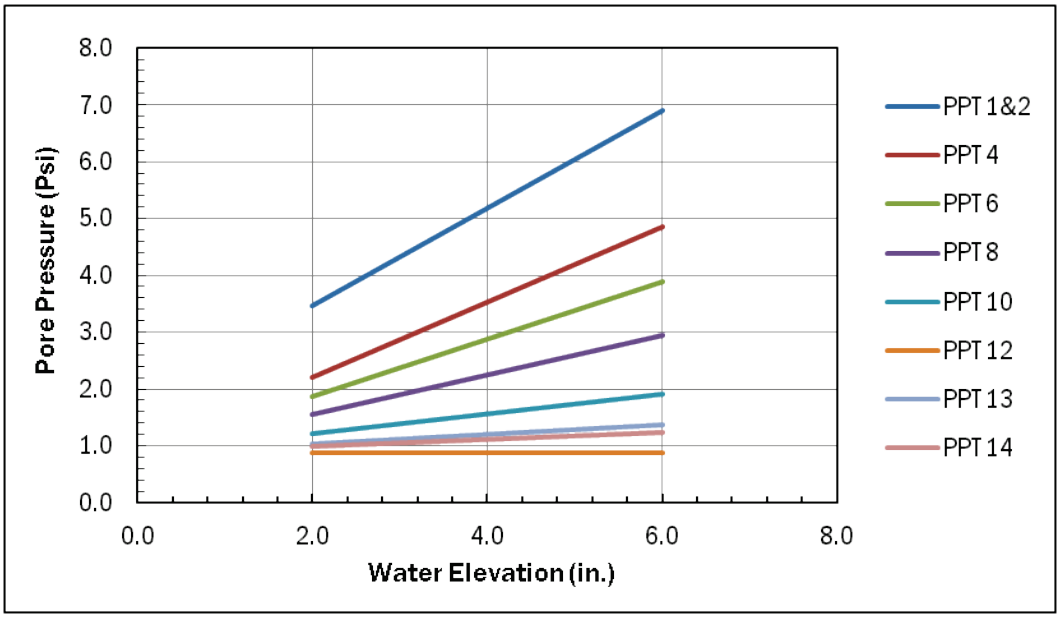

Figure 59. Pore pressure transducer (PPT) responses at sand-clayey sand interface versus increasing upstream reservoir head above base of levee with a pressure relief hole downstream of levee for Model 3 at 24 *g*.

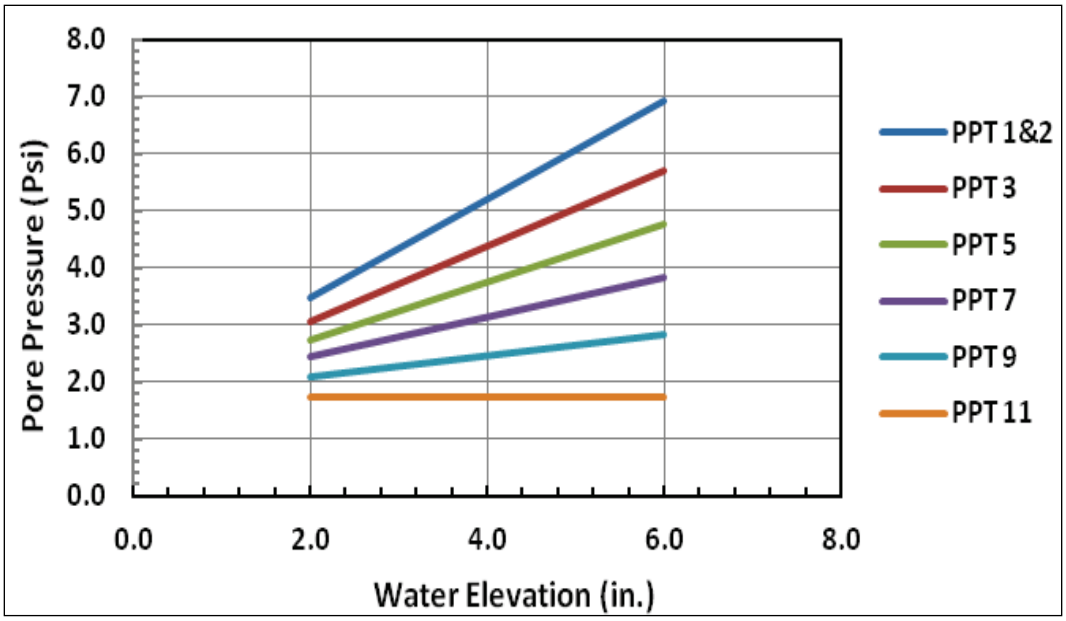

The magnitude of each response curve from the third analysis is double that from the second analysis.

5.3 General comments

The data from the centrifuge experiments compared favorably to the numerical results. The general data trends were what would be expected from a 2D analysis of this type of problem.

The distribution of pore water pressures before and after the insertion of the relief hole was expected and matched those found in the centrifuge tests. The pore pressures tended to differ between the analyses farther downstream. The PPTs close to the reservoir compared more favorably than those farther downstream. Higher pore pressures were calculated in the numerical analyses near the relief hole.

The difference between the experimental and numerical results may be caused by using a 2D model to analyze a 3D problem. Another possibility could be subsurface erosion. Subsurface erosion was not included in the numerical analyses because of limited program capabilities.

6 Conclusions

The preliminary centrifuge tests and companion numerical analyses discussed in this report clearly demonstrate that erosion and piping experiments in the centrifuge are valuable research tools, especially considering current research needs in improving the understanding in failure mode assessments. The approach discussed in this report to conduct physical and numerical modeling is critical to provide definitive and verifiable results. These tests were successful in design, construction, and execution of a realistic simulation of internal erosion leading to failure mode initiation, continuation, and failure. These results show that valuable laboratory data can be obtained in this manner.

Preliminary tests also provided the following insight and recommendations for improving research employing these tools:

- Design of the physical model should strive to be as succinct in purpose and simplistic in design as possible to accomplish a focused investigation of failure mode characteristics.
- The 2D numerical modeling is necessary but may not be sufficient in fully capturing the behavior of physical models in the centrifuge. First, conduct the 2D simulations, but continue with 3D models to gain further insight for improved assessment and verification of the companion physical model tests.
- Due to the relatively short history and limited experience in conducting centrifuge testing for this phenomena and to fully explore and account for possible "scale effects," "modeling of models" testing protocol should be included in the test program. Also, the model design should minimize the scale factor (gravitational level) because scale effects will compound or become more significant with increasing gravitational levels.

Specific recommendations for improving the centrifuge tests include the following:

- Design improved system for reservoir control to provide definitive and controlled reservoir water levels.
- The reservoir level (head pressure) must be carefully controlled to allow pore pressure data to be correctly interpreted. Capability to

maintain a constant head is important to maintain controlled known boundary conditions critically important in allowing accurate assessment of pore pressure response and correlation with active piping/erosion data.
- Provide for collection and monitoring of flow associated with the piping mechanism to provide important data to enable further analysis.
- Devise and include embedded soil markers to provide information for location and progression of piping.
- Conduct initial numerical modeling and response predictions to guide test design and assist in test monitoring.
- Develop and implement careful test protocol, data collection, and archiving procedures to improve test results and reduce posttest analysis effort. Test monitoring should include multiple windowed real-time PPT response data viewing superimposed on numerical results.
- For establishing the initial conditions, allow time for the model to reach a steady state seepage condition to attain uniform saturation and consolidation by removing entrapped air and excess water pressure. A head should be used with a sufficient gradient to affect these results, but well below a critical gradient.
- Additional tests should be performed using increased time frames between loading increments and more controlled conditions to better delineate the progression of subsurface erosion in sand or other soils.

Observed internal erosion mechanisms include the following:

- Erosion/piping occurs at the interface between two materials where their hydraulic properties (permeability) have a significant contrast.
- A sand layer overlain by clay resulted in erosion/piping to initiate along the sand/clay interface.
- Pore pressure measurements can be used to determine the progression of erosion/pipe under a levee or dam.
- The magnitude of confining stresses is a factor that contributes to the active status of a pipe as it progresses under a levee or dam.
- The results of numerical simulations and physical model tests were comparable where a 2D model reasonably captures the main features of the 3D physical model. The comparison also showed where the 3D flow field was not well captured with the simpler 2D assumptions.

References

de Wit, J. M., J. B. Sellmeijer, and A. Penning. 1981. Laboratory testing on piping. In *Soil mechanics and foundation engineering*, 517–520. Rotterdam, Netherlands.

Garnier, J., P. Audrain, V. D. Le, D. Marot, and L. Thorel. 1984. *Centrifuge modeling of an internal erosion mechanism*. Washington, DC: American Society of Civil Engineers.

Garnier, J., C. Gaudin, B. Kutter, and R. Phillips. 2007. Catalogue of scaling laws and similitude questions in geotechnical centrifuge modeling. *IJPMG International Journal of Physical Modeling in Geotechnics* 3.

Joseph, H., R. Einstein, and R. Whitman. 1988. A literature review of geotechnical modeling. Massachusetts Institute of Technology Dept of Civil Engineering for US Air Force Engineering and Services Laboratory, Tyndall AFB, Florida.

Le, V., D. Marot, L. Thorel, J. Garnier, and P. Audrain. 2010. Centrifuge modeling of an internal erosion mechanism. ASCE. *International Conference on Scour and Erosion* 2010:629–638.

Ng, C. W. W., P. Van Lark, W. H. Tang, X. S., and L. M.Zhang. 2001. Hong Kong geotechnical centrifuge. In *Soft soil engineering,* ed. Lee et al. Leiden, Netherlands: Swets and Zeitlinger.

Richards, K. S., and K. R. Reddy. 2007. Critical appraisal of piping phenomena in earth dams. *Bulletin of Engineering Geology and the Environment* 66(4):381–402.

Sellmeijer, J. B. 1988. On the mechanism of piping under impervious structures. PhD diss., Delft University of Technology.

Sellmeijer, J. B., and M. A. Koenders. 1991. A mathematical model for piping. *Applied Mathematical Modeling* 15(11-12):646–651.

van Beek, V., A. Bezuijen, and V. M. V. Beek. 2010. Piping: Centrifuge experiments on scaling effects and levee stability. In *Physical modeling in geotechnics,* 183–189. Delft, Netherlands.

Waterways Experiment Station. 1991. *Large centrifuge: A critical Army capability for the future*. Miscellaneous Paper GL-91-12, ed. L. Ledbetter. Vicksburg, MS: US Army Engineer WES.

Appendix A: Pictorial - Levee Piping Model

Figure A1. Model box with an upstream reservoir on right and downstream (overflow) reservoir on left.

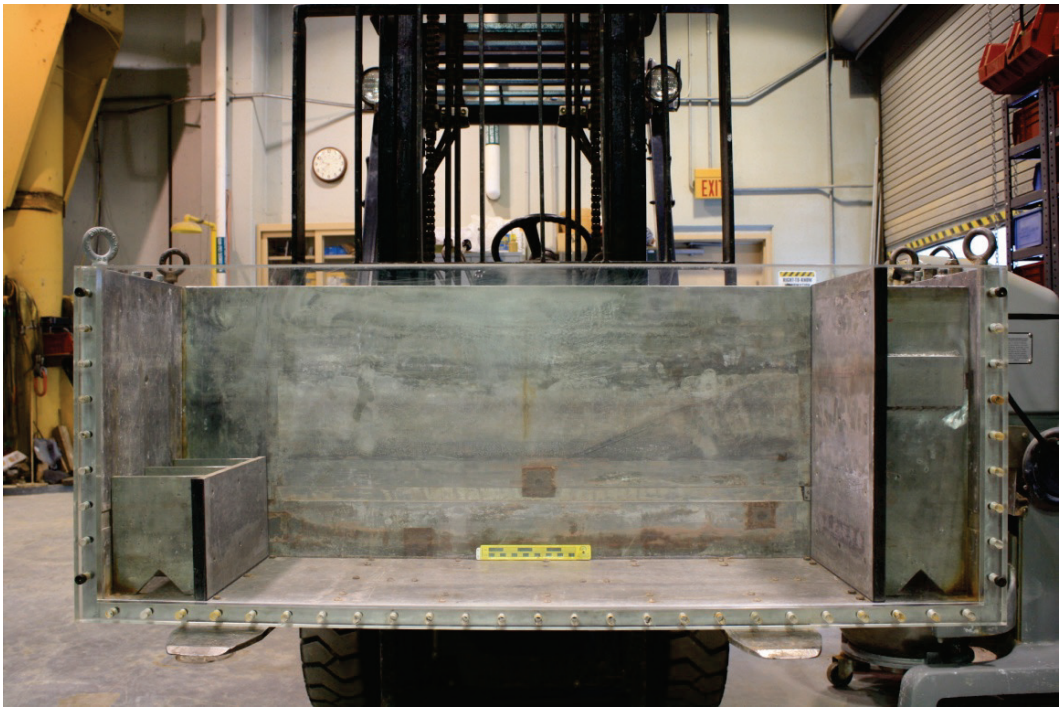

Figure A2. Absorbent paper used to enhance reservoir boundary leakage during model box checkout. Cameras are mounted on both reservoirs to view the boundaries as the centrifuge is spinning.

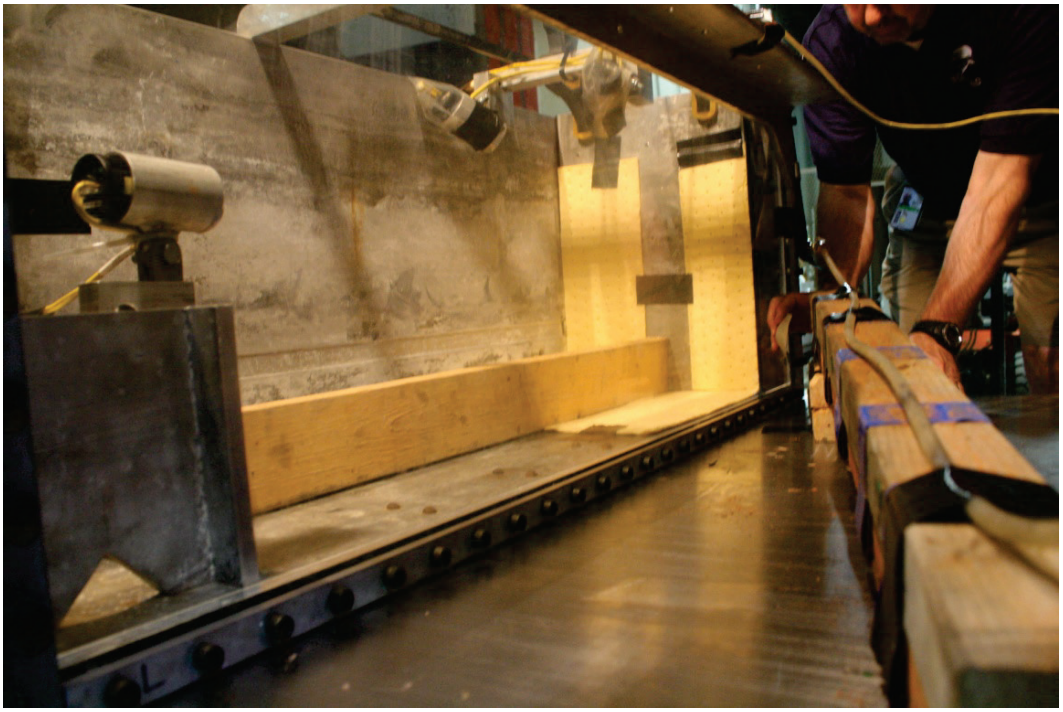

Model construction

Figure A3. The first two sections of bottom clay layer placed against back wall of model box. Edges of each section beveled at 45-deg angle for overlap and layer integrity.

Figure A4. The bottom clay layer is almost complete. The clay layer requires placement of the front 3-in. clay sections.

Figure A5. The bottom clay layer is complete and approximately 1 -in. thick.

Figure A6. Placement of the back 1-in.-thick clay wall.

Figure A7. Construction of the bottom clay layer and clay walls of the foundation completed. The model is ready for placement of remaining layer(s) of the foundation.

Figure A8. Model foundation flooded with water before pluviation of sand layer.

Figure A9. Pluviating sand through water to attain target density. Placement of the sand through water ensured the sand was saturated.

Figure A10. Completed sand layer with the sand layer brought to top edge of clay boundaries for Models 1 and 2.

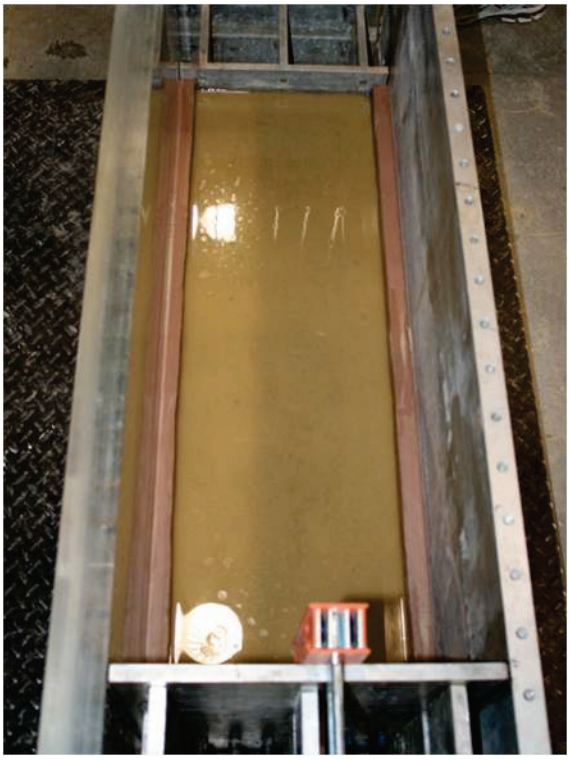

Figure A11. Clayey sand layer placed on top of sand layer for Model 3. Sand layer is 1 in. below the edge of the clay walls. For Model 3, clayey sand layer compacted until level with top edge of clay walls.

Figure A12. Clayey sand layer removed to expose sand layer on all models. The exposed sand layer is an exit point for water flowing through the model.

Figure A13. A top clay section is placed over clayey sand layer. The internal edges of each clay section are beveled at 45 deg. The bevel provides overlapping/sealing of each clay section and overall integrity of top clay layer.

Figure A14. Side view of completed model foundation before levee is constructed. Notice that the sand layer is exposed at the downstream reservoir.

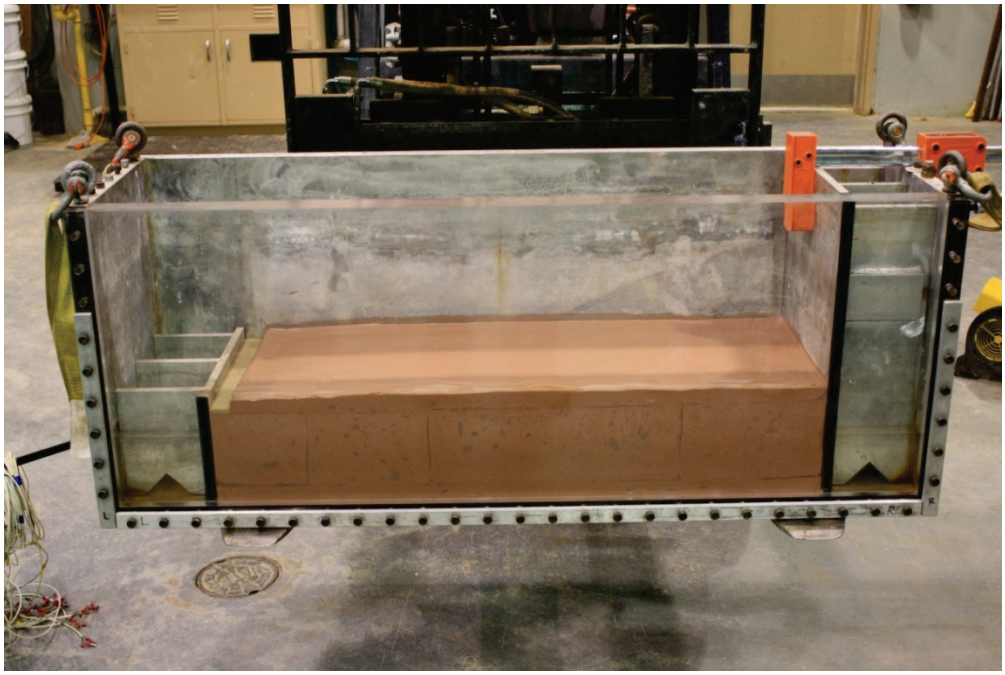

Figure A15. Construction of first two sections of levee completed. The pore pressure transducers will be inserted to the appropriate depth and sandwiched between these and next sections.

Figure A16. The installation of first row of PPTs between levee sections is complete. The second row has two PPTs installed with open holes awaiting remaining two PPTs.

Figure A17. Levee will be complete after placement of the final section. Notice the PPTs are sandwiched between sections, which provide a natural seal against leakage.

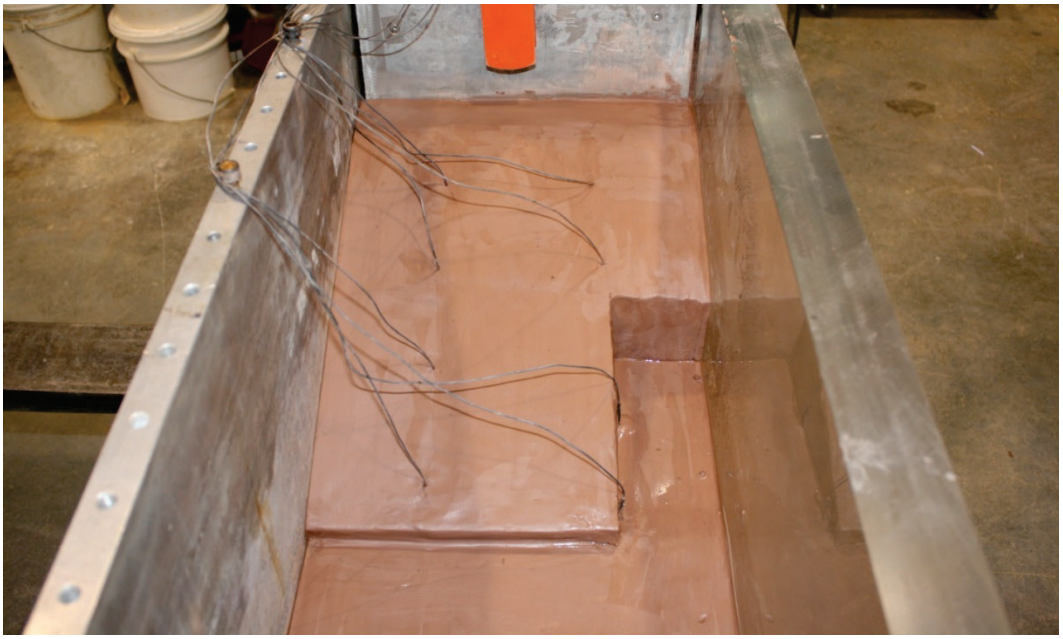

Figure A18. Placement of the relief hole at toe of levee and beginning construction of surface channels, which keep the surface of the model dry during the test.

Figure A19. Construction of relief hole and drainage channel completed. Notice the PPTs next to and downstream of the relief hole and berms. Berms provide added protection against leakage.

Figure A20. Close up view of relief hole and fanned area that leads into the drainage channels.

Post analysis of Model 1

Figure A21. Test of Model 1 is complete. The sand foundation has eroded and covers the area downstream of the levee toe.

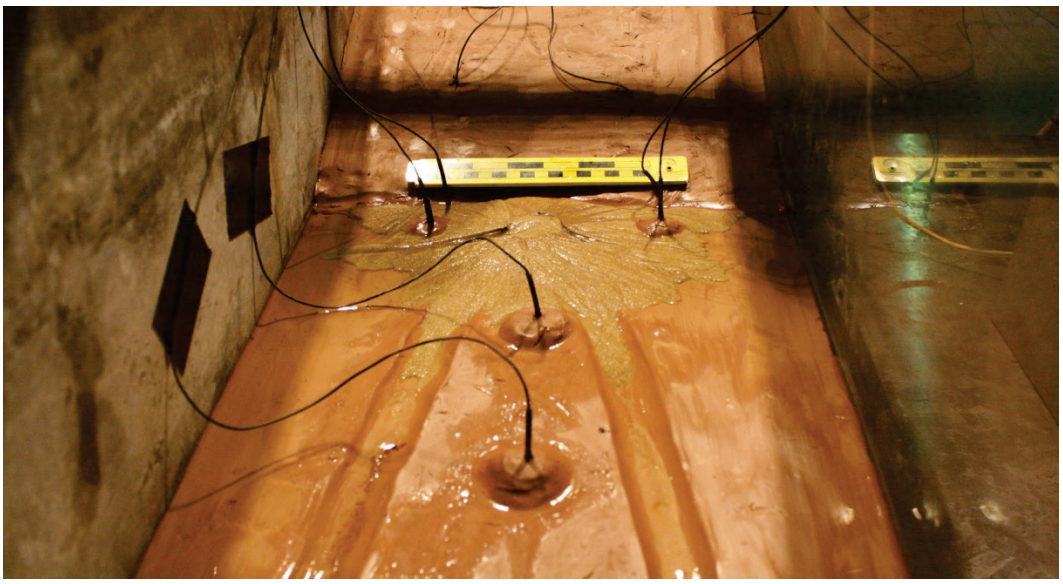

Figure A22. The eroded sand was collected from the model surface and weighted to determine the volume lost by the foundation.

Figure A23. The enlarged pressure relief hole after the sand was removed from the surface of the model.

Figure A24. Most of clay surface and levee removed. There is an erosion pattern next to the remnants of the levee.

Figure A25. The erosion pattern and the relief hole were outlined. No erosion channel appears to have formed. Notice the red staining from the top clay layer in the eroded area.

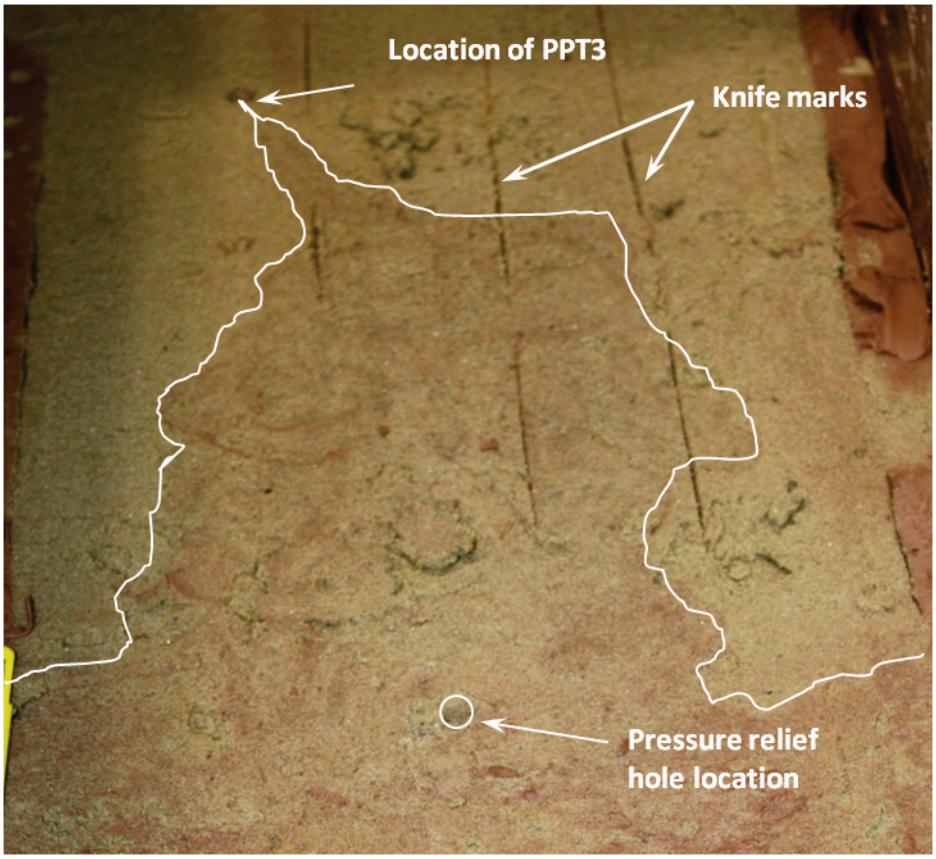

Figure A26. No erosion occurred with depth. All eroded sand appeared to come from the sand-clay interface.

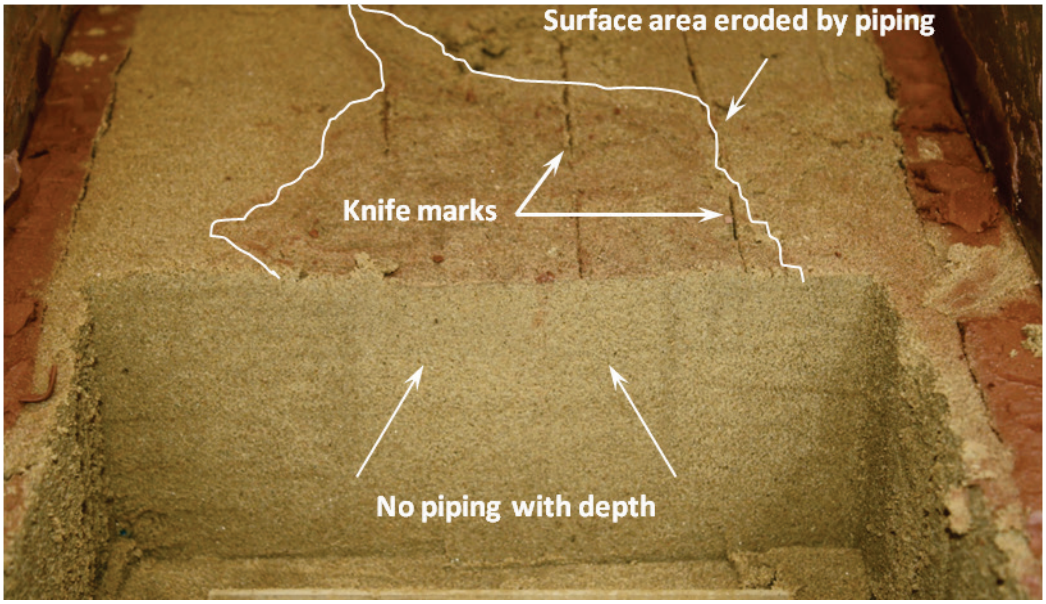

Post analysis of Model 2

Figure A27. View of the relief hole at the completion of Model 2.

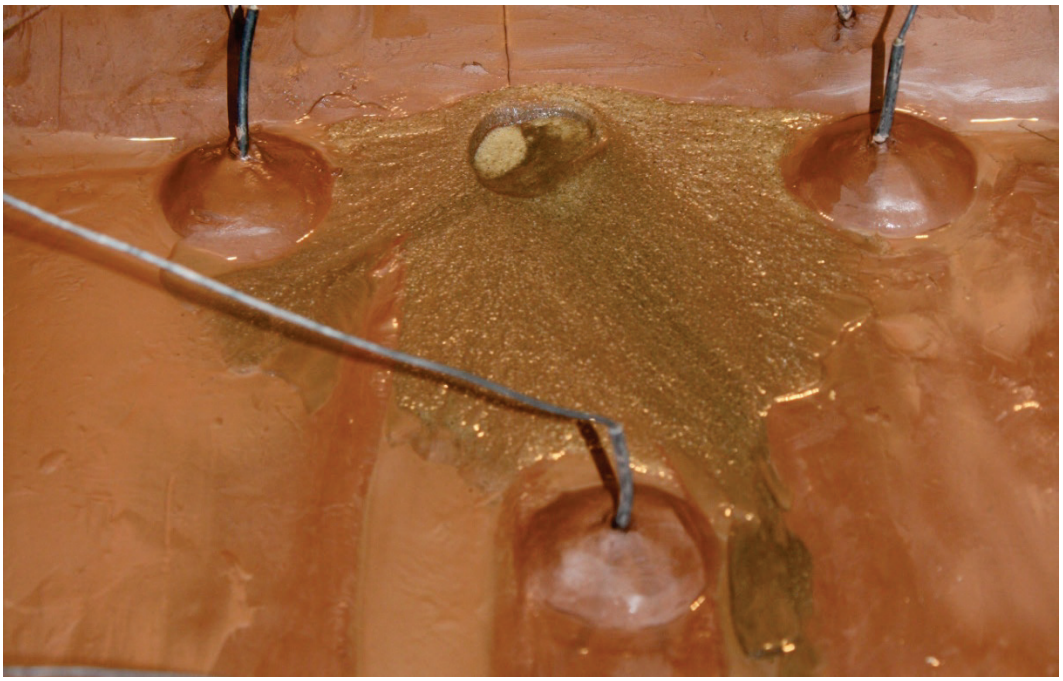

Figure A28. Removal of the top clay layer shows the eroded area under the levee.

Figure A29. Top view of Model 2 after the levee and top clay layer were removed.

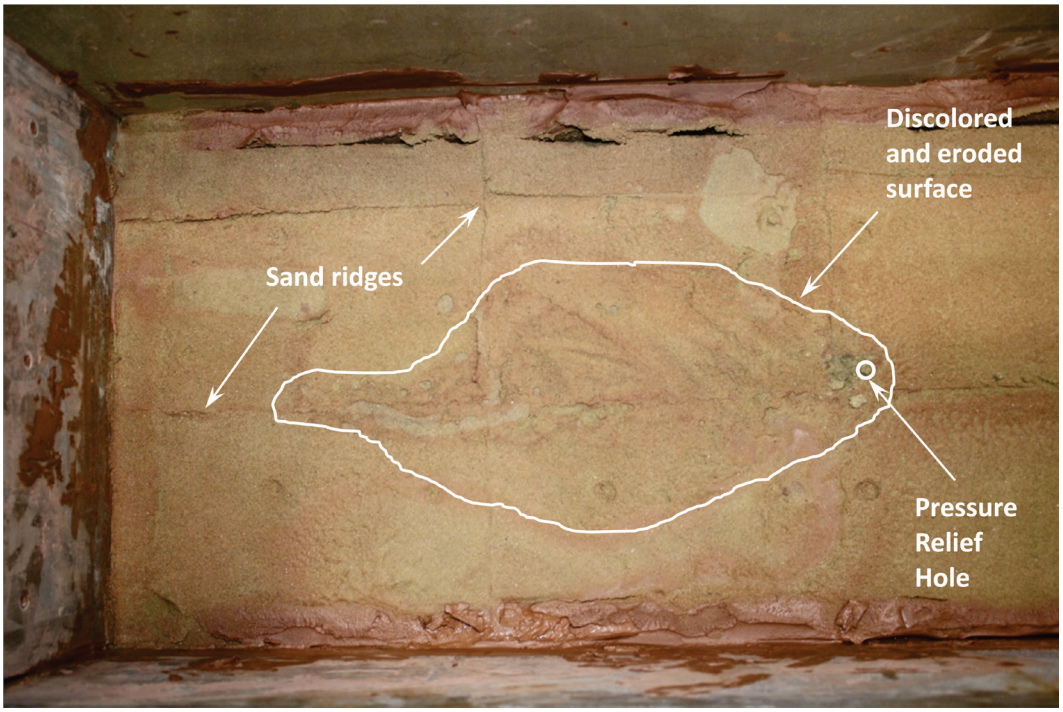

Figure A30. Little erosion occurred with depth. All eroded sand appeared to come from the sand-clay interface.

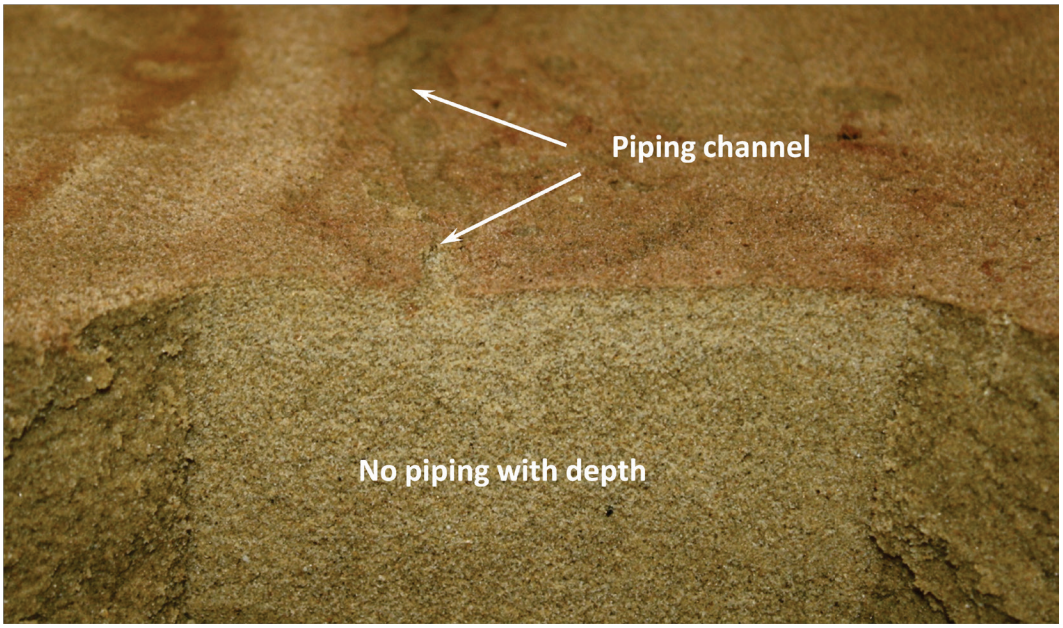

Post analysis of Model 3

Figure A31. View of Model 3 relief hole at the end of the test. The eroded clayey sand-sand mixture that covers the model surface is about 1-in. thick. Notice the cavity under the top clay layer.

Figure A32. Top view of Model 3 showing the downstream model surface after levee removal.

Figure A33. View of piping channel that formed in the clayey sand layer. Mirror image of channel shown on bottom of top clay layer.

Figure A34. View of the clayey sand layer excavation. Notice the clean sand in the center of the relief-hole area with the red clayey sand all around.

Figure A35. View of the combined piping channel with the sand pipe below and the mixture of soils in the clayey sand channel.

Figure A36. Top view of piping channel in the sand layer.

Figure A37. Top view of partially excavated clayey sand layer revealing the piped channel in the underlying sand layer. Notice that the channel enlarged as it traveled back to the reservoir.

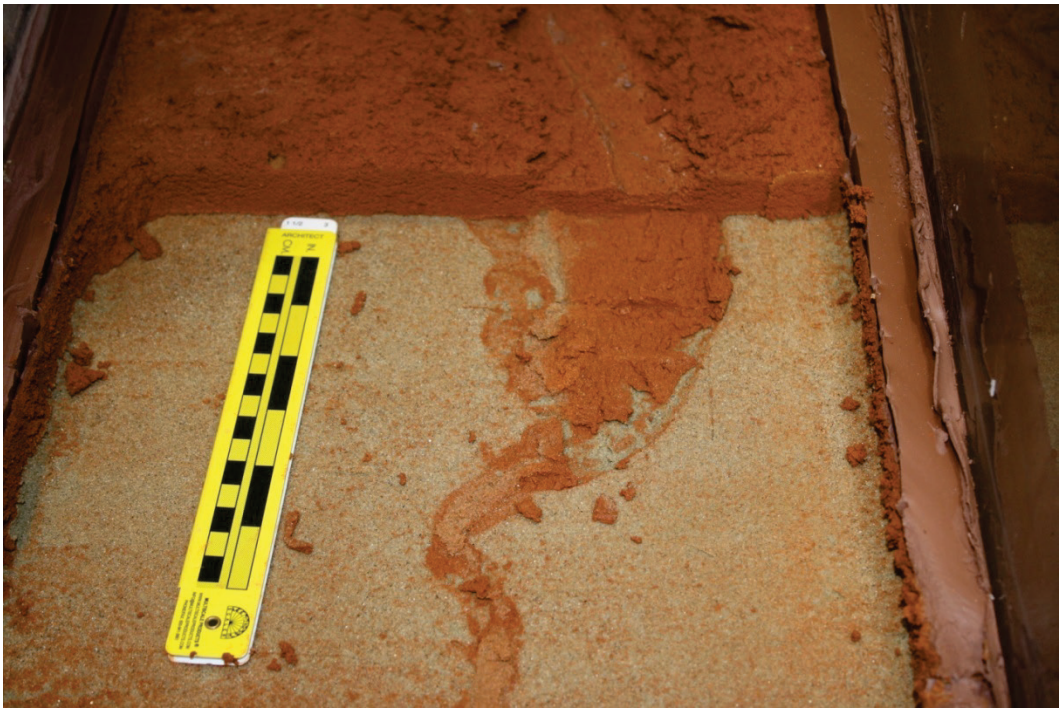

Figure A38. Top view of model after the removal of the red clayey sand layer. Notice that, at the reservoir wall, the channel covers half the width of the wall.

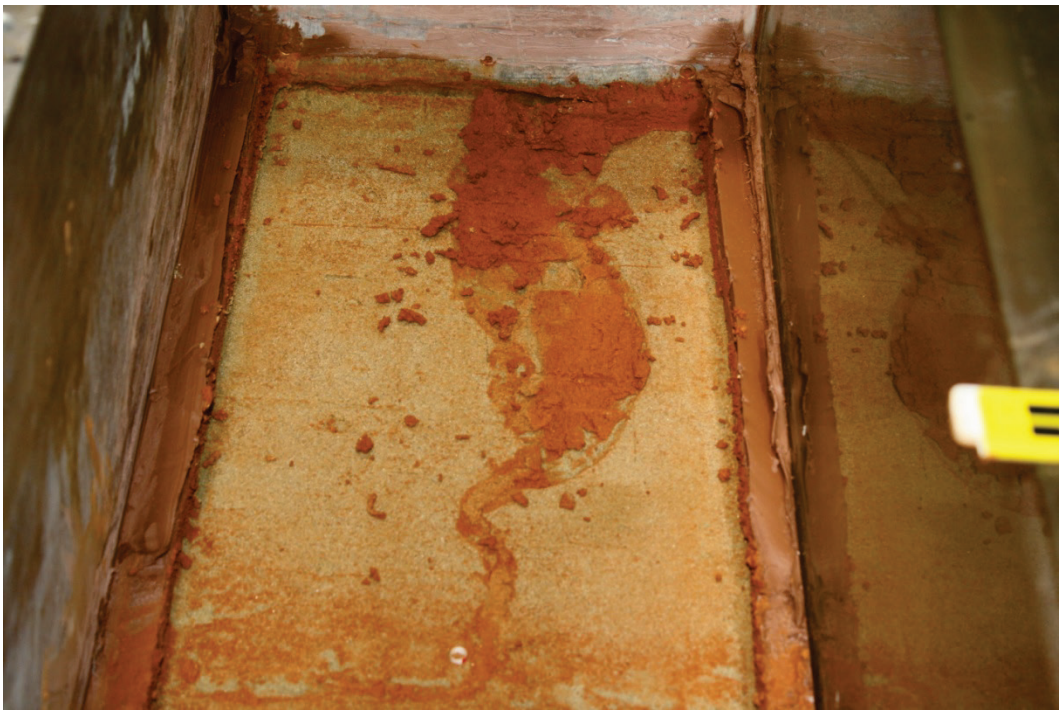

Figure A39. Top view of sand layer after the red clayey sand was carefully removed from the piped channel in the sand.

Appendix B: Centrifuge Piping Model Results

Raw and analyzed data for Model 1

Table B1. Raw data for the 10-*g* levee piping test (Model 1, with relief hole).

Model 1 with Relief hole, 10-*g* Levee Piping Test							
Pore Pressure Transducer	Initial Water Level (in.)	*g* Level	Reservoir Initial Pressure Offset, 6.7 in. of Water (psi)	Foundation Pressure Offset, 6.0 in. of Water (psi)	PPT Initial Offset, 0.7 in. of Water (psi)	psi/in. of Water Head	Distance Downstream of Water Source (in.)
	6.7	10	0.242	2.167	0.025	0.03611	
	Head on Levee (inches of water) @ 10 *g*						
	0.69	1.80	2.73	3.77	4.85	5.65	
	Pore Pressure Transducer Measurements (psi) @ 10 *g*						
1	2.53	2.93	3.26	3.64	4.03	4.31	0.0
2	2.54	2.94	3.29	3.66	4.04	4.34	0.0
3	0.50	0.82	1.06	1.30	1.49	1.69	4.0
4	0.46	0.78	1.03	1.27	1.48	1.68	4.0
5	0.43	0.68	0.87	1.06	1.19	1.33	8.0
6	0.42	0.68	0.89	1.07	1.22	1.37	8.0
7	0.43	0.67	0.85	1.01	1.08	1.20	12.0
8	0.39	0.64	0.82	0.98	1.06	1.17	12.0
9	0.48	0.66	0.79	0.88	0.90	0.93	16.0
10	0.40	0.55	0.72	0.83	0.87	0.88	16.0
11	0.63	0.76	0.81	0.81	0.82	0.81	18.0
12	0.46	0.63	0.73	0.81	0.84	0.82	18.0
13	0.31	0.47	0.57	0.66	0.67	0.67	23.0
14	0.44	0.56	0.63	0.68	0.69	0.67	28.0

Table B2. Datum for pore water pressure data changed to top of sand layer for 10-*g* levee piping test (Model 1, with relief hole).

Model 1 with Relief hole, 10-*g* Levee Piping Test							
Pore Pressure Transducer	Initial Water Level (in.)	*g* Level	Reservoir Initial Pressure Offset, 6.7 in. of Water (psi)	Foundation Pressure Offset, 6.0 in. of Water (psi)	PPT Initial Offset, 0.7 in. of Water (psi)	psi/in. of Water Head	Distance Downstream of Water Source (in.)
	6.7	10	0.242	2.167	0.025	0.03611	
	Head on Levee (inches of water) @10 *g*						
	0.69	1.80	2.73	3.77	4.85	5.65	
	Head at Top of Sand Layer (inches of water) @ 10 *g*						
	1.69	2.80	3.73	4.77	5.85	6.65	
	Pressures w/Datum at Top of Sand Layer (psi) @ 10 *g*						
1	0.60	1.00	1.33	1.71	2.10	2.38	0.0
2	0.62	1.02	1.36	1.73	2.12	2.42	0.0
3	0.53	0.84	1.08	1.32	1.51	1.71	4.0
4	0.48	0.80	1.05	1.30	1.51	1.71	4.0
5	0.45	0.71	0.90	1.08	1.22	1.36	8.0
6	0.44	0.71	0.91	1.10	1.25	1.39	8.0
7	0.45	0.69	0.87	1.04	1.11	1.23	12.0
8	0.42	0.66	0.85	1.01	1.09	1.20	12.0
9	0.51	0.69	0.82	0.91	0.92	0.95	16.0
10	0.43	0.58	0.75	0.85	0.89	0.90	16.0
11	0.66	0.78	0.84	0.83	0.84	0.84	18.0
12	0.49	0.66	0.76	0.84	0.87	0.85	18.0
13	0.34	0.49	0.60	0.68	0.70	0.69	23.0
14	0.47	0.59	0.66	0.71	0.71	0.69	28.0

Table B3. Raw data for 20-*g* levee piping test (Model 1, with relief hole).

Model 1 with Relief hole, 20-*g* Levee Piping Test											
Pore Pressure Transducer	Initial Water Level (in.)	*g* Level	Reservoir Initial Pressure Offset, 7.0 in. of Water (psi)		Foundation Pressure Offset, 6.0 in. of Water (psi)		PPT Initial Offset, 1.0 in. of Water (psi)		psi/in. of Water Head		Distance Downstream of Water Source (in.)
	7.0	20	0.253		4.333		0.03611		0.03611		
	Head on Levee (inches of water) @ 20 *g*										
	1.09	2.06	3.06	3.51	3.92	4.57	5.02	5.76	6.05	6.86	
	Pore Pressure Transducer Measurements (psi) @ 20 *g*										
1	5.59	6.26	7.00	7.31	7.62	8.10	8.41	8.93	9.14	9.72	0.0
2	5.59	6.31	7.02	7.36	7.63	8.10	8.44	8.98	9.19	9.80	0.0
3	1.30	1.81	2.35	2.48	2.66	2.83	3.07	3.32	3.44	3.71	4.0
4	1.17	1.69	2.25	2.39	2.58	2.77	3.01	3.27	3.49	3.66	4.0
5	1.10	1.52	1.96	2.06	2.14	2.25	2.38	2.48	2.66	2.94	8.0
6	1.09	1.52	1.98	2.07	2.16	2.30	2.43	2.59	2.80	3.02	8.0
7	1.07	1.46	1.76	1.93	1.92	1.98	1.98	1.99	2.14	2.70	12.0
8	0.97	1.36	1.77	1.83	1.83	1.90	1.95	2.03	2.10	2.45	12.0
9	1.00	1.31	1.64	1.68	1.57	1.57	1.53	1.46	1.55	1.92	16.0
10	0.87	1.17	1.49	1.53	1.43	1.48	1.53	1.72	1.82	2.08	16.0
11	1.12	1.40	1.69	1.72	1.64	1.68	1.70	1.77	1.85	2.11	18.0
12	0.93	1.22	1.48	1.36	1.35	1.34	1.34	1.40	1.50	1.62	18.0
13	0.75	1.00	1.25	1.14	1.20	1.25	1.28	1.34	1.39	1.45	23.0
14	0.85	0.99	1.14	1.11	0.97	0.84	0.76	0.69	0.58	0.64	28.0

Table B4. Datum for pore water pressure data changed to top of sand layer for 20-*g* levee piping test (Model 1, with relief hole).

Model 1 with relief hole, 20 *g* Levee Piping Test											
Pore Pressure Transducer	Initial Water Level (in.)	*g* Level	Reservoir Initial Pressure Offset, 7.0 in. of Water (psi)	Foundation Pressure Offset, 6.0 in. of Water (psi)		PPT Initial Offset, 1.0 in. of Water (psi)		psi/in. of Water Head		Distance Downstream of Water Source (in.)
	7.0	20	0.253	4.333		0.03611		0.03611		
	Head on Levee (inches of water) @20 *g*										
	1.09	2.06	3.06	3.51	3.92	4.57	5.02	5.76	6.05	6.86	
	Head at Top of Sand Layer (inches of water) @ 20 *g* (adjusted to 10 *g*)										
	4.18	6.12	8.11	9.03	9.83	11.13	12.05	13.51	14.10	15.73	
	Pressures w/Datum at Top of Sand Layer (psi) @ 20 *g*										
1	1.51	2.18	2.92	3.23	3.54	4.02	4.33	4.85	5.06	5.64	0.0
2	1.51	2.23	2.94	3.28	3.55	4.02	4.36	4.90	5.11	5.72	0.0
3	1.33	1.84	2.39	2.51	2.70	2.87	3.10	3.35	3.48	3.74	4.0
4	1.21	1.73	2.29	2.42	2.62	2.81	3.05	3.31	3.53	3.70	4.0
5	1.14	1.56	2.00	2.10	2.18	2.29	2.42	2.52	2.70	2.98	8.0
6	1.13	1.56	2.01	2.10	2.20	2.33	2.47	2.63	2.83	3.06	8.0
7	1.11	1.50	1.80	1.97	1.96	2.02	2.02	2.03	2.18	2.74	12.0
8	1.01	1.40	1.80	1.87	1.86	1.94	1.98	2.07	2.14	2.49	12.0
9	1.04	1.34	1.67	1.71	1.61	1.61	1.56	1.50	1.59	1.96	16.0
10	0.91	1.21	1.53	1.57	1.47	1.52	1.57	1.76	1.86	2.12	16.0
11	1.15	1.44	1.72	1.76	1.67	1.72	1.73	1.80	1.89	2.15	18.0
12	0.97	1.25	1.52	1.40	1.39	1.38	1.38	1.43	1.54	1.65	18.0
13	0.79	1.03	1.29	1.17	1.24	1.28	1.31	1.38	1.42	1.49	23.0
14	0.89	1.03	1.17	1.15	1.01	0.88	0.79	0.73	0.61	0.67	28.0

Raw and analyzed data for Model 2

Table B5. Raw data for the 12-*g* levee piping test (Model 2, no relief hole).

Model 2 without Relief hole, 12-*g* Levee Piping Test							
Pore Pressure Transducer	Initial Water Level (in.)	*g* Level	Initial Pressure Offset @ 1 *g*, 0.00 in. of Water (psi)	Foundation Pressure Offset @ 12 *g*, 6.0 in. of Water (psi)	PPT Initial Offset, 0.00 in. of Water (psi)	psi/in. of Water Head	Distance Downstream of Water Source (in.)
	6.00	12	0.00	2.600	0.00	0.03611	
	Head on Levee (inches of water) @ 12 *g*						
	-1.00	-0.43	0.05	0.45	1.23	2.02	
	Pore Pressure Transducer Measurements (psi) @ 12 *g*						
1	2.70	2.93	3.15	3.32	3.66	4.00	0.0
2	2.62	2.88	3.08	3.26	3.59	3.94	0.0
3	0.14	0.32	0.50	0.64	0.91	1.14	4.0
4	0.19	0.37	0.56	0.71	1.00	1.25	4.0
5	0.10	0.25	0.42	0.54	0.78	0.98	8.0
6	0.10	0.27	0.45	0.59	0.85	1.05	8.0
7	0.16	0.31	0.49	0.62	0.86	1.04	12.0
8	0.16	0.30	0.46	0.57	0.81	1.00	12.0
9	0.16	0.33	0.52	0.64	0.89	1.06	16.0
10	-0.05	0.08	0.26	0.37	0.60	0.75	16.0
11	0.00	0.00	0.00	0.00	0.00	0.00	18.0
12	0.00	0.00	0.00	0.00	0.00	0.00	18.0
13	0.00	0.00	0.00	0.00	0.00	0.00	23.0
14	0.31	0.38	0.53	0.69	0.81	0.88	28.0

Table B6. Datum for pore water pressure data changed to top of sand layer for 12-*g* levee piping test (Model 2, no relief hole).

Model 2 without Relief hole, 12-*g* Levee Piping Test							
Pore Pressure Transducer	Initial Water Level (in.)	*g* Level	Initial Pressure Offset @ 1 *g*, 0.00 in. of Water (psi)	Foundation Pressure Offset @ 12 *g*, 6.00 in. of Water (psi)	PPT Initial Offset, 0.00 in. of Water (psi)	psi/in. of Water Head	Distance Downstream of Water Source (in.)
	6.00	12	0.00	2.600	0.00	0.03611	
	Head on Levee (inches of water) @12 *g*						
	-1.00	-0.43	0.05	0.45	1.23	2.02	
	Head at Top of Sand Layer (inches of water) @12 *g*						
	0.00	0.57	1.05	1.45	2.23	3.02	
	Pressures w/Datum at Top of Sand Layer (psi) @12 *g*						
1	0.00	0.23	0.45	0.62	0.96	1.30	0.0
2	0.00	0.26	0.46	0.64	0.97	1.32	0.0
3	0.14	0.32	0.50	0.64	0.91	1.14	4.0
4	0.17	0.35	0.54	0.69	0.98	1.23	4.0
5	0.10	0.24	0.41	0.53	0.78	0.98	8.0
6	0.10	0.27	0.45	0.59	0.85	1.05	8.0
7	0.15	0.30	0.48	0.60	0.85	1.03	12.0
8	0.17	0.30	0.46	0.58	0.82	1.01	12.0
9	0.18	0.34	0.54	0.65	0.90	1.07	16.0
10	0.04	0.17	0.34	0.46	0.68	0.84	16.0
11	0.00	0.00	0.00	0.00	0.00	0.00	18.0
12	0.00	0.00	0.00	0.00	0.00	0.00	18.0
13	0.00	0.00	0.00	0.00	0.00	0.00	23.0
14	0.30	0.37	0.52	0.69	0.80	0.87	28.0

Table B7. Raw data for 12-*g* levee piping test (Model 2, with relief hole).

Model 2 with Relief hole, 12-*g* Levee Piping Test														
Pore Pressure Transducer	Initial Water Level (in.)	*g* Level	Initial Pressure Offset @ 1 *g*, 1.0 in. of Water (psi)		Foundation Pressure Offset @ 12 *g*, 6.0 in. of Water (psi)		PPT Initial Offset, 0.00 in. of Water (psi)		psi/in. of Water Head		Distance Downstream of Water Source (in.)			
	6.00	12	0.03611		2.600		0.0000		0.03611					
	Head on Levee (inches of water) @ 12 *g*													
	-1.14	-0.11	0.97	1.45	1.94	2.39	3.00	3.48	4.01	4.64	5.07	5.52	5.87	
	Pore Pressure Transducer Measurements (psi) @ 12 *g*													
1	2.50	2.95	3.42	3.62	3.83	4.02	4.33	4.53	4.77	5.04	5.22	5.43	5.57	0.0
2	2.58	3.02	3.49	3.70	3.92	4.12	4.34	4.55	4.77	5.05	5.24	5.42	5.58	0.0
3	0.01	0.40	0.74	0.85	1.01	1.15	1.24	1.36	1.50	1.65	1.71	1.75	1.82	4.0
4	0.01	0.44	0.74	0.87	1.04	1.20	1.33	1.46	1.61	1.77	1.84	1.90	1.98	4.0
5	-0.04	0.34	0.59	0.70	0.83	0.96	1.02	1.11	1.21	1.34	1.36	1.35	1.36	8.0
6	-0.04	0.37	0.65	0.76	0.91	1.04	1.12	1.22	1.32	1.44	1.48	1.49	1.53	8.0
7	-0.01	0.40	0.70	0.81	0.94	1.04	1.05	1.13	1.22	1.32	1.31	1.24	1.27	12.0
8	-0.04	0.36	0.61	0.70	0.83	0.93	1.01	1.09	1.18	1.27	1.28	1.26	1.30	12.0
9	0.06	0.53	0.71	0.82	0.94	0.97	0.97	1.03	1.10	1.15	1.12	1.10	1.13	16.0
10	-0.08	0.35	0.54	0.62	0.74	0.78	0.00	0.00	0.00	0.00	0.00	0.00	0.00	16.0
11	-0.17	0.13	0.39	0.45	0.52	0.52	0.64	0.68	0.73	0.77	0.76	0.76	0.78	18.0
12	0.06	0.56	0.00	0.00	0.00	1.21	0.68	0.70	0.73	0.75	0.75	0.73	0.76	18.0
13	-0.21	0.20	0.41	0.48	0.56	0.62	0.59	0.63	0.68	0.71	0.71	0.72	0.74	23.0
14	0.14	0.46	0.60	0.66	0.70	0.67	0.85	0.86	0.88	0.90	0.86	0.82	0.82	28.0

Table B8. Datum for pore water pressure data changed to top of sand layer for 12-*g* levee piping test (Model 2, with relief hole).

Model 2 with Relief hole, 12 *g* Levee Piping Test														
Pore Pressure Transducer		Initial Water Level (in.)	*g* Level	Initial Pressure Offset @ 1 *g*, 1.00 in. of Water (psi)		Foundation Pressure Offset@ 12 *g*, 6.00 in. of Water (psi)		PPT Initial Offset, 0.00 in. of Water (psi)		psi/in. of Water Head		Distance Downstream of Water Source (in.)	
		6.00	12	0.03611		2.600		0.00		0.03611			
	Head on Levee (inches of water) @12 *g*													
	-1.14	-0.11	0.97	1.45	1.94	2.39	3.00	3.48	4.01	4.64	5.07	5.52	5.87	
	Head at Top of Sand Layer (inches of water) @ 12 *g*													
	-0.14	0.89	1.97	2.45	2.94	3.39	4.00	4.48	5.01	5.64	6.07	6.52	6.87	
	Pressures w/Datum at Top of Sand Layer (psi) @ 12 *g*													
1	-0.10	0.35	0.82	1.02	1.23	1.42	1.73	1.93	2.17	2.44	2.62	2.83	2.97	0.0
2	-0.02	0.42	0.89	1.10	1.32	1.52	1.74	1.95	2.17	2.45	2.64	2.82	2.98	0.0
3	0.01	0.40	0.74	0.85	1.01	1.15	1.24	1.36	1.50	1.65	1.71	1.75	1.82	4.0
4	0.01	0.44	0.74	0.87	1.04	1.20	1.33	1.46	1.61	1.77	1.84	1.90	1.98	4.0
5	-0.04	0.34	0.59	0.70	0.83	0.96	1.02	1.11	1.21	1.34	1.36	1.35	1.36	8.0
6	-0.04	0.37	0.65	0.76	0.91	1.04	1.12	1.22	1.32	1.44	1.48	1.49	1.53	8.0
7	-0.01	0.39	0.70	0.81	0.94	1.04	1.05	1.13	1.22	1.32	1.31	1.24	1.27	12.0
8	-0.05	0.35	0.60	0.69	0.82	0.92	1.00	1.08	1.17	1.26	1.27	1.25	1.29	12.0
9	0.06	0.53	0.71	0.82	0.94	0.97	0.97	1.03	1.10	1.15	1.12	1.10	1.13	16.0
10	-0.07	0.36	0.54	0.63	0.74	0.79	0.00	0.00	0.00	0.00	0.00	0.00	0.00	16.0
11	-0.17	0.13	0.39	0.45	0.52	0.52	0.64	0.68	0.73	0.77	0.76	0.76	0.78	18.0
12	0.07	0.57	0.01	0.01	0.01	1.22	0.69	0.71	0.74	0.76	0.75	0.74	0.77	18.0
13	-0.21	0.20	0.41	0.48	0.56	0.62	0.59	0.63	0.68	0.71	0.71	0.72	0.74	23.0
14	0.15	0.47	0.61	0.67	0.71	0.68	0.86	0.87	0.89	0.91	0.87	0.83	0.83	28.0

Raw and analyzed data for Model 3

Table B9. Raw data for 12-*g* levee piping test (Model 3, no relief hole).

Model 3 without Relief hole, 12-*g* Levee Piping Test								
Pore Pressure Transducer		Initial Water Level (in.)	*g* Level	Initial Pressure Offset @ 1 *g*, 1.0 in. of Water (psi)	Reservoir Pressure Offset @ 12 *g*, 5.0 in. of Water (psi)	PPT Initial Offset, 0.0 in. of Water (psi)	psi/in. of Water Head	Distance Downstream of Water Source (in.)
	na	6.00	12	0.03611	2.167	0.00	0.03611	
	Head on levee (inches of water) @ 12 *g*							
	-0.98	-0.33	0.05	0.50	1.03	1.53	1.97	
	Pore Pressure Transducer Measurements (psi) @ 12 *g*							
1	2.61	2.89	3.05	3.25	3.48	3.70	3.89	0.0
2	0.00	0.00	0.00	0.00	0.00	0.00	0.00	0.0
3	0.26	0.51	0.70	0.83	1.02	1.19	1.34	4.0
4	0.22	0.47	0.66	0.80	1.00	1.19	1.38	4.0
5	0.40	0.62	0.80	0.92	1.08	1.24	1.38	8.0
6	0.17	0.38	0.55	0.67	0.84	1.01	1.17	8.0
7	0.38	0.61	0.80	0.93	1.10	1.26	1.40	12.0
8	0.13	0.33	0.50	0.62	0.78	0.93	1.08	12.0
9	0.00	0.00	0.00	0.00	0.00	0.00	0.00	16.0
10	0.20	0.41	0.58	0.70	0.88	1.01	1.16	16.0
11	0.45	0.68	0.85	0.96	1.08	1.18	1.31	18.0
12	0.23	0.43	0.60	0.70	0.82	0.94	1.02	18.0
13	0.36	0.55	0.69	0.79	0.91	1.00	0.97	23.0
14	0.38	0.55	0.67	0.73	0.75	0.79	0.80	28.0

Table B10. Datum for pore water pressure data changed to different interfaces for 12-*g* levee piping test (Model 3, no relief hole).

Model 3 without Relief hole, 12-*g* Levee Piping Test								
Pore Pressure Transducer		Initial Water Level (in.)	*g* Level	Initial Pressure Offset @ 1 *g*, 1.00 in. of Water (psi)	Reservoir Pressure Offset@ 12 *g*, 5.0 in. of Water (psi)	PPT Initial Offset, 0.0 in. of Water (psi)	psi/in. of Water Head	Distance Downstream of Water Source (in.)
		6.00	12	0.03611	2.167	0.00	0.03611	
	Head on Levee (inches of water) @ 12 *g*							
	-0.98	-0.33	0.05	0.50	1.03	1.53	1.97	
	Head at Top of Clayey Sand Layer (inches of water) @ 12 *g*							
	0.02	0.67	1.05	1.50	2.03	2.53	2.97	
	Head at Top of Sand Layer (inches of water) @ 12 *g*							
	1.02	1.67	2.05	2.50	3.03	3.53	3.97	
	Pressures w/Datum at Top of Sand Layer (psi) @ 12 *g*							
1	0.44	0.72	0.89	1.08	1.31	1.53	1.72	0.0
2	0.00	0.00	0.00	0.00	0.00	0.00	0.00	0.0
3	0.29	0.55	0.73	0.86	1.05	1.23	1.38	4.0
4	0.22	0.47	0.66	0.80	1.00	1.19	1.38	4.0
5	0.43	0.65	0.83	0.95	1.12	1.28	1.42	8.0
6	0.17	0.38	0.55	0.67	0.84	1.01	1.17	8.0
7	0.42	0.65	0.83	0.96	1.14	1.30	1.44	12.0
8	0.13	0.33	0.50	0.62	0.78	0.93	1.08	12.0
9	0.00	0.00	0.00	0.00	0.00	0.00	0.00	16.0
10	0.20	0.41	0.58	0.70	0.88	1.01	1.16	16.0
11	0.49	0.71	0.89	1.00	1.11	1.22	1.35	18.0
12	0.23	0.43	0.60	0.70	0.82	0.94	1.02	18.0
13	0.36	0.55	0.69	0.79	0.91	1.00	0.97	23.0
14	0.38	0.55	0.67	0.73	0.75	0.79	0.80	28.0

Table B11. Raw data for 12-*g* levee piping test (Model 3, with relief hole).

Model 3 with Relief hole, 12-*g* Levee Piping Test																	
Pore Pressure Transducer		Initial Water Level (in.)		*g* Level	Initial Pressure Offset @ 1 *g*, 1.0 in. of Water (psi)			Reservoir Pressure Offset @ 12 *g*, 5.0 in. of Water (psi)			PPT Initial Offset, 0.0 in. of Water (psi)			psi/in. of Water Head		Distance Downstream of Water Source (in.)
		6.00		12	0.03611			2.167			0.00			0.03611		
	Head on Levee @ 12 g's (inches of water)																
	-0.98	-0.35	0.13	0.45	0.98	1.49	1.98	2.65	3.02	3.50	4.05	4.49	5.05	5.48	6.02	6.45	
	Pore Pressure Transducer Measurements @ 12 g's (psi)																
1	2.61	2.88	3.09	3.23	3.46	3.68	3.89	4.18	4.34	4.55	4.79	4.98	5.22	5.41	5.64	5.83	0.0
2	0.00	0.00	0.00	0.00	0.00	0.00	0.00	0.00	0.00	0.00	0.00	0.00	0.00	0.00	0.00	0.00	0.0
3	0.26	0.49	0.66	0.79	1.02	1.19	1.36	1.60	1.74	1.89	2.09	2.24	2.40	2.53	2.66	2.80	4.0
4	0.23	0.47	0.66	0.80	1.00	1.19	1.38	1.52	1.65	1.81	2.00	2.18	2.36	2.51	2.66	2.81	4.0
5	0.39	0.62	0.79	0.92	1.09	1.24	1.38	1.46	1.57	1.71	1.87	1.99	2.13	2.23	2.31	2.41	8.0
6	0.18	0.38	0.55	0.68	0.84	1.01	1.17	1.29	1.40	1.54	1.72	1.85	1.98	2.09	2.18	2.30	8.0
7	0.38	0.61	0.80	0.93	1.10	1.26	1.41	1.53	1.64	1.76	1.92	2.04	2.15	2.24	2.26	2.34	12.0
8	0.13	0.33	0.50	0.61	0.78	0.93	1.08	1.30	1.40	1.52	1.69	1.81	1.92	2.03	2.05	2.13	12.0
9	0.00	0.00	0.00	0.00	0.00	0.00	0.00	0.00	0.00	0.00	0.00	0.00	0.00	0.00	0.00	0.00	16.0
10	0.20	0.39	0.58	0.70	0.85	0.98	1.13	1.08	1.16	1.26	1.39	1.43	1.49	1.55	1.52	1.56	16.0
11	0.45	0.64	0.83	0.95	1.05	1.17	1.30	1.36	1.40	1.48	1.57	1.57	1.63	1.73	1.70	1.71	18.0
12	0.00	0.00	0.00	0.00	0.00	0.00	0.00	0.00	0.00	0.00	0.00	0.00	0.00	0.00	0.00	0.00	18.0
13	0.36	0.52	0.69	0.78	0.87	0.98	0.98	1.07	1.10	1.27	1.09	1.09	1.10	1.08	1.06	1.00	23.0
14	0.38	0.54	0.67	0.72	0.75	0.79	0.81	1.21	1.27	1.37	1.41	1.29	1.31	1.31	1.26	1.19	28.0

Table B12. Datum for pore water pressure data changed to different interfaces for 12-*g* levee piping test (Model 3, with relief hole).

Model 3 with Relief hole, 12-*g* Levee Piping Test																	
Pore Pressure Transducer		Initial Water Level (in.)	*g* Level	Initial Pressure Offset @ 1 *g*, 1.0 in. of Water (psi)		Reservoir Pressure Offset @ 12 *g*, 5.0 in. of Water (psi)		PPT Initial Offset, 0.0 in. of Water (psi)		psi/in. of Water Head		Distance Downstream of Water Source (in.)				
		6.00	12	0.03611		2.167		0.00		0.03611						
	Head on Levee (inches of water) @ 12 *g*															
	-0.98	-0.35	0.13	0.45	0.98	1.49	1.98	2.65	3.02	3.50	4.05	4.49	5.05	5.48	6.02	6.45	
	Head at Top of Clayey Sand Layer (inches of water) @ 12 *g*																
	0.02	0.65	1.13	1.45	1.98	2.49	2.98	3.65	4.02	4.50	5.05	5.49	6.05	6.48	7.02	7.45	
	Head at Top of Sand Layer (inches of water) @ 12 *g*																
	1.02	1.65	2.13	2.45	2.98	3.49	3.98	4.65	5.02	5.50	6.05	6.49	7.05	7.48	8.02	8.45	
	Pressures w/Datum at Top of Sand Layer (psi) @ 12 *g*																
1	0.44	0.71	0.92	1.06	1.29	1.51	1.72	2.01	2.17	2.38	2.62	2.81	3.05	3.24	3.47	3.66	0.0
2	0.00	0.00	0.00	0.00	0.00	0.00	0.00	0.00	0.00	0.00	0.00	0.00	0.00	0.00	0.00	0.00	0.0
3	0.30	0.53	0.70	0.83	1.06	1.23	1.40	1.64	1.78	1.93	2.13	2.28	2.44	2.57	2.70	2.84	4.0
4	0.23	0.47	0.66	0.80	1.00	1.19	1.38	1.52	1.65	1.81	2.00	2.18	2.36	2.51	2.66	2.81	4.0
5	0.43	0.66	0.83	0.95	1.13	1.28	1.42	1.50	1.61	1.75	1.91	2.03	2.17	2.27	2.35	2.45	8.0
6	0.18	0.38	0.55	0.68	0.84	1.01	1.17	1.29	1.40	1.54	1.72	1.85	1.98	2.09	2.18	2.30	8.0
7	0.42	0.65	0.84	0.96	1.14	1.30	1.44	1.57	1.68	1.80	1.96	2.08	2.19	2.28	2.30	2.38	12.0
8	0.13	0.33	0.50	0.61	0.78	0.93	1.08	1.30	1.40	1.52	1.69	1.81	1.92	2.03	2.05	2.13	12.0
9	0.00	0.00	0.00	0.00	0.00	0.00	0.00	0.00	0.00	0.00	0.00	0.00	0.00	0.00	0.00	0.00	16.0
10	0.20	0.39	0.58	0.70	0.85	0.98	1.13	1.08	1.16	1.26	1.39	1.43	1.49	1.55	1.52	1.56	16.0
11	0.49	0.68	0.87	0.98	1.09	1.21	1.34	1.40	1.44	1.52	1.61	1.61	1.67	1.77	1.74	1.75	18.0
12	0.00	0.00	0.00	0.00	0.00	0.00	0.00	0.00	0.00	0.00	0.00	0.00	0.00	0.00	0.00	0.00	18.0
13	0.36	0.52	0.69	0.78	0.87	0.98	0.98	1.07	1.10	1.27	1.09	1.09	1.10	1.08	1.06	1.00	23.0
14	0.38	0.54	0.67	0.72	0.75	0.79	0.81	1.21	1.27	1.37	1.41	1.29	1.31	1.31	1.26	1.19	28.0

Table B13. Raw data for 24-*g* levee piping test (Model 3, with relief hole).

Model 3 with Relief hole, 24-*g* Levee Piping Test													
Pore Pressure Transducer		Initial Water Level (in.)	*g* Level	Initial Pressure Offset @ 1 *g*, 1.0 in. of water (psi)		Reservoir Pressure Offset @ 24 *g*, 5.0 in. of Water (psi)		PPT Initial Offset, 0.0 in. of Water (psi)		psi/in. of Water Head		Distance Downstream of Water Source (in.)
	na	6.00	24	0.03611		4.333		0.00		0.03611		
	Head on Levee (inches of water) @ 24 *g*												
	0.94	2.52	3.00	3.50	4.03	4.50	5.01	5.54	6.05	6.59	7.25	6.00	
	Pore Pressure Transducer Measurements (psi) @ 24 *g*												
1	6.88	8.25	8.67	9.10	9.56	9.97	10.41	10.87	11.31	11.78	12.35	11.27	0.0
2	0.00	0.00	0.00	0.00	0.00	0.00	0.00	0.00	0.00	0.00	0.00	0.00	0.0
3	2.24	3.30	3.64	3.97	4.34	4.65	4.92	5.29	5.59	5.92	6.21	5.09	4.0
4	2.02	3.05	3.39	3.76	4.14	4.45	4.75	5.12	5.44	5.78	6.10	5.06	4.0
5	2.14	3.04	3.32	3.60	3.88	4.11	4.34	4.62	4.83	5.09	5.24	4.21	8.0
6	1.79	2.65	2.95	3.25	3.60	3.82	4.08	4.38	4.64	4.89	5.04	3.95	8.0
7	2.14	3.01	3.25	3.51	3.75	3.92	4.14	4.37	4.57	4.73	4.77	3.61	12.0
8	0.00	0.00	0.00	0.00	0.00	0.00	0.00	0.00	0.00	0.00	0.00	0.00	12.0
9	0.00	0.00	0.00	0.00	0.00	0.00	0.00	0.00	0.00	0.00	0.00	0.00	16.0
10	1.97	2.68	2.90	3.14	3.30	3.28	3.40	3.43	3.44	3.44	3.48	2.68	16.0
11	2.12	2.70	2.86	2.98	3.13	3.16	3.34	3.17	3.41	3.46	3.89	2.69	18.0
12	0.00	0.00	0.00	0.00	0.00	0.00	0.00	0.00	0.00	0.00	0.00	0.00	18.0
13	1.68	2.13	2.16	2.26	2.23	2.32	2.34	2.31	2.28	2.32	2.70	1.92	23.0
14	0.00	0.00	0.00	0.00	0.00	0.00	0.00	0.00	0.00	0.00	0.00	0.00	28.0

Table B14. Datum for pore water pressure data changed to different interfaces for 24-*g* levee piping test (Model 3, with relief hole).

Model 3 with relief hole, 24-*g* Levee Piping Test													
Pore Pressure Transducer		Initial Water Level (in.)	*g* Level	Initial Pressure Offset @ 1 *g*, 1.0 in. of Water (psi)		Reservoir Pressure Offset @ 24 *g*, 5.0 in. of Water (psi)		PPT Initial Offset, 0.0 in. of Water (psi)		psi/in. of Water Head		Distance Downstream of Water Source (in.)
	na	6.00	24	0.03611		4.333		0.00		0.03611		
	Head on Levee (inches of water) @ 24 *g*											
	0.94	2.52	3.00	3.50	4.03	4.50	5.01	5.54	6.05	6.59	7.25	6.00	
	Head at Top of Clayey Sand Layer (inches of water) @ 24 *g*											
	1.94	3.52	4.00	4.50	5.03	5.50	6.01	6.54	7.05	7.59	8.25	7.00	
	Head at Top of Sand Layer (inches of water) @ 24 *g*											
	2.94	4.52	5.00	5.50	6.03	6.50	7.01	7.54	8.05	8.59	9.25	8.00	
	Pressures w/Datum at Top of Sand Layer (psi) @ 24 *g*											
1	2.55	3.92	4.34	4.77	5.23	5.64	6.08	6.54	6.98	7.45	8.02	6.94	0.0
2	0.00	0.00	0.00	0.00	0.00	0.00	0.00	0.00	0.00	0.00	0.00	0.00	0.0
3	2.28	3.34	3.68	4.01	4.38	4.69	4.96	5.33	5.63	5.96	6.25	5.13	4.0
4	2.02	3.05	3.39	3.76	4.14	4.45	4.75	5.12	5.44	5.78	6.10	5.06	4.0
5	2.18	3.08	3.36	3.64	3.92	4.15	4.38	4.66	4.87	5.13	5.28	4.25	8.0
6	1.79	2.65	2.95	3.25	3.60	3.82	4.08	4.38	4.64	4.89	5.04	3.95	8.0
7	2.18	3.05	3.29	3.55	3.79	3.96	4.18	4.41	4.61	4.77	4.81	3.65	12.0
8	0.00	0.00	0.00	0.00	0.00	0.00	0.00	0.00	0.00	0.00	0.00	0.00	12.0
9	0.00	0.00	0.00	0.00	0.00	0.00	0.00	0.00	0.00	0.00	0.00	0.00	16.0
10	1.97	2.68	2.90	3.14	3.30	3.28	3.40	3.43	3.44	3.44	3.48	2.68	16.0
11	2.16	2.74	2.90	3.02	3.17	3.20	3.38	3.21	3.45	3.50	3.93	2.73	18.0
12	0.00	0.00	0.00	0.00	0.00	0.00	0.00	0.00	0.00	0.00	0.00	0.00	18.0
13	1.68	2.13	2.16	2.26	2.23	2.32	2.34	2.31	2.28	2.32	2.70	1.92	23.0
14	0.00	0.00	0.00	0.00	0.00	0.00	0.00	0.00	0.00	0.00	0.00	0.00	28.0

REPORT DOCUMENTATION PAGE

Form Approved
OMB No. 0704-0188

1. REPORT DATE *(DD-MM-YYYY)*	2. REPORT TYPE	3. DATES COVERED *(From - To)*
May 2014	Final	

4. TITLE AND SUBTITLE

Geotechnical Centrifuge Experiments to Evaluate Piping in Foundation Soils

5a. CONTRACT NUMBER

5b. GRANT NUMBER

5c. PROGRAM ELEMENT NUMBER

6. AUTHOR(S)

Johannes L. Wibowo, Donald E. Yule, Daniel A. Leavell, and Ryan A. Strange

5d. PROJECT NUMBER

5e. TASK NUMBER

5f. WORK UNIT NUMBER

7. PERFORMING ORGANIZATION NAME(S) AND ADDRESS(ES)

Geotechnical and Structures Laboratory
US Army Engineer Research and Development Center
3909 Halls Ferry Road
Vicksburg, MS 39180-6199

8. PERFORMING ORGANIZATION REPORT NUMBER

ERDC/GSL TR-14-14

9. SPONSORING / MONITORING AGENCY NAME(S) AND ADDRESS(ES)

Headquarters, US Army Corps of Engineers
Washington, DC 20314-1000

10. SPONSOR/MONITOR'S ACRONYM(S)

HQ-USACE

11. SPONSOR/MONITOR'S REPORT NUMBER(S)

12. DISTRIBUTION / AVAILABILITY STATEMENT

Approved for public release; distribution is unlimited.

13. SUPPLEMENTARY NOTES

14. ABSTRACT

The general objectives of the centrifuge tests for this research were to model a realistic geologic prototype of a levee with a foundation containing a sand layer that is susceptible to an internal erosion/piping failure mechanism with objectives to initiate and monitor piping. Parameters that could influence piping/erosion in levee foundation soils were evaluated (i.e., depth of erodible material, density of erodible material, and confining stress). Centrifuge testing and numerical modeling were performed on three geotechnical models constructed with soils similar to those found in the US Army Corps of Engineers levee portfolio. Models 1 and 2 had a clay levee that was founded on a Nevada Sand layer sandwiched between two Longhorn Red Clay layers. Model 3 had a foundation consisting of a Longhorn Red Clay top layer, then a clayey sand layer, followed by Nevada Sand and, finally, a bottom layer of Longhorn Red Clay. Varying gravity loadings were selected based on a prototype structure 5 to 12 ft. in height. All models developed piping that moved from a downstream relief hole back under the levee toward the upstream reservoir. The results from the three centrifuge tests showed that subsurface erosion could be modeled in a centrifuge.

15. SUBJECT TERMS

Piping
Centrifuge
Seepage
Erosion

16. SECURITY CLASSIFICATION OF:			17. LIMITATION OF ABSTRACT	18. NUMBER OF PAGES	19a. NAME OF RESPONSIBLE PERSON M. Corcoran
a. REPORT	b. ABSTRACT	c. THIS PAGE			19b. TELEPHONE NUMBER *(include area code)*
Unclassified	Unclassified	Unclassified		107	601-634-3334